Techno-economical feasibility study of ammonia as a fuel to decarbonize a trailing suction hopper dredger

Masters thesis

by

B.W. den Tonkelaar

to obtain the degree of Master of Science at the Delft University of Technology,

Student number:

Project duration: November 14, 2022 – August 29, 2023

Thesis committee:

Dr. ir. P. de Vos, Delft University of Technology, chair Dr. ir. R.L.J. Helmons, Delft University Technology, supervisor

Ir. M. de Geus, Van Oord, supervisor



Acknowledgement

With this thesis I am completing my Offshore and Dredging engineering masters at the Delft University of Technology. This Master's thesis marks the final step in my six years of education at the TU Delft. During my thesis I have had help from a lot of people, and I want to thank the people that played key part in my thesis.

Firstly, I would like to express my gratitude to Martin de Geus, my supervisor at Van Oord, for his guidance and insightful discussions. Martin provided good advice, pushed me in the right direction and was always ready to help. Thanks to Jan Westhoeve for all the feedback and engaging discussions.

A special note of appreciation goes to Cees van Rhee, who recommended this thesis subject and was my chair during the first months of this thesis. Finally, I want to thank Peter de Vos from the TU Delft, for all his help and effort during my thesis.

B.W. den Tonkelaar Rotterdam, August 2023

Summary

To keep the global warming of the Earth to a minimum, the greenhouse gas emissions need to be reduced. Van Oord aims to be carbon neutral by 2050; therefore, Van Oord is exploring alternative fuels. Ammonia is a promising option to use as a fuel due to the forty times lower well-to-wake emissions than MGO when it is produced with green energy. There is no carbon content in ammonia. Furthermore, the expected cost of using ammonia as a fuel is lower than other competitive 'green' fuels, such as hydrogen or methanol, due to the lower storage or fuel cost of ammonia. The goal of this research is to determine if and when it is economically viable to use ammonia as a fuel to decarbonize a trailing suction hopper dredger (TSHD). This is expressed in cost per dredged material $[\in /m^3]$.

Ammonia needs to be handled, stored and consumed taking into account safety precautions to have a safe operable ship. Additionally, ammonia has poor combustion characteristics, and therefore a promoter such as hydrogen (7-11%) or MGO (40-60%) is necessary to initiate the combustion. Additionally, internal combustion engines (ICE) using ammonia as a fuel are expected to have a low transient load capability. Therefore, if there is no MGO present, the loading capability of the ICE with the load variation of the dredging process is a challenge. This dredging process has a dynamic loading. The same challenge applies for a Solid oxide fuel cell (SOFC), where the SOFC does hardly have transient load capabilities.

A TSHD has a dynamic engine load, and the main reasons for this transient load is the change in propulsion power, which is dependant on the friction of the draghead and the sailing speed of the vessel. Furthermore, a sudden change in mixture density in the dredging tube during dredging will result in a sudden transient load. To cope with these transient loads, the energy supply on board of a TSHD must have transient load capabilities.

A fuel consumption model has been developed to compare five drive train configurations for the dredging project Kustlijnzorg with an operational profile of 30 days. The total power demand [kW] and the dP/dt [kW/s] was included on a boolean way in this model. By means of this model, the main particulars of the engines, fuel cells and batteries regarding power and energy were determined. The output of this model was the amount of fuel consumed during 30 days. This fuel consumption model was validated with another project.

The Construction Industry Research and Information Association (CIRIA) has developed a method to valuate a TSHD. With this CIRIA methods, the value of a conventional TSHD is determined and compared with the value of the ammonia driven configurations. The value of a new vessel that operates on ammonia can be estimated with the help of a sustainability factor. It is found that the CAPEX and OPEX are mainly dependent on the value of the vessel and the fuel consumption.

Currently, it is not economically feasible to use ammonia as a fuel to decarbonize a TSHD. However, when green ammonia is used in combination with a SOFC, then a TSHD can be fully decarbonized, but that is not economically feasible. In order to make ammonia an economically feasible option for a TSHD, the price of MGO and carbon has to increase, or the price of the SOFC and ammonia (grey and green) has to decrease significantly.

Currently it is unclear if the carbon tax in the future applies to wake-to-tank (WTT) or well-to-wake (WTW) emissions. If the WTW emissions are taxed, then grey ammonia is never a better choice than MGO in terms of cost. Which is also the case when considering the \mathcal{CO}_{2eg} emissions.

To conclude, it is currently not economically feasible to decarbonize a TSHD using ammonia as a fuel based on the cost per dredged material $[\in/m^3]$. The limited transient load capabilities of drive train configurations on ammonia, need a battery or MGO to cope with the transient load of a TSHD. Future progress in the technology or developments in the reduction of transient loads could make ammonia as a fuel for a TSHD a better option. Finally, future developments in the price of: carbon, ammonia and MGO can make it economically feasible to decarbonize a TSHD.

Contents

troduction		1
	ground	1
	, arch problem	
	s outline	
		4
	•	
2.2.1		
2.2.2		
2.2.3	Carbon dioxide equivalent	5
3 Engin	e technologies for ammonia	6
2.3.1	Compression ignition	6
2.3.2	Spark ignition	6
2.3.3	Nitrogen oxides regulations	7
2.3.4	Selective catalytic reduction	7
4 Fuel c		
	· · · · · · · · · · · · · · · · · · ·	
-	•	
	•	
	·	
o Conci	usion	
		12
2 Drive	systems for a trailing suction hopper dredger	12
3 Energ	ıy storage systems	13
3.3.1	Battery	13
3.3.2	Capacitor	14
3.3.3	Flywheel	14
4 Vox A	malia	14
3.4.1	Installed power	14
5 Trans	·	
	•	
3.8.1	Cycle time	
U.U. I		- '
	mmonia 1 Ammo 2.1.1 2.1.2 2.1.3 2 Ammo 2.2.1 2.2.2 2.2.3 3 Engin 2.3.1 2.3.2 2.3.3 4 Fuel of 2.4.1 2.4.2 2.4.3 5 Ammo 6 Comb 7 Safety 2.7.1 2.7.2 2.7.3 2.7.4 8 Concl railing su 1 Dredo 2 Drive 3 Energ 3.3.1 3.3.2 3.3.3 4 Vox A 3.4.1 5 Trans 6 Trans 7 Produ 8 Hoppo	1 Ammonia as a maritime fuel . 2.1.1 Ammonia production . 2.1.2 Ammonia characteristics . 2.1.3 Ammonia storage . 2 Ammonia related emissions . 2.2.1 Well-to-tank . 2.2.2 Tank-to-wake . 2.2.3 Carbon dioxide equivalent . 3 Engine technologies for ammonia . 2.3.1 Compression ignition . 2.3.2 Spark ignition . 2.3.3 Nitrogen oxides regulations . 2.3.4 Selective catalytic reduction . 4 Fuel cell technologies for ammonia . 2.4.1 Alkaline fuel cell (AFC) . 2.4.2 PEMFC . 2.4.3 Solid oxide fuel cell (SOFC) . 5 Ammonia cracker . 6 Combination of fuel cell and engine . 7 Safety aspects of ammonia . 2.7.1 Health risks . 2.7.2 Corrosion . 2.7.3 Legislation . 2.7.4 Impact on sea life . 8 Conclusion . 3.3.1 Battery . 3.3.2 Capacitor . 3.3.3 Flywheel . 9 Transient profile . 1 Installed power . 1 Installed power . 5 Transient profile . 1 Transient load during dredging . 7 Production estimation . 8 Hopper sedimentation . 8 Hopper sedimentation . 9 Ho

Contents

	3.10	Fuel Consumption	23 24 26 26
4		Ifigurations Conventional 1 MGO ICE + battery 2 dual-fuel ammonia MGO ICE 3 Dual-fuel ammonia MGO ICE + battery 4 Ammonia SOFC + battery 5 Ammoniadrive + battery Conclusion	27 28 30 30 30
5		delling approach	34
	5.1 5.2 5.3 5.4 5.5 5.6	Input: Power demand Input: Configuration with setup Power management strategy Output: fuel consumption Simulation strategy Conclusion	35 35 36 37
6			39
	6.1	Value estimation of a (new) trailing suction hopper dredger	40
	6.2 6.3 6.4	Wear and tear cost	40
	6.5 6.6	Carbon cost	41 41
	6.7 6.8 6.9	Insurance	41
7	Res	ults	42
	7.1	7.1.1 Price of equipment	42
	7.2	7.1.2 Price of fuel	43
	7.3 7.4	Carbon dioxide equivalent emissions for each configuration	45
	7. 4 7.5 7.6	Cost of dredged material	46
	7.0	Sensitivity analysis	48
		7.6.2 MGO cost	50
	7.7	7.6.5 SOFC degradation	52
8	Disc	cussion	54
9		Clusion Recommendations	57

vi Contents

Bi	liography	60
Α	Appendix A	67
В	Appendix B B.1 Results B.1.1 Carbon tax B.1.2 MGO cost B.1.3 Ammonia cost B.1.4 SOFC cost B.1.5 SOFC degradation	68 69 70 71
С	Python code C.1 simulation	73 73
D	Simulations	74

Introduction

1.1. Background

The maritime industry is responsible for around 3 percent of the global emissions caused by humans [1]. In order to meet the ambitious climate goals that are widely accepted it is necessary for the expanding maritime industry to reduce its harmful greenhouse gas emissions. Nowadays Van Oord as a company aims to reduce their carbon footprint by 2.5 percent every year, this reduction will be increased to 4.2 percent in the near future. In order to achieve this Van Oord needs to reduce their emissions in all business units, including the operation of their trailing suction hopper dredger fleet. Carbon dioxide is not the only green house gas that is taken into account when looking into decarbonisation. The four different green house gases that exist are: carbon dioxide, methane, nitrous oxide and fluorinated gases [2]. When looking into decarbonisation it is important to speak of CO_2 equivalent. One kilogram of N_2O is as harmful for the environment as 298 kilograms of CO_2 [2].

Currently the fleet of Van Oord consist among other types of vessels out of 18 trailing suction hopper dredgers. A trailing suction hopper dredger is a self-propelled that can suck up material from the seabed to depths up to 100 meters deep depending on the vessel. The most common activities of a TSDH are deepening canals and harbors and spraying up sand for coastal protection [3]. These trailing suction hopper dredgers of Van Oord use HFO, MGO or LNG as fuel, which are fossil fuels and emit too much emissions to meet the climate goals. The goal is to use sustainable fuels having a net zero carbon footprint. Ammonia could be such a sustainable fuel if the production is done with renewable energy sources. Furthermore, ammonia can serve as an hydrogen carrier or can be directly used as a fuel [4]. If ammonia is directly used as a fuel in a combustion engine then there are no carbon emissions [5]. Therefore ammonia as a fuel for a hopper dredger can contribute to the decarbonisation of the world. Currently, there is still a lot of uncertainty in the costs of the technology involved.

1.2. Research problem

The goal of this research is to determine if it is economical feasible to use ammonia as a fuel to decarbonize a trialling suction hopper dredger. To answer the main research question, the following questions need to be answered:

- 1. Why has ammonia the potential to decarbonize the maritime industry over alternative fuels?
- 2. What are the different prime movers that can power a vessel using ammonia as a fuel?
- 3. What operational profile does a trailing suction hopper dredger have during its operation?
- 4. What is the origin of the transient load condition during dredging?
- 5. Which configuration can match the operational profile of a trailing suction hopper dredger?
- 6. Is it economically feasible to use ammonia as fuel for a TSHD in 2030?
- 7. How can future scenarios in prices affect the economic feasibility of an ammonia driven TSHD?

2 1. Introduction

For this thesis the following three scenarios are investigated:

- Scenario 1, Only the TTW \mathcal{CO}_{2eq} emissions are taxed
- Scenario 2, the WTW CO_{2eq} emissions are taxed and grey ammonia is used
- Scenario 3, The WTW CO_{2eq} emissions are taxed and green ammonia is used

1.3. Thesis outline

Chapter 2 introduces ammonia as a fuel with a literature study. First it is explained how ammonia can be produced and what the difference is between green, blue and grey ammonia. Then, the characteristics of ammonia such as energy density, auto ignition temperature and storage conditions are explained. After that the difference between the well to tank and well to wake emissions is discussed. Then, the drive train systems with ammonia are explained

In Chapter 3 the trailing suction hopper dredger (TSHD) introduced. First, the dredging cycle of a TSHD will be introduced. Then it is explained why the Vox Amalia is chosen and which data is used. The transient profile of the Vox Amalia is investigated and the fuel consumption is estimated. Then, the hopper sedimentation will be explained. Due to the possible weight increase, due to heavier equipment, the hopper capacity decreases. This relation is linearized over time for simplification reasons.

Chapter 4 explains the modelling approach for this research. The output of this model is the fuel consumption. The fuel consumption was estimated with one engine instead of four engines to prevent the need of a power management strategy.

Chapter 5 explains the following configurations that are used for this research:

- Conventional
- 1 MGO ICE + battery
- · 2 DF MGO NH3
- 3 DF MGO NH3 + battery
- · 4 NH3 SOFC + battery
- 5 Ammoniadrive + battery

For each configuration a simplified power layout is given. furthermore, the specific fuel consumption for each configuration is given. Finally the MCR/s for configurations that use ammonia as a fuel is explained.

Chapter 6 introduces a cost estimation framework for a TSHD. The value of a TSHD can be determined with the Construction Industry Research and Information Association (CIRIA) method. By using this method and the price of equipment for each configuration, the OPEX of each configuration can be determined. Furthermore, the OPEX of a TSHD consist of the following six components:

- · Maintenance and Repair
- · Wear and Tear
- Fuel
- Lubricant
- Carbon
- Crew

Finally, the total weekly cost of a TSHD are divided by a the amount of dredged material in a week. The result is the cost per dredged material.

Chapter 7 discusses the results. The cheapest setups for each configurations are illustrated. Furthermore, the total weekly costs are investigated. Finally an sensitivity analysis is done for the following four components:

1.3. Thesis outline 3

- Carbon tax
- MGO cost
- Ammonia cost
- SOFC cost
- SOFC degradation

Ammonia

2.1. Ammonia as a maritime fuel

Ammonia is a translucent colorless substance that has the potential to be a promising fuel for the transportation sector [6]. Nowadays, ammonia is mainly used as a fertilizer [7]. Therefore the infrastructure for ammonia does already exist, however the infrastructure is not large enough to deliver enough ammonia to support the maritime industry at this moment in time [8]. Furthermore, ammonia can be stored more easy than hydrogen. Additionally, the price of ammonia is predicted to be lower than e-methanol [9].

2.1.1. Ammonia production

In 2019, the global ammonia production was 146 metric tonnes and it is projected that in 2050 1.2 billion tonnes of ammonia will be produced [10]. Currently, large scale ammonia production is generated with fossil fuels such as coal and natural gas [11]. Around 80 percent of the ammonia is nowadays produced with natural gas and therefore, the ammonia prices are directly related to the gas prices [12]. Most ammonia is nowadays produced with the Haber-Bosch process which is an exothermic process and the reaction equation is shown in Equation 2.1 [13].

$$N_2 + 3H_2 \Leftrightarrow 2NH_3 \tag{2.1}$$

The building blocks of ammonia are Hydrogen and Nitrogen and these are mixed with a molar ratio of 3:1 [14]. During the Haber-Bosch process nitrogen and hydrogen are put under high temperature (450-600°) and pressure (100-250 bar) [15]. Ammonia can be classified into three different categories:

- · Grey ammonia
- · Blue ammonia
- · Green ammonia

Grey ammonia is produced with the use of conventional fossil fuels, like most ammonia. For blue ammonia fossil fuels are used for the production of ammonia just like grey ammonia, however carbon capture systems are used or trees are planted in order to be carbon neutral [16]. To meet the needs of a sustainable world green ammonia is preferred. Green ammonia is produced by renewable energy sources. Large scale green hydrogen production needs to exist, before large scale green ammonia production can take place because hydrogen is a component for ammonia. Next to the conventional ammonia production process, algae could also produce ammonia, this is currently not done on a commercial scale [17].

2.1.2. Ammonia characteristics

Ammonia is 10 times more energy dense than a lithium ion battery. However, ammonia has a lower energy density than MGO as is shown in Table 2.1. This means that bigger storage tanks are necessary for ammonia to store the same energy if MGO was stored. Hydrogen has a higher gravimetric energy

density than ammonia (120 vs 18.8 MJ/kg), but the volumetric energy density of hydrogen is lower than that of ammonia. These volumetric energy densities that are shown in Table 2.1 do not include the storage tanks and equipment itself, but only the volume of the fuel. The auto ignition temperature of ammonia is at 930 kelvin at ambient pressure and therefore ammonia is more difficult to ignite then diesel [6].

Table 2.1: Energy densities and auto ignition temperature of various fuels [6], [18]–[24].

Fuel	Energy density LHV [MJ/kg]	Volumetric liquefied energy density LHV [MJ/L]	Auto ignition temperature [°C]
Ammonia	18.6	12.7	630
Marine gas oil	42.7	36.6	225
LNG	48.6	20.8	537
Hydrogen	120	8.5	560
Methanol	19.9	18.2	464

2.1.3. Ammonia storage

Marine gas oil can in contrast to ammonia be stored at ambient pressure and temperatures. Ammonia is preferably stored in its liquid phase and this is possible when ammonia is stored at -33°Celsius at ambient pressure [25]. Another way for ammonia to be liquefied is to pressurize ammonia with around 9 bar at room temperature[26]. Hydrogen has a lower boiling point than ammonia and needs to be stored at -253°Celsius at ambient pressure to be in its liquid phase[27]. Therefore the cost of storing liquid ammonia is around 30 times lower than storing liquid hydrogen [11], [28].

2.2. Ammonia related emissions

First of all, when looking into emissions it is important to look at the whole life cycle where these emissions are produced and the ${\it CO}_2$ equivalent emissions. As a final point in this section, carbon taxes are discussed.

2.2.1. Well-to-tank

Well-to-wake is the entire process chain a fuel goes through in its cycle. Meaning from raw resources in the ground to a usable fuel to storing the fuel inside a tank and to transforming the fuel into energy. Well-to-tank (WTT) is only the first part of this process until storing the fuel inside a tank. The WTT emissions for ammonia and MGO are shown in table 2.2.

Table 2.2: The emission factor in CO_2eq for MGO and ammonia used in an ICE [9].

Fuel type	WTT [kg CO _{2eq} /kg]	TTW [kg ${\it CO}_{2eq}$ /kg]	WTW [kg CO _{2eq} /kg]
MGO	0.72	3.25	3.97
Ammonia (grey)	2.25	0.10	2.35
Ammonia (green)	0	0.10	0.10

2.2.2. Tank-to-wake

Tank-to-wake (TTW) emissions are the emissions that are emitted when the fuel is converted into energy. For an ammonia fuel cell the tank to wake emissions are expected near zero. Furthermore, for an ammonia engine the tank to wake emissions can be near zero when all the NO_x is captured [29]. Ammonia has no carbon content and therefore no carbon dioxide is emitted when ammonia is combusted, however N_2O can be formed in the exhaust gasses.

2.2.3. Carbon dioxide equivalent

The four different green house gasses are: Carbon dioxide, methane, nitrous oxide and fluorinated gasses. Fluorinated gasses are the only green house gasses that do not occur naturally and are therefore fully generated by human activities [2]. The three most common fluorinated gases are: hydrofluorocarbons, perfluorocarbons and sulphur hexafluoride. The impact of each gas is different as is shown in Table 2.3. CO_2 equivalent is a way to compare emissions of different green house gasses to CO_2 . For

6 2. Ammonia

example, one tonne of methane has same impact on the environment as 25 tonnes of carbon dioxide has.

Table 2.3: The CO₂ equivalent for the green house gasses [2], [30].

Green house gas	Carbon equivalent [tonne CO2/tonne]
Carbon Dioxide	1
Methane	25
Nitrous oxide	298
Fluorinated gases	up to 22800

2.3. Engine technologies for ammonia

There have been several studies about using ammonia as a fuel for the maritime industry. The history of an engine running on ammonia goes back to 1822 where an ammonia engine was used for a small locomotive [31]. One of the first patents where the idea of running an engine of an ammonia/hydrogen mixtures originates back from 1938 [32]. Research on ammonia as a fuel for internal combustion engines has been done for a very long time already. However, large scale applications of ammonia engines for the marine industry do not exist yet. Recently, a large scale test on a 4-stroke engine that was powered by ammonia was done by $W\ddot{a}rts\ddot{i}la$ and in the coming years such engines will become available [33].

Ammonia has a low flammability and therefore it is difficult to ignite when it is used as a fuel in combination with an internal combustion engine (ICE) [34]. Using a hydrogen/ammonia mixture can help the combustion process [35]. Diesel can like hydrogen serve as a promoter for the combustion process of ammonia. Furthermore, the ideal operating point of an dual fuel ammonia/diesel engine is at an energy ratio of about 40-60 percent [36]. The diesel is necessary to burn the ammonia, due to the poor combustion characteristics of ammonia .Such an ammonia diesel dual fuel engine could serve as a solution if no hydrogen is available, because diesel is more widely available. NO_x , N_2O emissions and ammonia slip remain a problem with the ammonia engine technology [37], [38]. Selective catalytic reduction (SCR) can capture NO_x emissions by using ammonia slip [38]. However, nitrous oxide can be formed in SCR processes and is a problem in diesel oxidation catalysts [39].

2.3.1. Compression ignition

A conventional marine diesel engine is a CI (compression ignition) engine, the working principle of such an engine is that the air and fuel are ignited due to the heat from the compression [40]. The octane rating of ammonia is about 110 - 130 which is higher than that of diesel [41]. Due to the higher octane rating than hydrogen and gasoline, ammonia is more difficult to auto ignite and it must be used at engines with a higher compression ratio [42]. Ammonia has a low flammability range and a high auto ignition temperature and therefore higher compression ratios are necessary to ignite the fuel. These higher compression ratios will result in higher combustion temperatures and therefore the NO_{χ} emissions will rise [43]. There are no big engine modifications necessary for running a compression engine on a ammonia diesel mixture, however the corrosive nature of ammonia can impose a problem to the materials used [44].

2.3.2. Spark ignition

Next to fuel for CI engines ammonia is a option for spark ignition (SI) engines [45]. The ignition process of a SI engine is initiated with a spark that ignites the fuel air mixture, most of the time this fuel is petrol and these engines are commonly used in cars [46]

A higher power (MW) will naturally result in more NO_x emissions and ammonia slip [47]. The minimum hydrogen to ammonia energy ratio is higher at half engine load in comparison to a full engine load in a four stroke spark ignition engine (11% versus 7 %) [48]. This does suggest that there is a relation with the engine load and the minimum amount of hydrogen that is needed for a good combustion.

2.3.3. Nitrogen oxides regulations

The International maritime organization (IMO) has set certain limits for NO_x emissions that marine diesel engines that need to comply with in the North sea and the Baltic sea and these are shown in table 2.4 [49]. Since 2021, new build vessels that are longer than 24 meter, have an installed power higher than 130 kW and have a gross tonnage higher than 500 GT, have to comply with IMO tier III. A low speed two stroke dual fuel marine engine that works on a diesel/ammonia mixture does meet the tier IMO II, but not the tier III limits for NO_x emissions without aftertreatment systems [50].

Table 2.4: The maximum NO_x emissions allowed for different engine speed according to IMO TIER III.

n = engine rated speed (rpm)	n < 130	130 > n > 1999	n > 2000
NO_x emission limit (g/kWh)	3.4	0.9n(-0.2)	2.0

2.3.4. Selective catalytic reduction

Selective catalytic reduction (SCR) is an aftertreatment process where a catalyst is used to capture NO_x emissions. Traditionally, urea is used for NO_x aftertreatment processes, however ammonia can also serve as a catalytic agent [51]. Ammonia will then react with the NO_x gasses and both of those gasses will be converted to nitrogen and water as is shown in Equation 2.2 which is shown in Figure 2.1. Thus ammonia slip can be used as an reacting agent [47]. When there is not enough ammonia slip to react with the NO_x gasses then additional ammonia can be added. This addition of extra ammonia does not impose a problem because there is already ammonia on board that is used as fuel. Thus an SCR is can prevent ammonia slip and NO_x emissions.

$$4NO + 4NH_3 + O_2 \rightarrow 4 N_2 + 6H_2O$$

$$6NO_2 + 8NH_3 \rightarrow 7 N_2 + 12H_2O$$
(2.2)

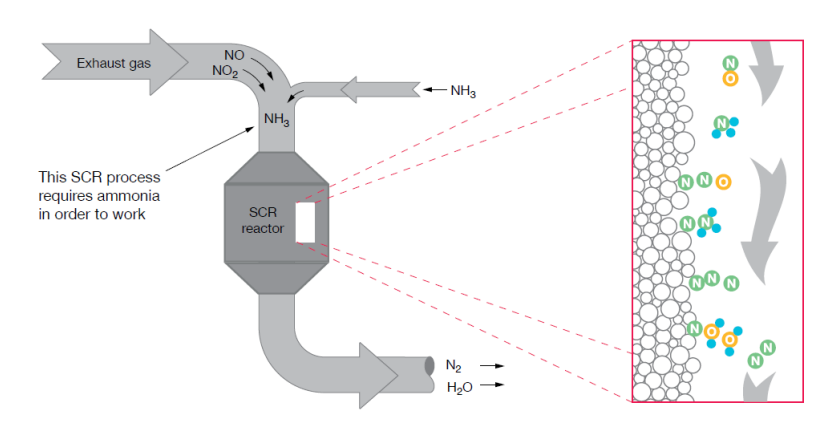


Figure 2.1: SCR process with ammonia as a reacting agent to capture the NO_x emissions [51].

At low temperatures ammonium nitrate (NH_4NO_3) can be formed in SCR catalysts that uses ammonia as a reacting agent and the reaction is shown in Equation 2.3 [52].

$$2NH_3 + 2NO_2(g) \rightarrow NH_4NO_3(s) + N_2(g) + H_2O(g)$$
 (2.3)

This ammonia nitrate has an almost irreversible reaction at temperatures between 230 and 260 °Celsius into water and nitrous oxide as is shown in Equation 2.4 [53].

$$NH_4NO_3 \rightarrow N_2O + 2H_2O \tag{2.4}$$

At high temperatures the formation of nitrous oxide happens due to the oxidation of ammonia and this total reaction is shown in Equation 2.5 [54].

$$2NH_3 + 2NO_2 \rightarrow N_2 + 3H_2O + N_2O$$
 (2.5)

8 2. Ammonia

2.4. Fuel cell technologies for ammonia

Some of the advantages of fuel cells over conventional internal combustion engines are [55]:

- · Higher efficiency than an internal combustion engine.
- · Only a few moving parts.
- · (Almost) no emissions.
- · Less noise and vibrations than an internal combustion engine.

A fuel cell consist of an anode where the fuel (ammonia, hydrogen) is fed to and a cathode where air (oxygen) is fed to [56]. The hydrogen will be split into hydrogen protons and electrons, these positively charged hydrogen protons will transfer to the cathode [56]. As a result electrons will also transfer to the cathode by an external circuit and due to the flow of the electrons electricity will be generated [56]. This working principle of an SOFC-H is shown in Figure 2.2 that uses ammonia as fuel [57].

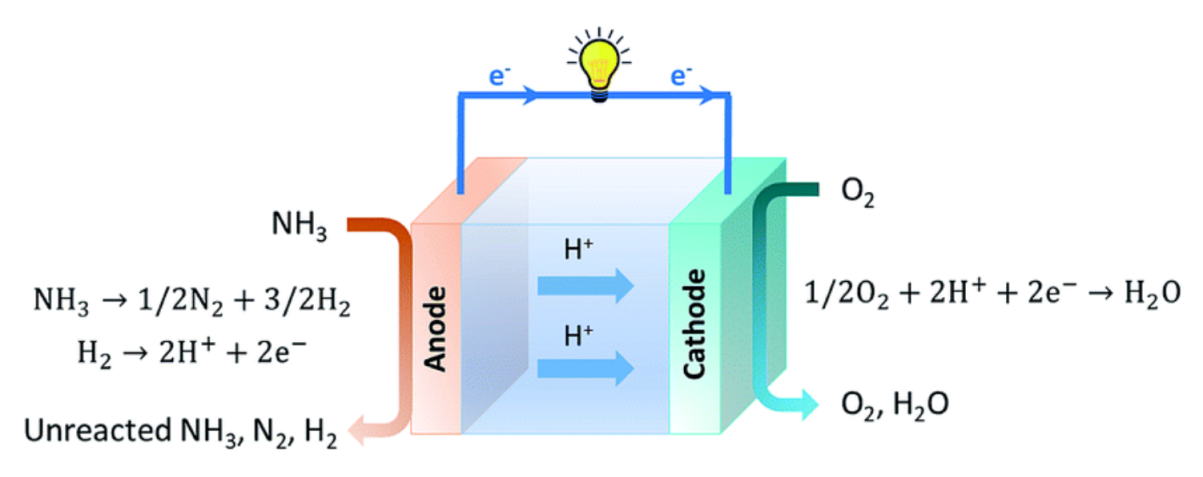


Figure 2.2: A schematic overview of a SOFC-H with ammonia as fuel [57].

The most promising fuel cells for shipping are Akaline fuel cell, Proton exchange membrane fuel cell and the solid oxide fuel cell [58]. A brief summary of the three fuel cells is shown in table 2.5, it should be noted that these low and high properties are relative to fuel cells [58]. These fuel cells can be classified into high temperature fuel cells and low temperature fuel cells where the AFC and PEMFC are low temperature fuel cells and the SOFC is a high temperature fuel cell [59]. Furthermore, the efficiency of a high temperature fuel cell is much higher than the efficiency of a low temperature fuel cells due to the possibility of waste heat recovery for high temperature fuel cells [58]. The power of a single fuel cell is not very high, therefore multiple fuel cells can be connected in arrays and this is called a stack [59]. Disadvantages of the fuel cells are the current prices and the availability of technologies.

Table 2.5: Some properties of different promising fuel cells [58] [60].

Fuel cell	Fuel	Temperature [°C]	Peak efficiency	Cost	Transient load capabilities	Size
AFC	H_2	65 - 220	50-60	Low	Good	Small
PEMFC	H_2	50 - 200	50-60	Low	Good	Small
SOFC	NH_3	500 - 1000	60-85	High	bad	Medium

2.4.1. Alkaline fuel cell (AFC)

The alkaline fuel cell is a low temperature fuel cell and can thus not be powered by ammonia, but it should be powered by pure hydrogen [61]. Therefore the ammonia needs to be cracked in to hydrogen first which is shown in Equation 2.6. The power density of the low temperature fuel cells can cause difficulties [57].

2.5. Ammonia cracker 9

2.4.2. PEMFC

The standard proton exchange membrane fuel cell (PEMFC) has an operating temperature between 50 and 100 °Celsius and requires hydrogen as fuel [58]. High temperature PEMFC have an operating temperature at 200 °Celsius and the is less sensitive to impurities in the fuel (hydrogen) [58]. Therefore, the cracking of ammonia into hydrogen can be done with less accuracy. However, ammonia poisons the fuel cell and this will reduces the performance of the PEMFC [62].

2.4.3. Solid oxide fuel cell (SOFC)

In contrast to the AFC and the normal PEMFC the solid oxide fuel cell (SOFC) can use different fuels due to its high operating temperature and therefore ammonia can directly be used as fuel [63]. Due to the high operating temperature (500-1000°C) of the SOFC the overall efficiency of the system can be improved. The waste heat can be used to improve the system efficiency. However, the costs of the SOFC are very high relative to the AFC and PEMFC. Moreover, an SOFC suffers from a much slower start up time than a low temperature fuel cell with start up times of 2.5 hours for commercially available SOFCs [64].

An advantage of the high operating temperature of a SOFC is that ammonia can be directly used as fuel, because the ammonia will due to the higher temperature be cracked inside the fuel cell into hydrogen that will be used for the electrochemical reaction [65]. If the temperature inside the SOFC is higher than 590 °Celsius then there will be full conversion of ammonia into hydrogen and nitrogen [66]. Two commonly used SOFCs are the SOFC-H and the SOFC-O. The difference in these two fuel cells is that for the SOFC-O works on a oxygen ion conducting electrolyte and that the SOFC-h works with a hydrogen proton conducting electrolyte [57]. A result of this working principle is that the SOFC-H fuel cell has the advantages that it will not produce any NO_x emissions while a SOFC-O will produce NO_x emissions without the right catalyst. The SOFC-H has a higher power density than a SOFC-O [57]. In 2023 the Viking Lady which is an offshore supply vessel will be the first fully SOFC powered vessel on ammonia with an SOFC of 2 MW [67]. Currently, an ammonia fed SOFC had an electrical efficiency of 52 % [68]. Currently, the degradation of a SOFC is 1% to 1.5% for every 1000 hours, however for 2030 the targeted degradation is lower than 0.2% [69].

2.5. Ammonia cracker

Instead of directly bunkering hydrogen, ammonia can serve as a hydrogen carrier. Ammonia is more easy to store than hydrogen due to the lower temperature required (-33°C versus -253 °C). When ammonia is used as a hydrogen carrier, an ammonia cracker can split ammonia into hydrogen and nitrogen as can be seen in Equation 2.6.

$$2NH_3 \to 3H_2 + N_2 \tag{2.6}$$

In order for ammonia to be suitable for low temperature fuel cell a 99.5 percent conversion ratio needs to be achieved [70]. The cracking of ammonia is an endothermic process that requires high temperatures in order to have a high conversion ratio into hydrogen as can be seen in table 2.6 [71]. Currently the Port of Rotterdam is performing a feasibility study for a large scale ammonia cracker that could produce a million tonnes of hydrogen a year [72].

Table 2.6: The conversion ratios of ammonia for different temperatures according to the Gibbs equation [71].

Temperature °C	300	400	500	600	700
NH ₃ conversion (%)	95.70	99.10	99.70	99.90	99.95

2.6. Combination of fuel cell and engine

Figure 2.3 shows the Ammoniadrive concept, which is a combination between a SOFC and a ammonia/hydrogen ICE [73]. The SOFC will crack the ammonia into hydrogen. Then, part of this hydrogen is used for the generation of electricity, while the remaining hydrogen is directed to the engine. The engine is supplied with ammonia, oxygen and the remainder of hydrogen that flows out of the SOFC. The idea is that the SOFC can supply the grid with constant energy and for the auxiliary systems and

10 2. Ammonia

the ICE can handle the transient loading. A version of this concept is also used in this research and is explained in Section 4.6.

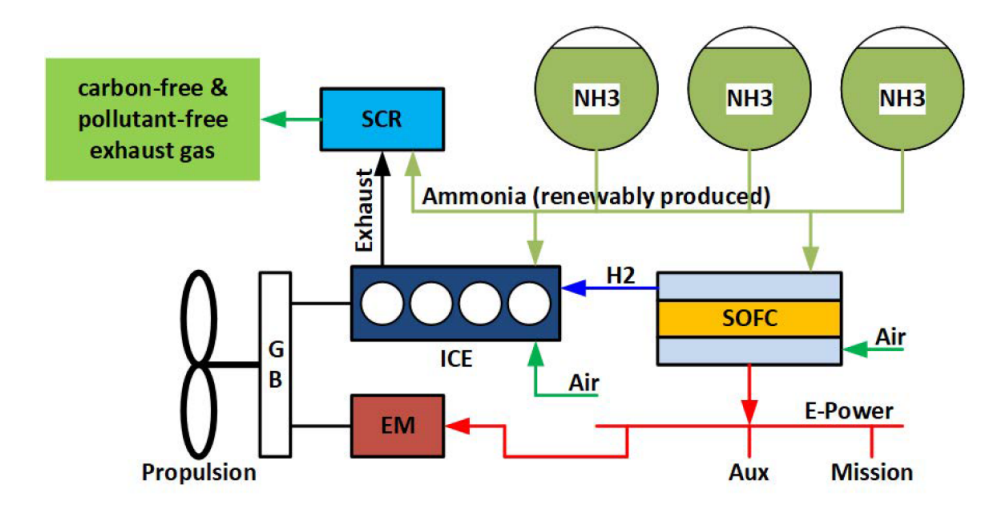


Figure 2.3: The Ammoniadrive concept where an ICE and SOFC are integrated into one power plant [73].

2.7. Safety aspects of ammonia

Ammonia is a chemical substance that has safety concerns that need to be addressed in order to be safely contained. Figure 2.7 shows the hazard rating of ammonia, this hazard rating is on a scale of 0 to 4. A score of zero means that there is no hazard and a score of 4 means that there is immediate danger [74]. Ammonia is not flammable and will not auto ignite, it can however ignite under higher pressures or if the temperature is 930 Kelvin. Furthermore, ammonia can be extinguished with conventional fire fighting procedures due to the stable behavior of ammonia [75].

Table 2.7: the Hazard ratings of ammonia according to the National Fire Protection Association (NPFA) [76].

Hazard	Value	Description
Health	3	Can cause serious or permanent injury
Flammability	1	Does not auto ignite, must be preheated
Instability	0	Normally stable, does not react

2.7.1. Health risks

Ammonia can however pose a serious threat to the health of people when they are exposed to ammonia. Exposure to ammonia means that it is inhaled, ingested or there is direct physical contact. Symptoms of ammonia exposure include [77]:

- Confusion
- · Headache
- · Skin burns
- Irritation of eyes, nose and throat
- Fever
- Sore throat

Humans are able to smell ammonia in the air from 5 ppm however, for some people the concentration of ammonia needs to be 53 ppm in order to smell it [78]. This is unfavorable because ammonia can already cause irritation when exposed to concentrations below 53 ppm. Doses at which ammonia could

2.8. Conclusion 11

be lethal are higher at around concentrations of 2500 to 4500 ppm when exposed for 30 minutes [79]. Exposure to lower concentrations than a fatal dose could still have long term impacts on the health [80].

To minimize the health risks there are laws and guidelines that state the maximum amount of ammonia that can be legally exposed to a human being. The national institute for occupational safety and health (NIOSH) advises the OSHA what the legal limits of chemicals should be. The NIOSH advises a maximum of 25 ppm ammonia averaged over 10 hours with a limit of 35 pm during a 15 minute time period [81]. The OSHA however decides the legal limits and states a maximum of 50 ppm ammonia averaged over 8 hours may be in the air [81]. In December 2022 a train that transported ammonia derailed and ammonia leaked into the air and as a result 50 people suffered from symptoms of ammonia poisoning [82]. Ammonia can thus either way be a real threat to the human health and therefore it needs to be handled with caution.

2.7.2. Corrosion

Stress corrosion cracking (scc) can occur in carbon steels if when ammonia is blended with oxygen and high stresses are present [83]. Therefore, it needs to be prevented that air is added to the ammonia. There are both double and single wall tanks used for ammonia currently. Double walled tanks have a safety advantage over a single walled tank when a crack develops [84]. The addition of water can prevent stress corrosion cracking for certain substances [85].

2.7.3. Legislation

On a vessel there should not be any direct contact between ammonia and the crew. The ammonia will be safely stored inside tanks, ammonia slip needs to be prevented to ensure a safe working environment. An ammonia leakage of 0.1 kg/s could inflict injury to people in a machine room of 180 cubic meters [86]. However, during maintenance of an ammonia engine, manual inspection can be necessary. This could impose a problem due to the ammonia fumes still present in the engine. Therefore, engines and equipment need to be vented before it can be manually inspected. Nowadays there are already some advisory regulations for using ammonia as a fuel on several aspect of vessel design for example: material of tanks, distance of vents and distance between tanks and machine rooms [87] [88].

2.7.4. Impact on sea life

When ammonia is diluted in water the pH value of the water will increase, causing an increase in toxicity [89]. This is harmful for the environment because ammonia is toxic for most fish species and the effect depends on the amount of ammonia that is leaked [90]. Hence, total loss of vessel that sails on ammonia would be disastrous for the aquatic life. If the whole marine industry would use ammonia as a fuel this could cause problems because in 2021 54 ships were lost [91]. Thus, when ships sink that use ammonia as a fuel, the result would be a big disaster.

2.8. Conclusion

currently ammonia is mainly used as a fertilizer. The Haber-Bosch process is used to produce ammonia. Ammonia can be produced carbon free, when it is produced with green electricity. However, currently almost all ammonia is produced by fossil fuels. Due to the poor combustion characteristics of ammonia, a promotor such as MGO or hydrogen is required to ignite the combustion. Additionally, ammonia can directly be used as a fuel in a SOFC. When ammonia is first cracked into hydrogen and nitrogen it can be used as a fuel for a low temperature fuel cell. The Ammoniadrive concept is a combination of a fuel cell and a ICE. Ammonia that is used as fuel for an ICE, will emit N_2O emissions, which is a harm full greenhouse gas. Ammonia is a toxic substance that is lethal at doses between 2500 and 4500 ppm. A accident with an vessel that uses ammonia as a fuel, will results in a natural disaster.

Trailing suction hopper dredger

This chapter will introduce the Vox Amalia as a vessel. Then, the operational modes will be presented. Thereafter, past dredging projects will be examined and the operational profile will be discussed. Finally, the actual fuel consumption reported of the Vox Amalia will be compared with the theoretical fuel consumption. This theoretical fuel consumption is based on the power demand signal data.

3.1. Dredging cycle of a trailing suction hopper dredger

A TSHD will have one or two arms depending on the configuration of the vessel. During dredging these arms are lowered to the seabed and the dragheads that are connected to the arms will suck up the material. Jets in the drag head will fluidize the sand and the teeth will cut in the seabed. The sucked up materials will then be pumped to the hopper, where the materials will be stored. Subsequently, the dredged material will be disposed at a chosen location which can be done in three different ways: dumping, pumping and rainbowing. A TSHD will mostly be used for sand or silt soils [92].

The power generation and energy demand of a trailing suction hopper dredger (TSHD) is not constant due to its operational cycle. Furthermore, the energy consumption during dredging is dependent on the soil conditions, depth, weather and the amount of material in the hopper [93]. The soil conditions are not 100 percent known and are not uniform and this results in a dynamic load during dredging as is shown in Figure 3.1. The finer the soil materials the lower the dynamic loading is during dredging and discharging [93]. During sailing the load on the engines is mainly dependant on the weather and the payload. It is important to investigate the energy profile more in depth to get a better understanding of the varying energy consumption. The typical operation of a trailing suction hopper dredger consist of the following four activities:

- Sailing with empty hopper
- · Dredging
- · Sailing with loaded hopper
- · Disposing of the material

3.2. Drive systems for a trailing suction hopper dredger

A trailing suction hopper dredger has a main power drive to power the propulsion systems and the pumps and a auxiliary power system to power the auxiliary systems such as hotel, jet pumps, lighting etc. From an investment perspective it is preferable to install multiple engines, however from a maintenance perspective it is preferable to have one big engine, because idle engines wear out faster [3].

For integrated drive systems the main engines will power both the ships propeller and power the electric generators. These electric generators generate electricity that will power the pumps and other auxiliary systems. Integrated drive systems need a load control, if during dredging the required power

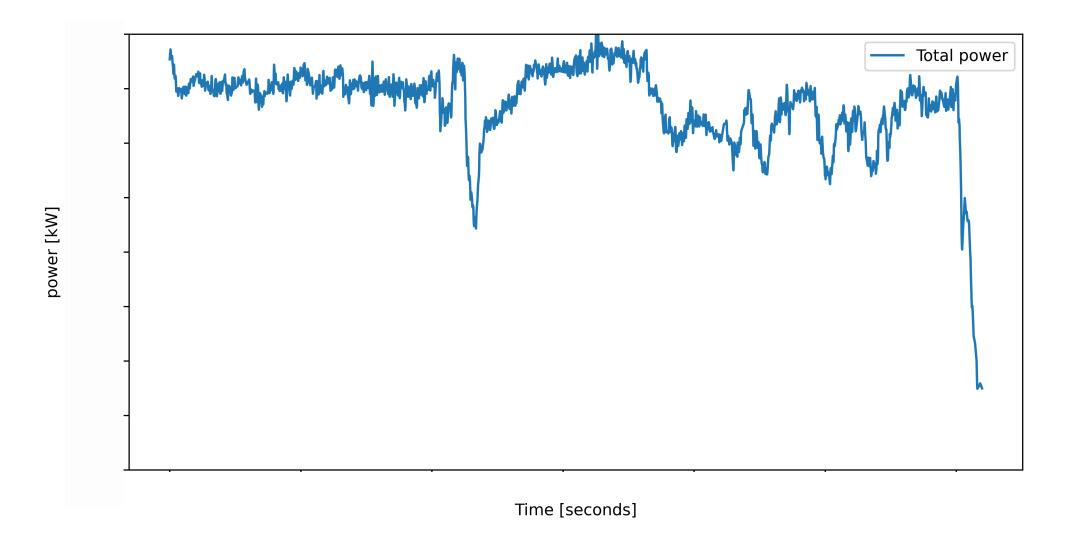


Figure 3.1: The of the Vox Amalia on 21 March 2020 during dredging.

is to high the rpm will drop. Overloading needs to be prevented and when the load is too high then the trailing speed of the hopper will decrease to cope with the load. Therefore, when the total installed power of a dredger is not high enough to cope with the high loading, the production of the hopper will be reduced [3].

3.3. Energy storage systems

In order to cope with dynamic loading of a hopper dredger an energy storage system (EST) can be a solution. Such solution can be used as an extra power source or temporary buffer to meet the required power in certain situations. Furthermore, an EST can improve the overall system efficiency because, an ICE is optimized for a certain load range and less efficient for low loads, where an EST system could handle the load fluctuations and a the diesel engine can keep running at its optimum engine load [94]. There are fast and slow load leveling systems. A battery is a slow load leveling system and for a fast load leveling system capacitors or flywheels can be used. For a cutter suction dredger these fast load leveling systems can handle the dynamic loading [95].

3.3.1. Battery

Although ammonia is 10 times more energy dense than a lithium ion battery a battery can still be a feasible solution [96]. A battery stores energy as chemical energy and can release its energy as electrical energy [97]. Batteries have a much higher gravimetric energy density than electrolytic capacitors. The power supply of batteries is however hundreds to thousands times smaller and therefore limited in comparison with capacitors[98]. The lifetime of a battery is heavily dependant on the temperature ranges that a battery is exposed to and the ideal operating temperatures are between 20 and 25 degrees Celsius [99]. Therefore, in order to preserve the lifetime of a battery the temperature has to be monitored closely. Additionally, batteries have a c-rating that is a scale for how fast batteries can be charged or discharged, a c-rating of 1 means that it takes an hour to charge or discharge a battery and a c rating of 2 means that a battery can be charged or discharged 2 times in an hour [100]. Besides a higher charging speeds does a higher c-rating also mean that there will be more stress on the battery and this can reduce the lifetime of a battery [101]. The depth of discharge (DoD) of a battery, is the percentage of the battery that is being used for discharging. The higher the DoD, the battery is exposed to, the lower the lifetime of the battery will be [102].

The production of lithium batteries has an impact on the environment and the production of 1 Wh of lithium battery storage capacity produces on average 110 grams of CO_2 equivalent [103]. Currently, a 6.8 MWh battery system is installed on a fully electric vessel [104].

3.3.2. Capacitor

As stated before, electrochemical capacitors have a lower energy density than batteries and the power density is at most 20 Wh/kg [105]. In contrast to batteries, electrochemical capacitors have an excellent cycle life, meaning that the capacitor can be loaded and unloaded often and very fast before the capacity of the cell becomes lower than 80 percent [106][107]. Super capacitors are less dependant on temperatures than batteries and will be operating stable in temperature ranges from -20 degrees to 40 degrees Celsius [108]. Some super capacitors can even operate at bigger temperature ranges [109]. Most commercially available supper capacitors are based on activated carbons [110]. The biggest polluter when producing capacitors is activated carbons with a 62.78 kg of ${\it CO}_2$ for every kilogram of activated carbon produced [111].

3.3.3. Flywheel

A flywheel can be used to store energy as kinetic energy where a wheel is rotating with a certain speed. The energy stored in a flywheel is dependant on the mass and rotational speed of the wheel. Flywheels are an existing technology and is used in the cutter suction dredger Spartacus [112].

3.4. Vox Amalia

The Vox Amalia is chosen as a reference for this research. One of the main reasons for this choice is that the Vox Amalia was build recently (2018) and is in operation since 2020. Furthermore, the Vox Amalia is capable to sail on the following fuels: HFO, MGO and biofuels. Some of the newest vessels of Van Oord use LNG as a fuel and for this research a vessel that uses MGO and or HFO is preferred.

This vessel complies with IMO tier III, and there is no SCR installed. Furthermore, the Vox Amalia equipped with two dragheads that can be lowered to the seabed. The Vox Amalia is able to use different discharging methods including: discharging, dumping and rainbowing.

3.4.1. Installed power

The total installed diesel power during normal operations is 23 MW. With three main engines and a auxilliary generator.

3.5. Transient profile 15

3.5. Transient profile

The dredging cycle is a dynamic process where the total engine power is fluctuating over time, so the required engine power is not constant compared with container or bulk carriers. It shows that for the 1st and 99th percentiles, the highest fluctuations occur during the sailing empty operation. However, for the other percentiles, the dredging and discharging operations show the highest power fluctuations over time. A visualization of this cumulative distribution can be seen in Figure 3.2.

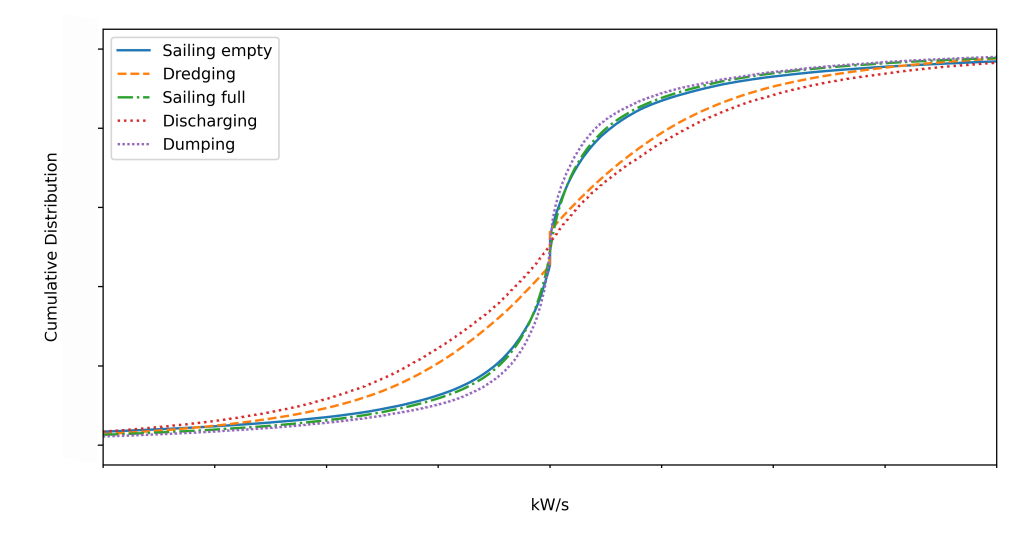


Figure 3.2: The cumulative distribution of the power change for each operation during the coastline project

This delta power is calculated for every second during the projects. During these calculations the first and last second of each cycle is the compared with the last and first second from the previous and next cycle. Therefore, two values in the analysed dataset should be excluded for each cycle. This is an error of 0.4% and is thereforeeemed negligible.

3.6. Transient load during dredging

To get a better understanding of the origins of the transient loading during dredging, the power signals on the Vox Amalia are investigated. A single dredging operation from 21 March 2020 (during the Kustlijnzorg project) is examined. The total power demand during this dredging operation is shown in Figure 3.1. It is evident that the power fluctuates heavily over time, with small changes occurring every second. At approximately 1,200 seconds, there is a significant change in power demand. Furthermore, between 2,000 and 2,500 seconds, there are also more substantial peaks in the total power demand.

The power demand of these three main engines is illustrated in Figure 3.3. Each of the signals varies over time, as the lines are not constant. The power of the main engines ps and sb almost completely overlap, while the power of the dredge engine remains more constant. The peaks at 1,200 and between 2,000 and 2,500 seconds from the total power demand in Figure 3.1 are smaller but also visible for the power of the main engines on port side and starboard in Figure 3.3.

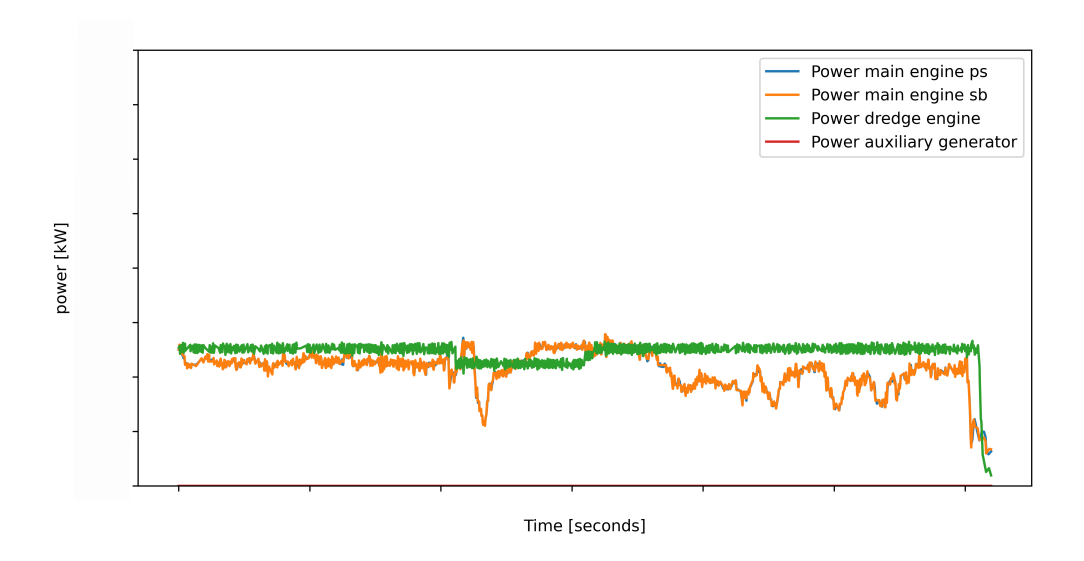


Figure 3.4: The power demand of the three main engines and the auxiliary generator of the Vox Amalia during dredging on 21 March 2020.

The power of the main engine starboard and port side is divided into generator power and propulsion power. The losses for the generator and the propulsion are approximately 95% and 98%, respectively, in reality. However, for this investigation, these losses are neglected. Figure 3.5 visualizes the total power for the propulsion and the total electrical power available on the boardnet. It is clear that there is again a drop in power at 1,200 seconds. Furthermore, the same peaks in power between 2,000 and 2,500 seconds are present in Figure 3.5 as in the total power demand in Figure 3.1.

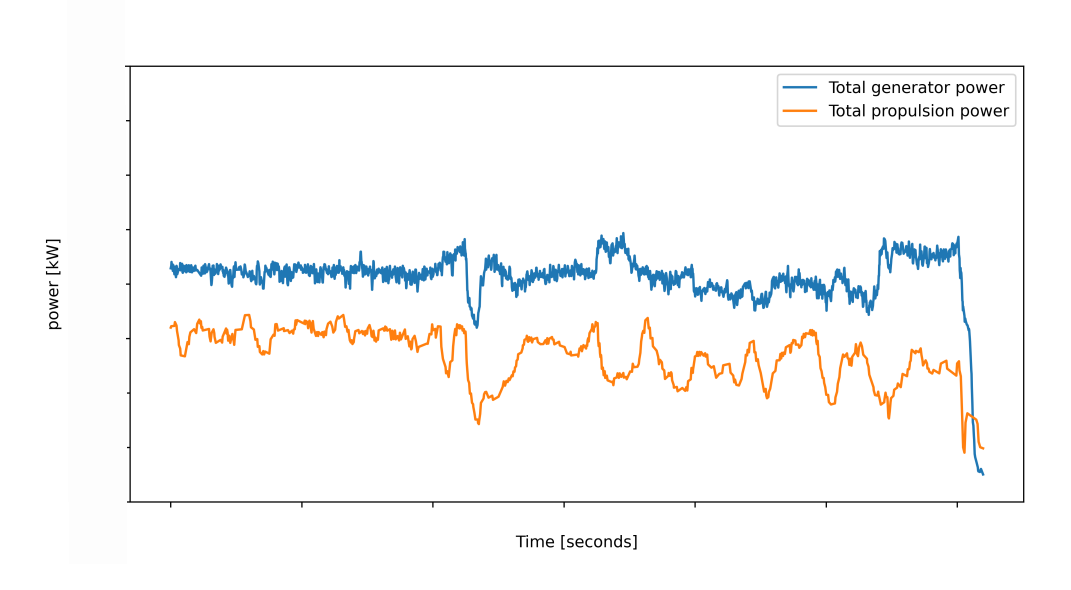


Figure 3.5: The generator and propulsion power of the Vox Amalia during dredging on 21 March 2020.

The propulsion power is a function of vessel speed and drag force. Figure 3.6 shows that the vessel speed varies between 0.5 and 4.0 m/s during dredging. Until 1,100 seconds, the vessel speed is fairly constant. After 1,100 seconds, the vessel speed fluctuates. At 1,200 seconds, there is a sudden spike in vessel speed followed by a sudden decrease in vessel speed.

The Vox Amalia experiences a drag force in the water due to the hull, suction tubes, and the draghead in the water. Additionally, there is a drag force between the draghead and the soil. This drag force varies with the amount of contact with the soil and the soil properties. During dredging, the visor

angle changes, and therefore the amount of soil cut by the teeth of the draghead. This amount of soil cut by the teeth is among other things dependent on the failure mechanism of the soil.

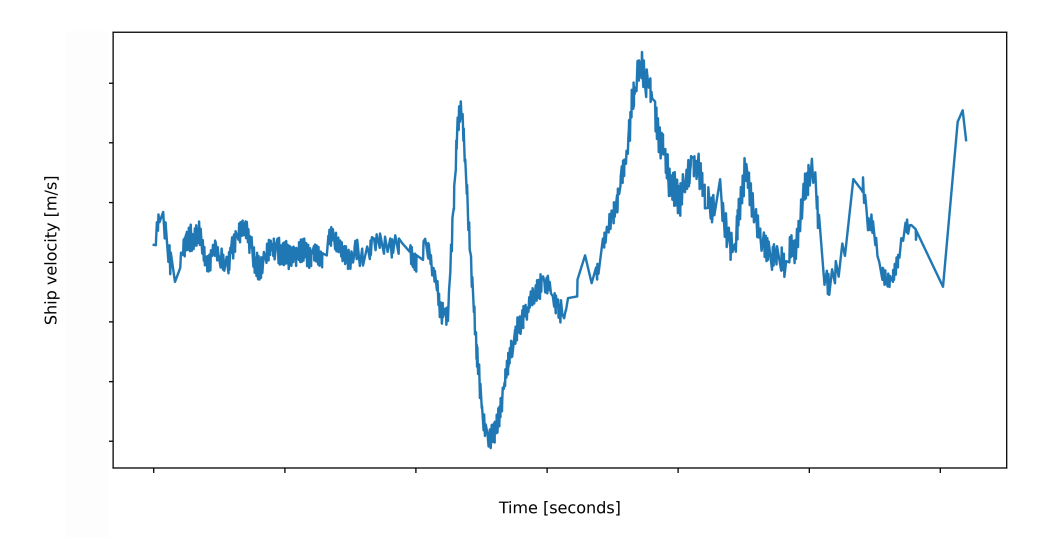


Figure 3.6: The ship velocity of the Vox Amalia during dredging on 21 March 2020.

The power of the jet pumps of the Vox Amalia remains fairly constant during dredging. Figure 3.7 visualizes the power of the underwater dredge pump on the starboard side of the Vox Amalia. The Vox Amalia is equipped with two underwater dredge pumps, one on the port side and one on the starboard side. At 1,200 seconds, there is a sudden drop in power. After 2,000 seconds, the power of the dredge pump fluctuates more than before.

The power of the dredge pump is a function of pressure and mass flow rate. This pressure is influenced by factors such as mixture density, inlet speed, outlet speed, depth of the dredge pump, and the vertical distance to the hopper and the ground [3].

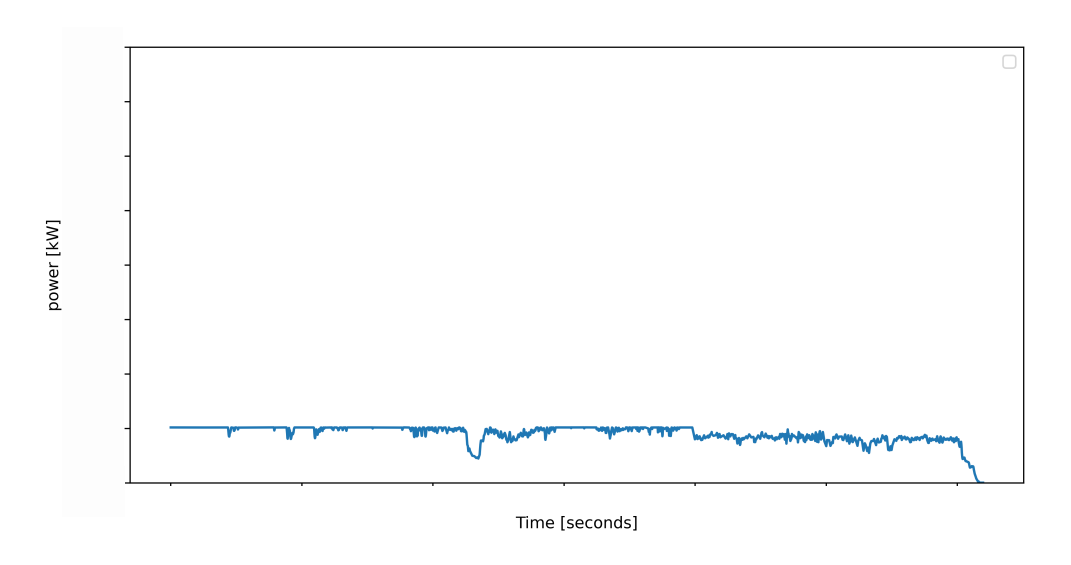


Figure 3.7: The power of the dredgepump on port side of the Vox Amalia during dredging on 21 March 2020

3.7. Production estimation 19

Figure 3.8 visualizes the density in the dredging tube during dredging. This density fluctuates more over time than the power of the underwater dredge pump. At 1,200 seconds, the density of the dredge pump is almost the same as the density of water, indicating that there is (almost) no sand in the dredging pipe. This explains the drop in underwater pump power at 1,200 seconds.

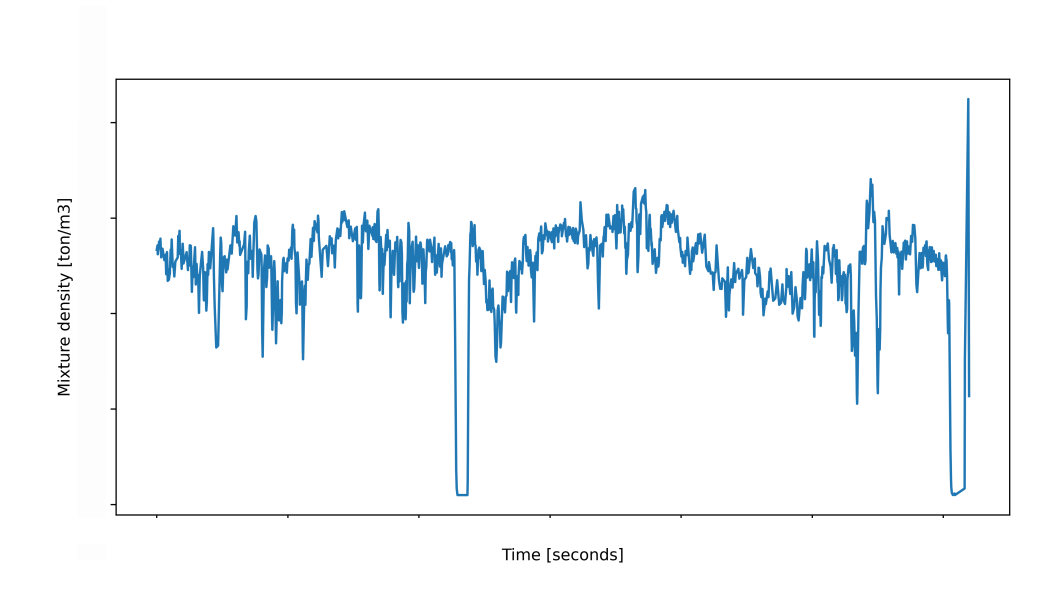


Figure 3.8: The mixture density in the dredging tube on port side of the Vox Amalia on 21 March 2020

Most of the transient behaviors originate from the propulsion of a dredging vessel. The dynamic propulsion power is the result of the change in friction that the draghead exhibits with the soil. Furthermore, the power of the dredge pumps is dependent on a lot of parameters. A change in mixture density will result in a change of underwater pump power. Finally, all the small power fluctuations of the other consumers on board will also have a small impact on the total transient power demand of a TSHD.

3.7. Production estimation

The loading process of a TSHD is not linear over time. The addition of extra weight due to equipment will result in a lower hopper capacity due to weight limitations. This influence will be discussed in this Section. The extra volume that is required due to the addition of extra weight of fuel is not taken in to account in this research.

3.8. Hopper sedimentation

In reality, the loading rate of a hopper is not a constant over time. At the beginning, when filling a hopper, all the material will settle in the hopper. After a certain point in time, the hopper will be filled up to overflow position with a mixture of sand and water. Then, this mixture in the hopper will partially flow overboard as long as more mixture is pumped into the hopper. This process is known as overflow. During overflow, some of the particles in the mixture will settle in the hopper, while the remaining (smaller) particles will flow overboard.

The settling velocity (w_s) of a sand particle determines whether the particle will flow overboard or settle in the hopper. This settling velocity represents the terminal velocity of the particle. If the settling velocity of the particle is lower than the required settling velocity for it to settle in the hopper, then the particle will flow overboard in the mixture [113]. Conversely, if settling velocity of the particle is higher than the required settling velocity to settle in the hopper, then the particle will settle in the hopper. The specific density of a mixture can be calculated using Formula 3.1 [113].

$$\Delta = \frac{\rho_s - \rho_w}{\rho_w} \tag{3.1}$$

Where

 Δ = Specific density (dimensionless)

 ρ_s = Density of mixture in kg/m^3

 ρ_s = Density of water in kg/m^3

The settling velocity of a single particle can be calculated with Formula 3.2 [114]. This formula holds for all three regimes, laminar, transient and turbulent.

$$w_0 = \frac{\Delta g d^2}{C_1 \nu + \sqrt{0.75 C_2 \Delta g d^3}}$$
 (3.2)

Where:

 w_o = Settling velocity in m/s

g = Gravitational acceleration in m/s^2

d = Particle diameter in m

 ν = Viscosity in $kgm^{-1}s^{-1}$

 \mathcal{C}_1 Dimensionless coefficient is equal to 18 for natural sands

 \mathcal{C}_2 Dimensionless coefficient is equal to 1 for natural sand

The concentration has an influence on the settling velocity, as it determines the number of particles present in a certain volume. This relationship can be calculated using Formula 3.3 [113]. It is assumed in this formula that all sand particles are of the same size. An increase in concentration will result in a decrease in the settling velocity of the mixture.

$$w_s = w_0 (1 - c)^n (3.3)$$

Where:

- w_s = Settling velocity of the mixture in m/s
- *c* = Volume concentration (dimensionless)
- *n* = Richardson-Zaki exponent (dimensionless)

The volume concentration can be calculated with Equation 3.4

$$c = V_s / V_m \tag{3.4}$$

Where:

- V = Volume of solid in the mixture in m^3
- V = Volume of the mixture in m^3

This Richardson-Zaki exponent is dependant on the grain size of the particles and this varies from 2.4 for coarse materials up to 4.65 for fine materials [113]. This Richardson-Zaki exponent can be calculated with formula 3.5 [113].

$$n = \frac{4.7 + 0.41Re_p^{0.75}}{1 + 0.175Re_p^{0.75}}$$
(3.5)

Where

• Re_p = Particle Reynolds number (dimensionless)

Finally the particle Reynolds number can be calculated with Formula 3.6 [113].

$$Re_p = \frac{w_0 d}{v} \tag{3.6}$$

3.8.1. Cycle time

During the 30 days of the Kustlijnzorg project, the Vox Amalia completed 200 dredging cycles, sailing empty, dredging, sailing full, and discharging dredged material 200 times during the simulation. The average hopper load for each cycle was 30,000 tonnes of material, with an average hopper density of $2.00\ kg/m^3$. It should be noted that the maximum overflow hopper capacity is $20,000\ m^3$. Considering a sand density of $1.95\ kg/m^3$, this results in a hopper load of 60,000 tons. Thus, during the Kustlijnzorg project, the hopper was not loaded to its maximum capacity. This is because there were limitations on the draft of the vessel for the Kustlijnzorg project. The draft of a vessel is related to its weight, and a fully loaded hopper would result in a higher draft compared to a hopper loaded to fifty percent.

During the 30 days, the time spent on each operation is different. It should be noted that during 13% of the time, it was unknown what the Vox Amalia was doing. It is assumed that during each operation, the unknown time was relative to the time spent on the specific operation. Thus, during each operation, 13% of the time was allocated to the unknown category. This correction allows for the calculation of average cycle times for each operation.

Additionally, it is worth noting that the average rainbowing time is only 500 seconds, which is too short to unload a whole hopper using the rainbowing method. This discrepancy arises because out of the 200 cycles, the hopper was unloaded using rainbowing only fourteen times, while dumping was used for the other 187 times. The actual rainbowing duration during the kustlijnzorg project for the Vox Amalia was 6,000 seconds.

3.8.2. Weight influence

It is assumed that during the Kustlijnzorg project, all sand particles have the same grain size. Additionally, the influence of the volume concentration in the hopper is considered negligible for the settling velocity. As a result, the filling and discharging of the hopper can be assumed to occur linearly over time.

It takes 7,500 seconds to fill the hopper with 30,000 tons of material. This indicates a filling speed of 5 ton/s per second. Furthermore, the total unloading time (rainbowing + dumping) is 2,000 seconds, resulting in an average unloading speed of 20 ton/s. If the hopper has an available capacity of 20,000 tons, the loading time will be approximately 5,500 seconds, and the unloading time will be 991 seconds. This will result in a cycle time of 17,000 seconds, allowing for 200 cycles within 30 days. Over the course of thirty days, a weight increase of 30 % will reduce the amount of dredged material by approximately 14%. Figure 3.9 illustrates the cycle time for a hopper at the original load capacity of 30,000 tons and the modified load capacity of 20,000 tons.

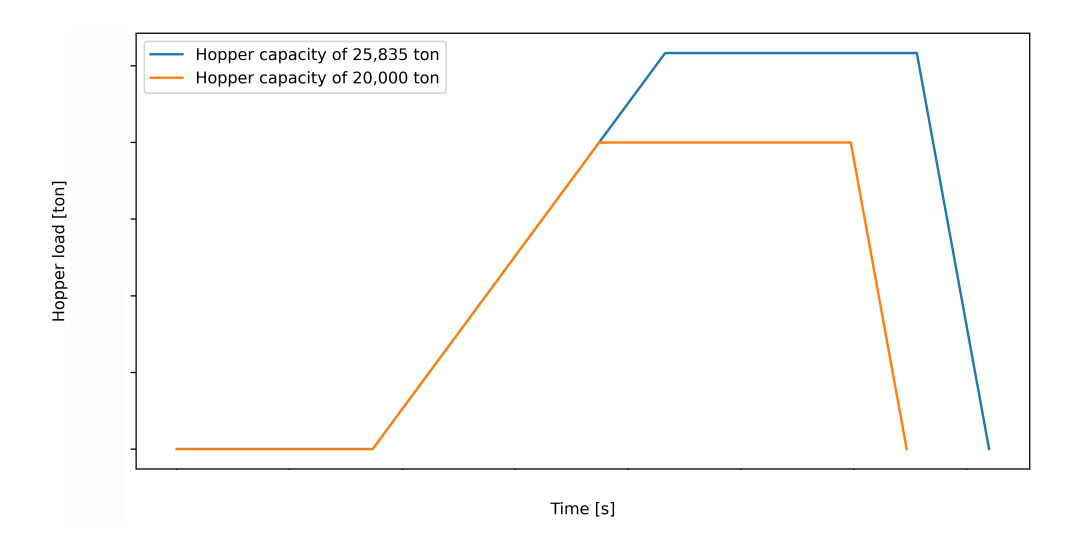


Figure 3.9: The cycle time for a TSHD depending on the amount of dredged material.

The extra weight that is taken into account during this research are:

- · Average fuel weight
- ICE weight
- · SOFC weight
- · Battery weight

The extra weight due to the tanks is not included in this research. For the fuel weight, the average fuel weight over the 30 days is considered. In reality, at the beginning of the 30 days, the fuel weight is higher than at the end, resulting in a lower trip capacity at the beginning of the period and a higher trip capacity at the end of the month. However, this difference is not taken into account for this research.

Furthermore, the main engine weight of the Vox Amalia is 150 tons, and with a power output of 10,000 kW, this results in a specific engine weight of 15 kg/kW. It is assumed that the engines for all configurations have the same specific weight. The specific weights of other technologies are shown in Table 3.1.

Table 3.1: The assumed specific weight for the: ICE, SOFC and the batteries [115]–[117]

Equipment	Weight
ICE	15 [kg/kW]
SOFC	48 [kg/kW]
Battery 0.4C	6 [kg/kWh]
Battery 0.7C	9 [kg/kWh]
Battery 2C	13 [kg/kWh]

3.9. Fuel Consumption

Specific fuel consumption (SFC) is the amount of fuel (grams) that is necessary to generate a certain amount of energy with an engine (kWh). Mechanical efficiency, combustion efficiency, and relative pump losses all contribute to changes in sfc at different engine loads. Table 3.2 shows SFC for all four engines installed on the Vox Amalia. The Table includes data for eight different engine loads, ranging from 1 % to 110 %. It should be noted that operating an engine at 110 % load can lead to overloading, although it is accepted for certain duration's. Missing data points are observed for three engines at 1 % and 10 % load, and for two engines at 85 % and 110 % load. Notably, at 1 % load, sfc is significantly higher compared to other engine loads, which is logical, because an ICE is not designed to operate at 1% load.

Table 3.2: Specific fuel consumption with MGO according to the engine test bench tests for all 4 engines on the Vox Amalia.

Engine load (%)	1	10	25	50	75	85	100	110
SFC main engine PS [% gr/kWh]	-	-	112	100	100	96	100	104
SFC main engine SB [% gr/kWh]	-	-	112	100	100	96	100	104
SFC dredge engine [% gr/kWh]	733	145	123	101	99	95	100	103
SFC auxiliary generator [% gr/kWh]	-	-	118	100	97	-	100	-

In this section the fuel consumption is estimated from week 50 in 2022 till week 22 in 2023. During these weeks the Vox Amalia is dredging on the Fehmarnbelt project and not the Kustlijnzorg project. The main reason to use another project for the fuel consumption is that during the Kustlijnzorg both HFO and MGO is used. While during the Fehmarnbelt project only MGO is used. Only the total fuel consumption of each fuel at the end of the week is noted and therefore it is more difficult to estimate the fuel consumption when multiple fuels are used.

3.9.1. Fuel Estimation

At the end of every week, the fuel consumption of the Vox Amalia is recorded and stored into a database. This database included the amount of fuel consumed, determined by the crew per week and as well as the type of fuel used. By utilizing the SFC data, it is possible to make an accurate estimation of the fuel consumption of the Vox Amalia. To achieve this, the SFC data needs to be extrapolated to cover and in between all eight engine loads that are shown in Table 3.2. The missing data in Table 3.2 was extrapolated using the closest available engine load data. The results of this extrapolation process are presented in Table 3.3. With the extrapolation of the SFC values, a more accurate estimation of the fuel consumption of the Vox Amalia can be achieved.

Table 3.3: Specific fuel consumption with MG0	extrapolated according to the engine manuation	If for all 4 engines on the Vox Amalia.
---	--	---

Engine load [%]	1	10	25	50	75	85	100	110
SFC main engine PS [% gr/kWh]	507	277.3	112	100	100	96	100	104
SFC main engine SB [% gr/kWh]	507	277.3	112	100	100	96	100	104
SFC dredge engine [% gr/kWh]	733	145	123	101	99	95	100	103
SFC auxiliary generator [% gr/kWh]	730	144	118	100	97	93	100	103

First an linear interpolation between the SFC for the main engine PS data points from Table 3.3 was done and is shown in Figure 3.10. Combustion of fuel is not a linear process, mainly due to the combustion efficiency and to a minor extent the other efficiency variations over engine load. Therefore, linear interpolation is not a good fit.

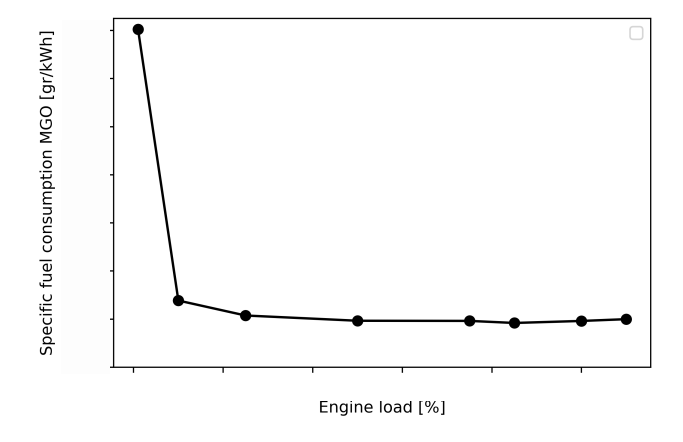


Figure 3.10: SFC data points main engine PS of the Vox Amalia interpolated linearly.

Figure 3.11 illustrates a second-order interpolation using the SFC data points for the main engine PS obtained from Table 3.2. This interpolation method does not provide a accurate estimation for this data set. Notably, at the minimum of the curve, the interpolated values are significantly lower than the original data points by a factor of more than two. Furthermore, the maximum sfc value at an engine load of 1 % is underestimated. Therefore, this second-order interpolation curve fails provide a fit in the line with the data points.

To achieve a more accurate interpolation between the datapoints, the piecewise cubic hermite interpolating polynomial (pchip) is used. The pchip method ensures that the curve passes through all data points. Figure 3.12 displays the pchip interpolated curve obtained using the pchip interpolation method. This method is suitable for accurately estimating the sfc values at various engine loads.

A total of 25 weeks, spanning from week 50 in 2022 to week 22 in 2023, were investigated to estimate weekly the fuel consumption of the Vox Amalia. The fuel consumption for each week was estimated using the sfc curves, and the results are presented in Figure 3.13. It is clear that the fuel consumption estimates exhibit both underestimations and overestimation's when compared to the actual data.

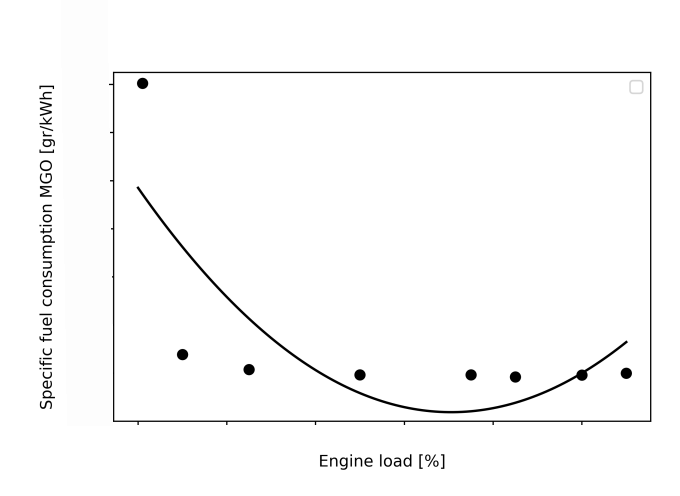


Figure 3.11: SFC data points main engine PS of the Vox Amalia interpolated with a second order.

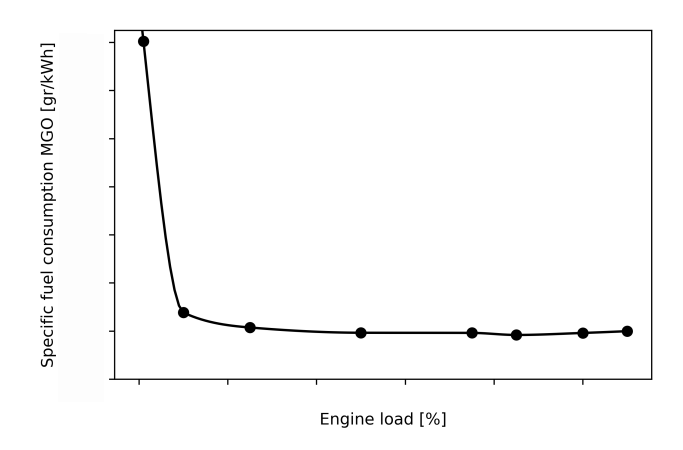


Figure 3.12: SFC data points main engine PS of the Vox Amalia interpolated with a piecewise cubic hermite interpolating polynomial.

To gain further insight in the variations between estimated fuel consumption and recorded fuel consumption by the crew, the average engine load for each week was investigated. It became clear that during the period from week 2023-8 till 2023-11, the Vox Amalia remained idle in the harbor. During this research only the weeks where the Vox Amalia was dredging were considered for this research. After filtering out those four weeks, a total of 21 weeks in operation remained. This means that the actual data is 5% higher than the estimation. It is therefore evident that there is a discrepancy between the estimated fuel consumption and the actual fuel consumption and this will be further explained in Section 3.9.2.

3.9.2. Fuel actual errors

In the analysis of the fuel consumption for the Vox Amalia, it is important that the potential errors are investigated. It is important to note that the fuel consumption on the Vox Amalia is measured with an automated tank sounding system. At the end of every week the fuel consumption will be automatically registered with flow sensors. The flow of fuel in and out of the engine is measured. On weekly basis on, manual sounding is done on all vessels to check what is in the bunkers compared to any available measurement system. Either based on automatic tank sounding or based on flow sensors. For this research it is assumed that the fuel consumption is manually measured with manual sounding. There are both errors on the actual data and on the estimation of the fuel consumption. The following errors can occur with the actual data:

· Time interval error

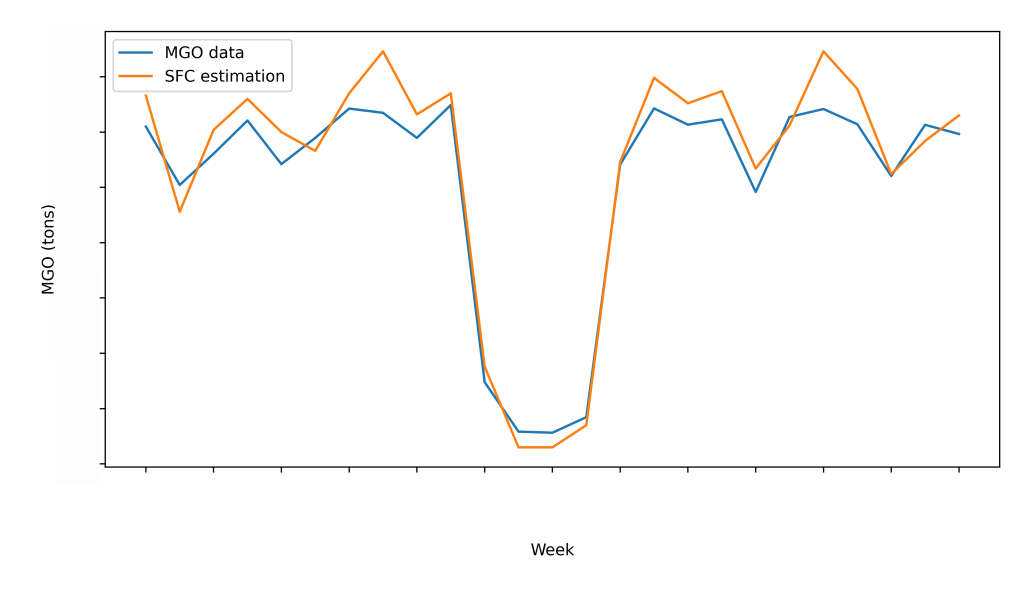


Figure 3.13: The fuel consumption estimated with SFC and compared with the actual fuel consumption of the Vox Amalia.

· Manual sounding error

Table 3.4: Actual fuel consumption with errors Vox Amalia.

Week	2022-50	2022-51	2022-52	2023-1	2023-2	2023-3
ACT. Data Fuel consumption MGO [%]	100	100	100	100	100	100
ACT 1.1 Time interval error lower [%]	94	94	94	94	94	94
ACT 1.2 Time interval error higher [%]	112	112	112	112	112	112
ACT 2.1 Manual sounding error lower [%]	96	96	96	96	96	96
ACT 2.2 Manual sounding error lower [%]	104	104	104	104	104	104

The first source of error in the actual fuel consumption is the time interval error. The data for fuel consumption is recorded at the end of each week, but in reality the timing of these recording can vary. It is reasonable to assume that the maximum delay in recording the data is 5 hours or that the data may be recorded up to 5 hours earlier than the supposed time. This introduces a potential deviation in the total time considered for fuel consumption over a week. Instead of the standard 168 hours in a week, the total time may range from 158 to 178 hours. This results in a maximum difference of 6% in total time for fuel consumption. The upper and lower bounds of the resulting fuel consumption, considering this time interval error, are presented in Table 3.4. It is important to note that in the subsequent analysis, the data is grouped into a consecutive 21-week period, which helps reduce the impact of this time interval error. Over a span of 21 weeks, where a total of 3528 hours are considered, a difference of 10 hours corresponds to a negligible 0 % deviation.

The second source of error is related to the manual sounding process. Measuring the amount of MGO in each tank is done using a sounding tape, which lowered into the tank to determine the fuel level. This measurement is corrected for any trim or is tried to measure at almost even keel during transit. The crew experiences challenges in reading the sounding tape as result of the transparency of MGO. According to the Vox Amalia crew, the measurement error can be typically in the order of centimeters. Assuming a measurement error of 1 cm in each tank, the cumulative error in fuel measurement amounts to 4 m^3 of MGO, based on the dimensions of the tanks. Additionally, a reasonable measurement error of 5 centimeters can result in a total error of 20 cubic meters of MGO.

3.9.3. Fuel estimation errors

On the estimation side the following three errors are investigated and shown in Table 3.5:

- ISO 3046 tolerance
- · NaN data error
- Lower fuel quality

The first error relates to the tolerance specified in ISO 3046, which allows for a 5% deviation in engine efficiency from the stated efficiency in product guises [118]. Considering this tolerance, the estimated fuel consumption could be up to 5% higher each week. However, this tolerance alone does not explain the variations in underestimation and overestimation observed across different weeks. It could, however, explain the overall 5% deviation observed over the 21-week period, as discussed in Section 3.9.1.

The second error on the estimation side is that there is NaN data present. NaN data indicates unknown values and require interpolation. Interpolation is done between the last known data point and the first subsequent known data point. Thus, everything in between is not known. If the slope of the total power (the power off all 4 engines added together) remains constant for 60 seconds, it is determined that interpolation occurred, indicating unknown data. Approximately 17 hours of unknown data were identified during the 21 weeks. This is means that less than 0.1 % of the data was unknown. This difference in NaN data is multiplied with the original SFC consumption and shown in Table 3.5.

The final error investigated concerns the difference in fuel quality during operation compared to the fuel quality used during engine testing. The sfc curves are valid for MGO having an energy content of 42.7 MJ/kg. However, lab test during the 21-week period indicated that the lowest measured energy content was 1% lower. The lower fuel quality used during operation results in higher fuel consumption, as more fuel is required to generate the same amount of energy. This difference in fuel quality amounts to 1%, leading to a 1% increase in fuel consumption compared to the estimated values.

Table 3.5: Estimated fuel consumption with error Vox Amalia

Week	2022-50	2022-51	2022-52	2023-1	2023-2	2023-3
EST. SFC consumption MGO [%]	100	100	100	100	100	100
EST. 1 ISO 3046 positive 5 percent tolerance [%]	105	105	105	105	105	105
EST 2.1 NaN data lower [%]	100	100	100	100	100	100
EST 2.2 NaN data higher [%]	100	100	100	100	100	100
EST 3. Lower fuel quality [%]	101	101	101	101	101	101

3.10. Conclusion

The Vox Amalia is equipped with four engines that provide power the power, with the highest power demand occurring during dredging and discharging operations. The kustlijnzorg project had the highest average and maximum power demand with respect to the other projects. The transient loading during dredging is mainly due to the change in propulsion power. This propulsion is dependant on the friction force of the draghead with the soil. Additionally, a sudden change in mixture density in the dredge tube, can also lead to a sudden transient load.

During the kustlijnzorg project, the Vox Amalia was not loaded to its maximum capacity. The settling of sand in a hopper is not a linear process in reality. However, for the purpose of this research, this process is assumed to be linear. With this assumption, the new cycle time can be calculated, and the resulting increase or decrease in dredged material per week can be determined. A weight increase of about 30 % will result in a 14% decrease in dredged material over thirty days. The weight of equipment is dependent on the amount of installed power, use of SOFC, and the type of battery used.

To estimate fuel consumption, the specific fuel consumption at different engine loads is used with pchip interpolation. The difference between the estimated and actual fuel consumption is primarily influenced by two factors. First, the time interval error introduces discrepancies in the fuel consumption data. The second factor contributing to the difference in fuel consumption is the 5% deviation observed over the 21-week period, which can be attributed to the 5% tolerance specified by ISO 3046.

Configurations

This chapter shows five different new configurations, covering aspects such as layout, drive train efficiencies, power train efficiency, power generation efficiencies and other necessary assumption for the simulation. The configuration discussed in this chapter are:

- Conventional
- 1 MGO ICE including battery
- 2 DF MGO/ammonia ICE
- · 3 DF MGO/ammonia ICE including battery
- · 4 Ammonia SOFC including battery
- · 5 Ammoniadrive including battery

4.1. Conventional

As mentioned in Section 3.4, the Vox Amalia was initially designed for HFO and MGO operation. However, it is currently operating with MGO as fuel. The layout diagram includes the tank, engine, and grid, which represent the main components.

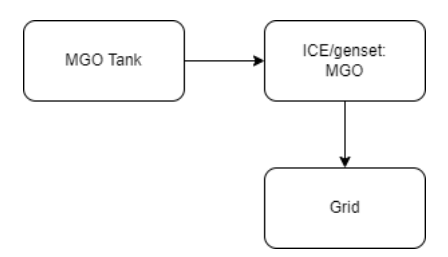


Figure 4.1: The conventional configuration on MGO excluding a battery.

As mentioned in Section 2.3.3, a vessel currently has to comply with the IMO tier III regulations. For this research the time frame was set at 2030 and therefore the MGO conventional configuration should also include a SCR.

4.2. 1 MGO ICE + battery

The first new configuration, as depicted in Figure 4.2, is an MGO ICE/genset in combination with a battery. A SCR is also included in this configuration to comply with IMO tier III. In this setup, the battery is charged during periods when the generated energy exceeds the energy demand of the grid. The battery is discharged during power shortages on the grid. The goal of integrating a ICE/genset with a battery is to enable the engine to operate at its optimal efficiency, while the battery can handle

28 4. Configurations

variation in power demand. Operating the engine at its peak efficiency point could result in a reduced fuel consumption and emissions. The optimal engine load, as indicated in Table 3.3, is set at 85% for all configurations that are equipped with batteries.

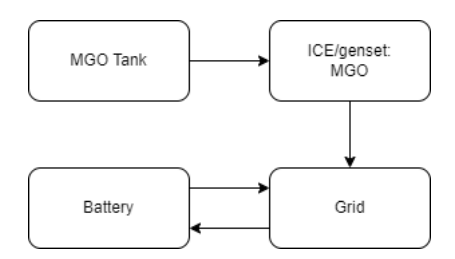


Figure 4.2: The configuration where a MGO genset is used in combination with a battery.

The discharge and charge power output of a battery is determined by its C-rate. The C-rate indicates the number of times a battery can be fully discharged or charged within an hour. A C-rate of 1 means that a battery can be fully charged or discharged once within an hour. Also, a C-rate of 2 means that a battery can be charged or discharged 2 times within an hour. It is worth noting that some batteries have a higher C-rate for short duration's (e.g. less than 30 minutes). However, for this research a continuous C-rate is used. The following C-ratings are used for this research:

- 0.4
- 0.7
- 2

These specific C-ratings are chosen, because there are marine batteries available with these specific C-ratings.

Not all energy that flows to the battery will be stored. The charge efficiency reflects the ratio of the amount of energy that flows into the battery and the amount of energy that will be stored in the battery. While the discharge efficiency indicates the ratio between the energy flowing out of the battery and the usable energy. These efficiencies vary on C-rate. For a lithium-ion battery with a C-rate of 2 the charge and discharge efficiency are around 97 percent, and batteries with a lower C-rate will have higher efficiencies [119]. In this research, a charge and discharge efficiency of 97% is assumed for all configurations with batteries. Furthermore, is the depth of discharge set at 0.5 To mitigate stress on the lifetime of the batteries.

4.3. 2 dual-fuel ammonia MGO ICE

The second configuration is a duel fuel ICE/genset with ammonia and MGO and can be seen in Figure 4.3. As mentioned in Section 2.3.3 a dual-fuel diesel/ammonia engine does not meet the IMO tier II regulations and therefore for this configuration a SCR is included.

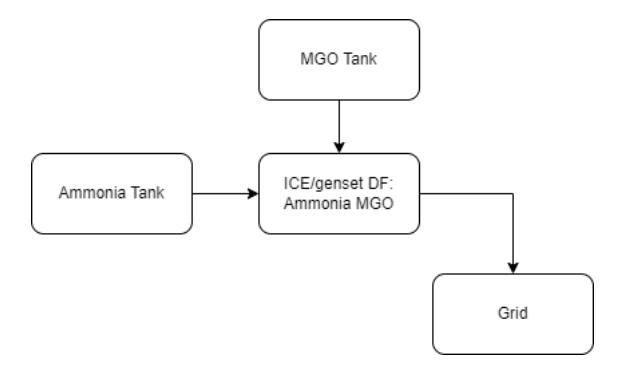


Figure 4.3: The configuration where a dual-fuel Ammonia/MGO genset is used without a battery.

The ideal operating point of an dual-fuel ammonia/diesel engine is at an energy ratio of about 40-60% as is mentioned in Section 2.3. Due to the poor combustibility of ammonia, MGO needs to be

present at low engine loads. Therefore, it is chosen that the amount of MGO in the engine is constant and ammonia will be used at engine loads above 40 percent. Figure 4.4 visualises the energy ratio between ammonia and MGO.

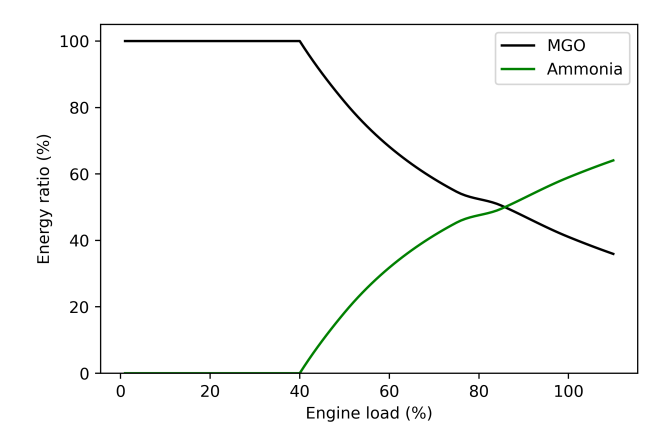


Figure 4.4: The energy ratio for the dual-fuel Ammonia/MGO genset.

Currently, there are no commercially available of the shelf dual-fuel ammonia/MGO engines. This limits the availability of data for reconstructing their SFC curves. However, it is assumed that the SFC curve of a dual-fuel ammonia/MGO engine will follow a similar trend to that of a conventional combustion engine. MGO engines have been studied and optimized for a long time already, while ammonia diesel dual-fuel engines are a relatively new technology and have not yet been fully optimized. The dual-fuel ammonia/MGO engine in this research is assumed to be 5% less efficient than a MGO engine. Therefore a correction factor of 0.95 will be applied on the original efficiency of the SFC to account for the performance difference.

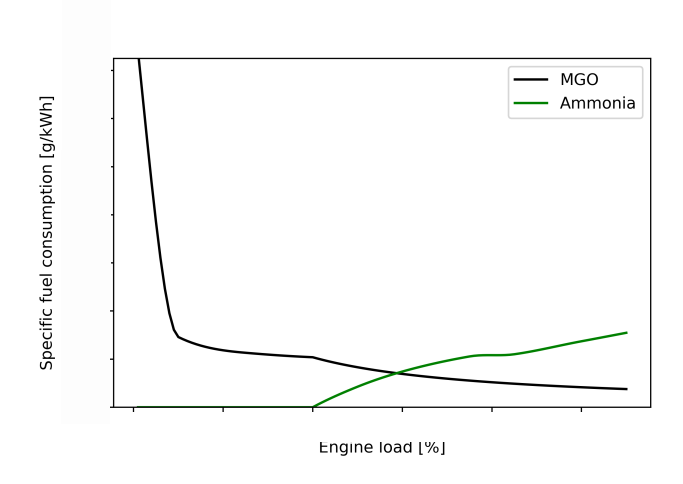


Figure 4.5: The specific fuel consumption for a dual-fuel MGO/ammonia engine.

Figure 4.5 visualizes the specific fuel consumption in g/kWh. The change in power is defined as dP/dt [kW/s]. MCR/s is the maximum change in engine load per second [%] an engine can handle in a safe manner. It is expressed as an percentage of the total engine capacity. For a dual-fuel LNG engine, the maximum change in engine load varies depending on the current engine load. For engine loads up to 75%, the maximum change in engine load per second is approximately 4% for a LNG/MGO dual-fuel engine [120]. As, the engine load further increases, then the maximum change of engine loads per second decreases to around 1.5%. Considering the higher flammability of LNG compared to ammonia, it is expected that an ammonia-based engine would have a maximum change of engine load. Therefore, the maximum change of engine load for an ammonia engine is assumed to be 2% per

30 4. Configurations

second. Consequently, if the load change exceeds 2% within a second, MGO will be used as the fuel to handle the transient load. The dP/dt is then to high to use ammonia as a fuel. For an engine with a installed power of 20,000 kW, a maximum change in engine loaf 2% per second results in a maximum dP/dt of 400 kW/s.

4.4. 3 Dual-fuel ammonia MGO ICE + battery

Figure 4.6 visualizes the dual-fuel ammonia MGO configuration including a battery. This configuration is similar to the configuration in Section 4.3, but with the addition of a battery for load levelling. Therefore, the same assumptions as in Section 4.3 regarding the engine efficiency and MCR/s apply to this configuration as well.

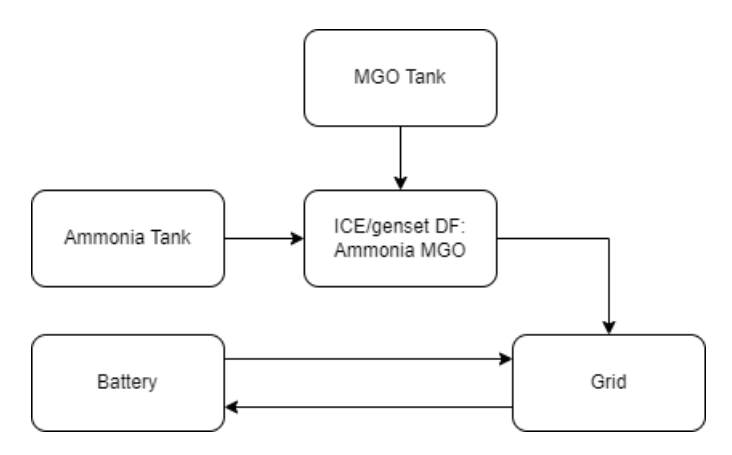


Figure 4.6: The configuration where a dual-fuel Ammonia/MGO genset is used with a battery.

4.5. 4 Ammonia SOFC + battery

The ammonia SOFC including battery configuration depicted in Figure 4.7. The SOFC in this configuration will operate at a constant load due to its inability to handle transient loads effectively. The maximum change in power this configuration is thus set at 0 kW/s (dP/dt = 0 kW/s). Therefore, a battery is required to cope with the transient loading. When the battery is fully charged and an energy surplus occurs, then the excess energy will be destroyed.

The loading point for the SOFC stack is set at 80% load. In this setup, the SOFC efficiency is set at 52% for electricity generation, which was mentioned in Section 2.4.3. Currently, the system degradation for a SOFC stack is 1% as was mentioned in Section 2.4.3. However, it is expected that by 2030 the system degradation is reduced. Therefore, the system degradation for the SOFC is set at 0.5% for every 1000 hours of operation. This means that approximately every 7 years the SOFC system has to be replaced by a new system considering a stack load of 80% and 38 operational weeks a year.

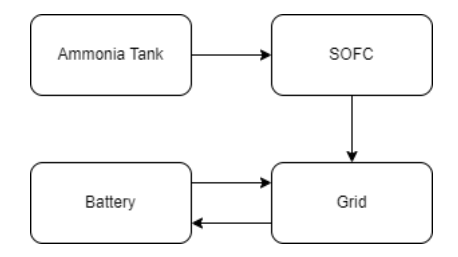


Figure 4.7: The configuration where a SOFC powered with ammonia is used with a battery.

4.6. 5 Ammoniadrive + battery

Figure 4.8 visualizes the configuration with a dual-fuel ammonia hydrogen engine in combination with a battery and a SOFC. The solid oxide fuel cell (SOFC) will convert ammonia into hydrogen. Then, a

part of this hydrogen will be used for the generation of energy, while the remaining hydrogen is directed to an intermediate hydrogen storage and thereafter supplied to the engine. The assumptions regarding the SOFC efficiency and degradation are the same as those mentioned in Section 4.6.

Furthermore, the conversion efficiency of ammonia into hydrogen is assumed to be 97%. This means that 97 percent of the ammonia is converted into hydrogen, while 3% of the ammonia remains unconverted. According to Equation 2.6 2 molecules of ammonia are required to create 3 molecules of hydrogen. The molar weight of hydrogen is approximately 1 gram/mol and the molar weight of ammonia is approximately 17 gram/mol. This means that with a conversion efficiency of 97%, 11.6 gram of ammonia is required to produce 1 gram of hydrogen. To determine, the required power of the cracker, the ammonia rate is multiplied with the lower heating value of ammonia. A ammonia rate of 11.6 gram per second, results in a SOFC power of 216 kW. This SOFC is also operating at a 80% load to extend the lifetime. Therefore, a SOFC of 270 kW is required to generate 1 gram of hydrogen every second.

Additionally, a small hydrogen tank is included in the configuration to store the hydrogen. The flow of hydrogen into the ICE is dependent on the engine load, while flow of hydrogen out of the SOFC remains constant. Therefore, the presence of hydrogen storage is necessary to ensure that enough hydrogen flow is possible into the engine and prevent to prevent excessive hydrogen cracking.

This configuration, which involves a dual-fuel ammonia/hydrogen engine, cannot be implemented without the presence of a battery. This is due to the maximum change in engine load of this setup. The same maximum change of engine load of 2% as in Section 4.3 is assumed for an ammonia hydrogen engine. However, in this configuration there is no MGO available to handle the transient loads. Therefore, transient loads higher than 2% must be managed by a battery. Thus when the installed power of the ICE is 20,000 kW, the maximum dP/dt that the ICE can handle is 400 kW/s. The engine load for this configuration is kept at a minimum of 85% due to the high dP/dt present when the engine load drops low. If this was not done, the simulation would be stopped every time the engine load lowered and needed to increase significantly.

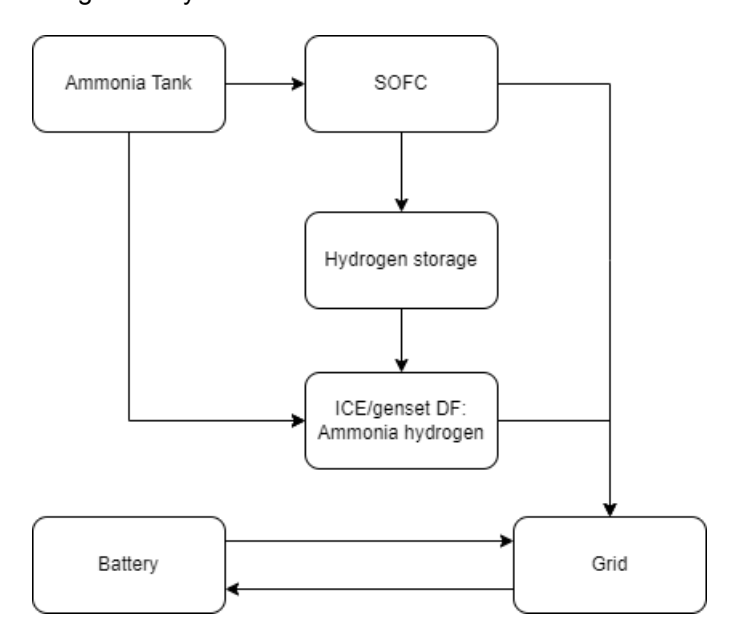


Figure 4.8: The configuration where a dual-fuel Ammonia/hydrogen genset is used in combination with an SOFC that is powered on ammonia and a battery.

The minimum amount of hydrogen that is necessary to keep an engine running is 7% at mid-load and 11% at full engine load as is mentioned in Section 2.3. Thus, this means then that at half engine load 89 percent of the energy is generated from ammonia, while at full engine load 93 % of the energy is generated from ammonia. These values are linearly extrapolated from 0 till 110 %. Figure 4.9 visualizes the energy ratio between ammonia and hydrogen.

Furthermore, a dual-fuel ammonia hydrogen engine has a lower technology readiness level compared to an ammonia/MGO dual-fuel engine discussed in Section 4.3. Therefore, the efficiency of the engine ammonia hydrogen engine is expected to be lower. To account for this lower assumed

32 4. Configurations

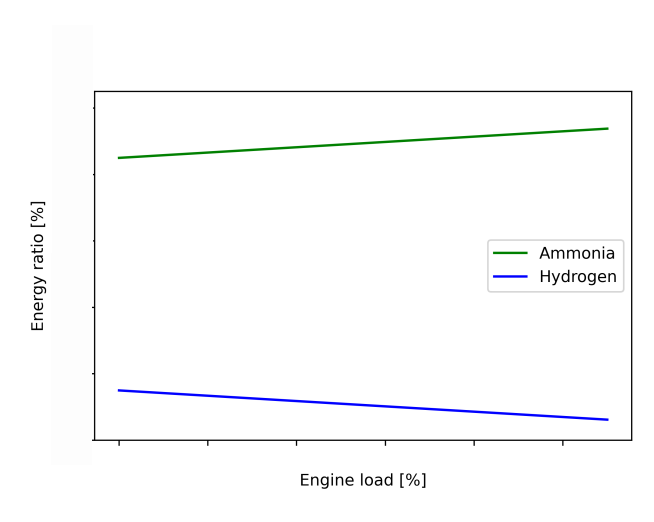


Figure 4.9: The energy ratio for the dual-fuel Ammonia/hydrogen genset.

efficiency, a correction factor of 0.9 is applied to the SFC. The resulting specific fuel consumption is visualized in figure 4.10. This curve is used to calculate the fuel consumption for this configuration.

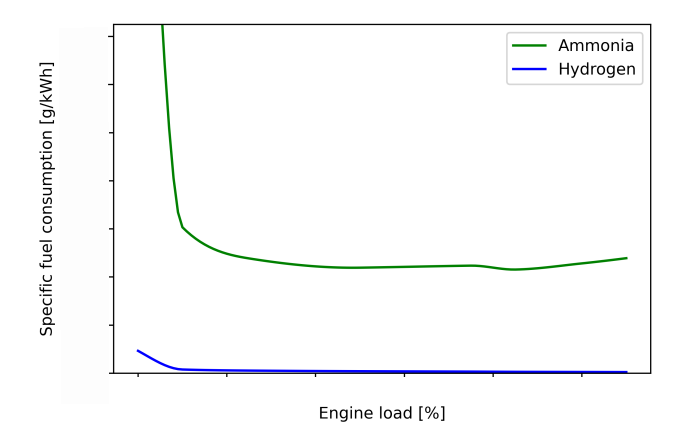


Figure 4.10: The specific fuel consumption for a dual-fuel hydrogen/ammonia engine expressed in g/kWh.

4.7. Conclusion 33

4.7. Conclusion

In this chapter, the SFC for each configuration has been determined. Additionally, assumptions regarding the engines, SOFC and batteries have been outlined in this section. Batteries are necessary when the transient load capabilities of the engine are low and there is no MGO available. To provide a concise overview, Table 4.1 provides a summary of the various configurations discussed.

Table 4.1

Configuration	Power	Battery	Fuel	TRL
Conventional	ICE	No	MGO	9
1 MGO ICE including battery	ICE	Yes	MGO	9
2 DF ammonia MGO ICE	ICE	No	MGO, Ammonia	5
3 DF ammonia MGO ICE including battery	ICE	Yes	MGO, Ammonia	5
4 Ammoniadrive including battery	ICE, SOFC	Yes	Ammonia	2
5 Ammonia SOFC	SOFC	Yes	Ammonia	7

Modelling approach

This chapter will explain the modelling approach. The input an the output of the simulation is explained and the available parameters that can be changed are discussed. The fuel consumption is estimated with one engine instead of four engines. Finally, the simulation strategy is explained.

5.1. Input: Power demand

The goal of this of modelling is to verify that the configurations have sufficient power and energy on board to support dredging operations under a high varying load for a duration of 30 days. In Section 3.4.2, the power demand of all the previous dredging projects for the Vox Amalia was examined. Among them, the Kustlijnzorg project exhibited the highest average and peak power. Consequently, the simulation will adopt the power demand from this project as a reference. If the configurations can handle the power demand of the kustlijnzorg project, it is assumed that the power demand of other projects can be handled as well.

The power demand profile starts on the 21st of March 2020 and runs till the 20th of April 2020. These specific dates were chosen because of data quality having minimal NaN data. A similar methodology as described in Section 3.9.2 is used to determine the amount of NaN data during these 30 days. This method resulted in approximately two hours of unknown data. Figure 5.1 illustrates the total engine power demand of the Vox Amalia on 21 March 2020.

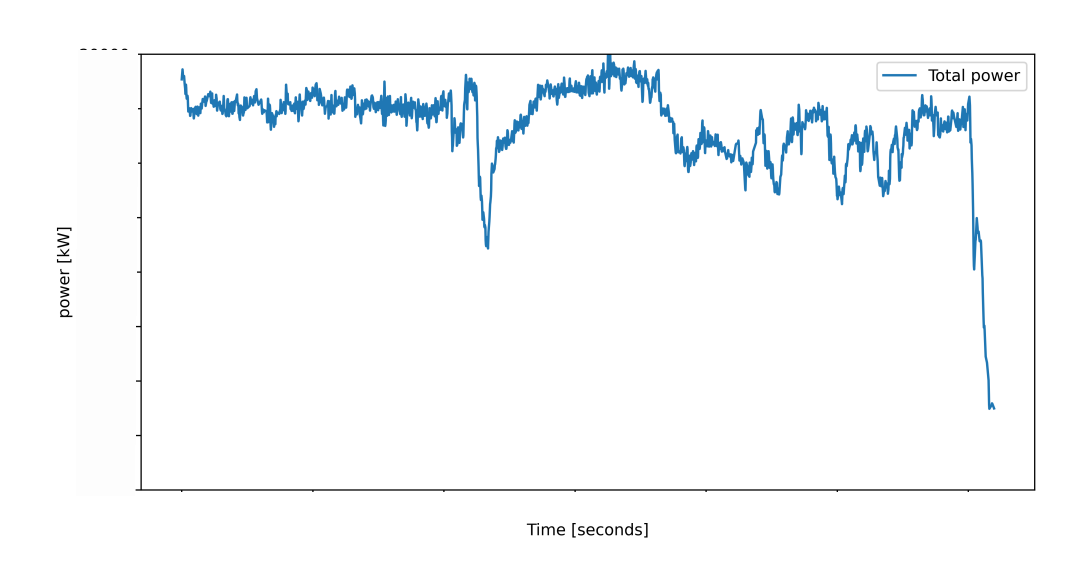


Figure 5.1: The power demand of the Vox Amalia during the Kustlijnzorg project on 21 March 2020.

5.2. Input: Configuration with setup

The following input parameters can be modified for each applicable simulation:

- · Installed power ICE
- · Installed power SOFC
- · Battery capacity
- · C-rating battery
- · Hydrogen rate out of SOFC
- · Hydrogen storage tank size

Each configuration is equipped with a specific amount of installed power, it is assumed that these can be adjusted in increments of 1,000 kW. Both the ICE and SOFC installed powers can be modified insteps of 1,000 kW. Furthermore, for configuration 4 (Ammoniadrive including battery), the hydrogen rate that flows out of the SOFC can be chosen with steps of 1 gram per second. The hydrogen tank capacity is assumed to have a minimum of 10 kg storage capacity. As for energy storage, the battery capacity can be adjusted in steps of 1,000 kWh. Table 5.1 lists three different battery options, each with varying capacities. It is assumed that these batteries are fully charged at the beginning of each simulation. Furthermore, the assumed lifetime of the battery are 50,000 cycles at a dept of discharge of 50% [117]. During this research all the battery use a 50% depth of discharge.

Table 5.1: The c-ratings for charging and discharging and the weight for the available batteries for different configurations [115]–[117].

Battery	C-rating charging	C-rating discharging	Weight [kg/kWh]
Corvus Dolphin	0.4	0.5	6
Corvus Whale	0.7	0.7	9
Echandia Energy	2	2	13

5.3. Power management strategy

Figure 5.2 shows the flow chart of the modelling approach. On one hand, it incorporates the power demand as an input, and on the other hand, it integrates the configuration setup discussed in Section 5.1 and Chapter 4. The simulation itself is implemented in Python.

At each time step, which is set to one second, the simulation verifies whether the configuration with the specified setup has sufficient installed power to meet the power demand at that specific moment. If the installed power falls short, the simulation checks if there is enough energy stored in the battery. If the battery has not enough energy stored or its maximum power output is too low, then the configuration does not meet the requirements. Therefore, the simulation will stop then. When there is charged battery capacity available and the power output of the battery is high enough, then the battery will discharge energy to meet the required energy demand.

The power output of the engine and SOFC is then high enough to cope with the power demand at that step in time. The engine load of the ICE will then be determined, the power plant load for a SOFC is constant. Then, the the engine load at that moment in time will be compared to the engine load in the previous second. If this delta engine load is larger than maximum engien load per second (The maximum change of engine load per second of each configuration are given in Chapter 4) than the installed power plant of the configuration can cope with, then the simulation will stop. For a installed power of 20,000 kW, a maximum change of engine load per second of 2% means a dP/dt of 400 kW/s. However, when the delta engine load is within the bounds of the dp/dt, then the configuration can cope with the transient load at that moment in time. The output of the simulation will then be the fuel consumption in MGO and or Ammonia for this particular step in time.

On the other hand, if there is enough power installed for the given moment in time. Then, the simulation checks if there is empty battery capacity available, to store the surplus of energy. However, if the battery is already fully charged, the power plant load will be reduced. For Configuration 4 (Ammoniadrive including battery) and 5 (ammonia SOFC including battery), it is not possible to lower the power

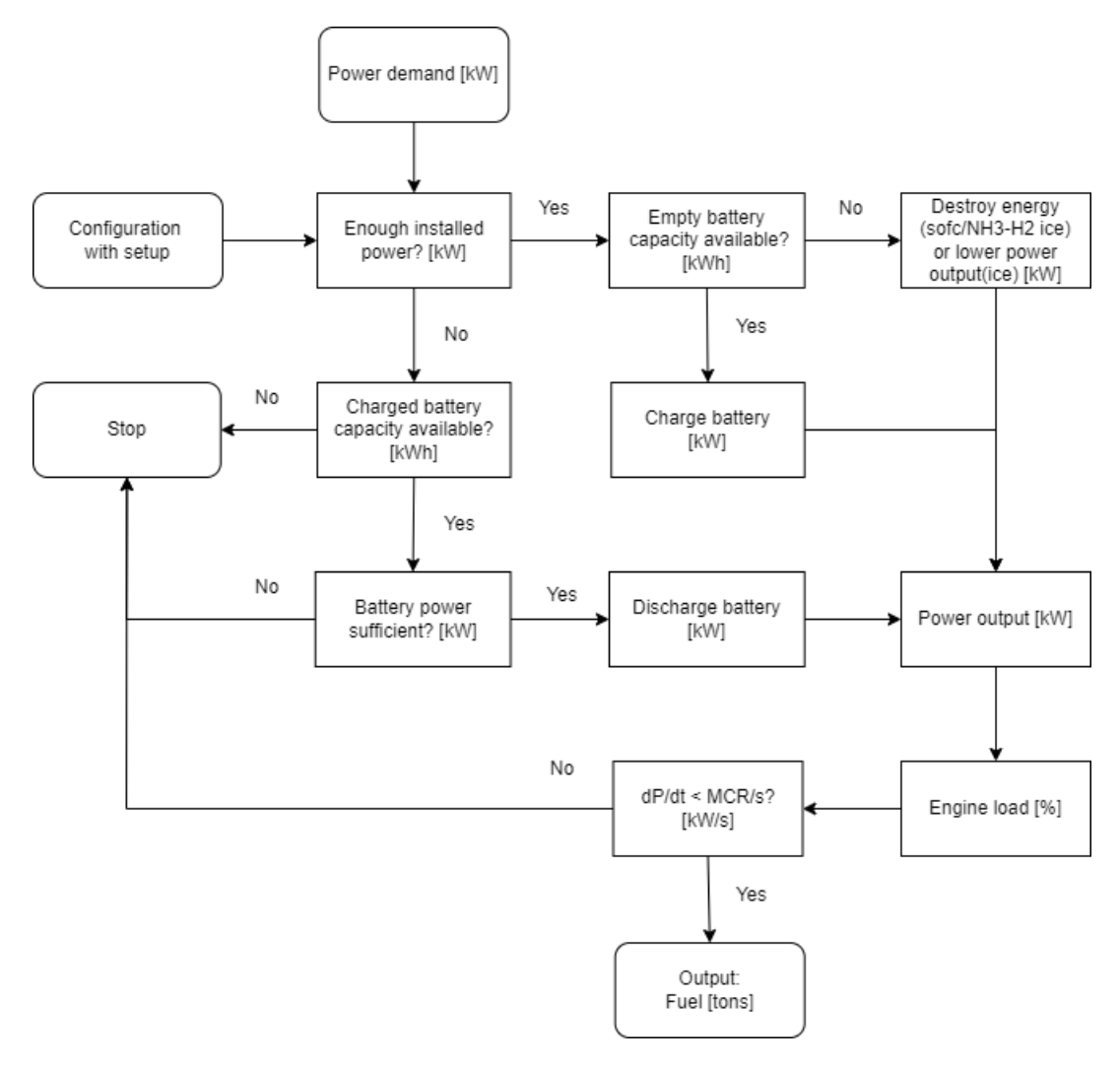


Figure 5.2: An overview of the modelling approach to verify if there is enough installed power and capacity.

output due to their low ability to cope with transient load [dP/dt]. Therefore, the surplus of energy has to be wasted. Then, the same steps are followed in the case when a battery was discharged. Then, the power output is determined and then the engine load at that moment in time is determined. Then, again it is checked if the configuration can handle the transient load [dP/dt] in that moment in time and then the fuel consumption is calculated in MGO and ammonia for this particular step in time.

If the simulation stops before every second in the 30 days of the power input were completed. Then the configuration with the setup parameters was insufficient. The input parameters of the configuration have to be changed to make the configuration sufficient. The changing of these input parameters was done manually. When the simulation has run for every second in the 30 days, then the fuel consumption of each section will be summed to a total fuel consumption for the 30 days.

5.4. Output: fuel consumption

After the simulation has run for every during the 30 days of power output, then the total fuel consumption can be determined. In Chapter 4 it will be discussed that the fuel consumption varies across setups, depending on the fuel type, and the type of ICE and or use of SOFC.

As mentioned in Section 3.4.1, the Vox Amalia is equipped three main engines and an auxiliary generator. These four engines provide the vessel with power during normal operation. Each engine has a specific fuel consumption curve providing the amount of fuel required for a certain engine power output. It is assumed that the power is equally distributed over the engines. Therefore, for this research, all configurations including the conventional configuration, are assumed to have a single big engine,

instead of multiple smaller ones. It is assumed that the three main engines and the auxiliary generator are always online, and the load is equally distributed. For the simulation the four engines are considered as one large engine with the same SFC curve. The engine load is then determined by dividing the total power by the installed capacity.

When assuming there is one big engine, the engine will operate continuously without being turned of. However, when multiple engines are utilized, it is possible to deactivate an additional engine in certain cases. Moreover, it should be noted that the engines' optimal efficiency point is at 85% load. However, when simulating with a single large engine, the engine load will often fall below 85%, resulting in non-optimal operating conditions.

For the determination of the fuel consumption, it is necessary to transition from four SFC curves to one SFC curve, as only one engine is considered. For the SFC, a combination between the SFC data points for the main engines and the SFC data points for the dredge generator engine is taken. The known data points The known data points from the SFC of the main engines are taken (25% to 110%) and the SFC values for the 1% and 10% engine loads of the dredge generator engine from Table 3.2. The resulting SFC for each engine load is presented in Table 5.2. Similar to Section 3.9.1, the pchip interpolation method is applied to create a smooth curve by interpolating between the engine loads.

Table 5.2: The specific fuel consumption values at different engine loads for the MGO engine.

Engine load [%]	1	10	25	50	75	85	100	110
SFC MGO engine [% gr/kWh]	739	146	112	100	100	96	100	104

To validate the combined SFC curve for the single MGO engine, the same 21-week period discussed in Section 3.9.1 is used. This 21 week period is used, because only one type of fuel was used during this period and during the Kustlijnzorg both HFO and MGO were used. There is a a difference of 1% by the estimated consumption and the actual consumption. By dividing the combined SFC curve, the fuel consumption with a single engine can be estimated for the 21-week period with an accuracy of less than one percent. The newly created SFC curve is depicted in Figure 5.3. This SFC curve serves as the basis for estimating the fuel consumption of each configuration, except for Configuration 5: Ammonia SOFC including battery. For configuration the fuel cell load is constant.

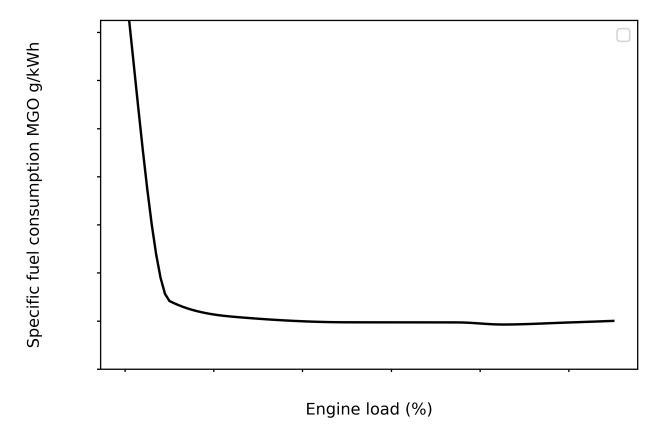


Figure 5.3: The specific fuel consumption for the conventional configuration where all engine are assumed as one big engine.

5.5. Simulation strategy

All the simulations can be found in Appendix 5. For every configuration the setup will be changed with regards to the installed power, and the battery properties, with the exception of the conventional and configuration 2. These configurations are set by the original specifications of the Vox Amalia. Furthermore, if a setup is sufficient for configuration 1, then it is also sufficient for configuration 3. If a simulation was insufficient, then the installed power or battery capacity would be increased. Furthermore, if a simulation was sufficient, then the installed power or the battery capacity would be decreased. This was

done to find the optimum. The installed engine power was set to a minimum of 70% of the original installed capacity. Furthermore, was the power split between the ICE and SOFC limited to 1:4 or 4:1.

5.6. Conclusion

In this chapter, the selection of the specific 30 day period during the Kustlijnzorg project is explained. These days were chosen due to the presence of a low amount of NaN data and a high power demand, making them suitable for this research. If a simulation is meets the required power demand, then the output of the simulation is the fuel consumption over the thirty days. This fuel consumption is estimated with one total engine load and thus one SFC curve. The accuracy of this curve has been validated over a span of 21 weeks.



Cost calculations

This chapter will explain the cost that are involved in operation a TSHD. The following seven cost components will be clarified:

- · Depreciation and Interest (CAPEX)
- · Maintenance and Repair (OPEX)
- · Wear and tear (OPEX)
- Fuel (OPEX)
- · Lubricant (OPEX)
- · Carbon (OPEX)
- Crew (OPEX)

The Depreciation and interest and the Maintenance and repair cost are both based on the value of a TSHD and therefore the value of a THSD needs to be determined first.

6.1. Value estimation of a (new) trailing suction hopper dredger

The costs for depreciation, interest, maintenance, and repair are determined based on the value of a vessel using the CIRIA method [121]. This method calculates the replacement cost of a vessel and is applicable to conventional self-propelled trailing suction hopper dredgers [121]. The formula for calculating the base value, as given in Equation 6.1

$$V = f(W, P_t, J_t, S)$$
(6.1)

Where:

V =Value of the vessel in euros

W =Lightweight of the vessel in ton

 P_t = Power of the dredgepumps during suction in kW

 J_t = Power of the jetpumps during suction in kW

S = Free sailing power in kW

Additionally, CIRIA published in 2023 a factor of 1.32 to compensate for the inflation from 2010 to 2022 [122]. This index accounts for the inflation of the value of a TSHD and is based on the Eurostat indices for engines, steel structures, and pumps [122].

Recent developments to make a vessel more sustainable are not included in Formula 6.1 to calculate the value. However, there are certain sustainability factors that can adjust the vessel's value. A

40 6. Cost calculations

vessel that has an LNG dual-fuel drive train configuration has a 10% increased value, and furthermore, if an aftertreatment system for NO_x (SCR) or a diesel particulate filter (DPF) is installed, the value is increased by 2 or 3 percent, respectively [122]. The sustainability factors are reviewed annually and updated or expanded based on recent developments.

The cost of equipment for an LNG-powered vessel can be estimated. From the values in Table 6.1, it is evident that the equipment cost for an LNG-powered vessel is 3.5 times higher than for an MGO-powered vessel. A 350 % increase in equipment cost would then result in a 10% increase in the value of the vessel, considering the CIRIA sustainability factors. Using this ratio between an LNG vessel and an MGO vessel, it is possible to estimate the value for the Vox Amalia across all configurations covered in Chapter 4.

Table 6.1: Equipment cost for LNG and MGO powered vessels [9].

Туре	Engine [€/kW]	Tank and add-ons [€/kW]
MGO	356	0
LNG	713	534

6.1.1. Depreciation and interest

A vessel has a specific lifetime during which it can be utilized, and as a result, the costs associated with the vessel must be allocated over its service life. This allocation is known as depreciation and interest. The service life, also referred to as the lifetime of the vessel, is the duration in years that the vessel can be economically and technically viable. The depreciation and interest expenses are expressed as a percentage of the current vessel's value. When a configuration needs to replace the SOFC within the 25 years of lifetime. Then, the total SOFC costs that are required for the 25 years are added to the current value of the vessel, before the depreciation and interest can be calculated.

6.1.2. Maintenance and repair

Maintenance and repair (M&R) activities encompass preventive maintenance, daily maintenance, and major maintenance. These costs are expressed as a percentage of the value of the vessel.

6.2. Wear and tear cost

The parts on a hopper dredger that are most sensitive to wear are: the draghead, suction pipes, dredgepumps and the hopper [123]. The extent of wear and tear is influenced by the soil conditions in which the dredger operates. The cost of wear and tear is dependent on the volume of dredged material.

Fourteen times the Vox Amalia unloaded by rainbowing and the other 186 cycles the vessel unloaded by dumping. This means that eight percent of the time the Vox Amalia unloaded by dumping. The weekly wear and tear cost can be calculated by multiplying the the production for each cycle times the type of unloading mode.

6.3. Fuel cost

The weekly fuel cost is determined by multiplying the amount of fuel that is burned in a week by the fuel price. The output of the simulation was the amount of fuel burned in 30 days. To convert 30 days to a week, a factor of 0.23 needs to be multiplied by the fuel output over thirty days. The fuel price is set in euros per ton, and recent fuel prices are shown in Table 7.4 and are discussed in Section 7.1.2. The weekly fuel costs are different for each configuration and setup due to the differences in fuel type and fuel consumption.

6.4. Lubricant cost

Lubricant costs can be estimated as between 8 to 10 % of the total fuel costs [123], [124]. However, it should be noted that newer vessels require less lubricants, and this percentage is based on conventional fuel prices [123]. The amount of lubricant required is related to the total installed power. The bigger the engine, the more heat is generated and the more lubricant is required. Therefore, the lubricant costs of each configuration are linearly related to the lubricant cost of the MGO base case. Which

6.5. Carbon cost 41

are assumed at 8 % of the weekly fuel cost. Additionally, the lubricant cost for the SOFC is assumed to be zero.

6.5. Carbon cost

A carbon tax means that there is a fee for every tonne of carbon that is emitted. The European Union will gradually introduce a carbon tax for the maritime industry in 2024 when 40 percent of the carbon emissions and in 2026 a 100 percent of the carbon emissions will be taxed [125]. The emissions that will be taxed are: Carbon dioxide, methane and nitrous oxide. This European carbon tax only applies to vessels which are sailing between port in the European Union and this carbon tax applies for 50 percent to vessels which will only depart or arrive from a port inside the European Union. In 2022 the mean price per tonne of carbon was approximately 82 euro in the European Unions [126].

The carbon dioxide emissions are calculated by multiplying the amount of fuel burned by an emission factor. These emission factors are shown in Table 2.2. However, it should be noted that these emission factors are for an ICE. If ammonia is used in a SOFC, WTT carbon dioxide emissions are assumed to be zero. With the weekly fuel consumption, the weekly \mathcal{CO}_{2eq} emissions can be calculated. The weekly carbon cost is calculated by multiplying the carbon price by the weekly \mathcal{CO}_{2eq} emissions. The set carbon price is the average carbon price from 2030 to 2055, which is the assumed lifetime of the vessel for this research.

6.6. Crew cost

There are both expat and non-European crew members onboard the Vox Amalia. The vessel has a crew capacity of 50 people, but typically there are 20 expat crew members and 20 non-European crew members onboard. The day rate for the crew and food rate can be found in Table 6.2. Based on these rates, the total weekly crew cost amounts to 364,000 euros.

Table 6.2: The day rates for the crew and food

Rate type	[€/day]
Expat day rate	1,000
Non European day rate	200
Food day rate	50

6.7. Insurance

The insurance cost for a vessel can vary depending on factors such as the material and the number of claims made by the company. For normal dredging operations, the annual insurance cost for a vessel typically ranges from 1 to 2.5 percent of the capital value of the dredger [127][123]. The specific deductibles and terms of conditions of the insurance can vary among companies and also impact the insurance price [123]. For this research, the yearly insurance cost is assumed to be 1 percent of the current value of the TSHD. To calculate the weekly cost, the yearly insurance cost is divided by the number of dredged weeks in a year (38 weeks).

6.8. Cost of dredged material

Finally, by summing all the weekly costs, the total weekly cost is known. The Vox Amalia dredged a total of 1,500 Megatons of material, with an average density of 2.00 kg/m³. By dividing the total weekly cost by the total amount of dredged material in a week, the cost of dredged material can be calculated.

6.9. Conclusion

The value of a vessel can be calculated using the CIRIA method. For each configuration, the new value can be calculated with the help of the sustainability factor for an LNG-powered vessel. Additionally, the costs are dependent on the value of the vessel, amount of dredged material, fuel consumption, carbon tax, crew and insurance. With all the weekly costs and the known production of the vessel, it is possible to calculate the cost of dredged material.

Results

In this chapter, the results are discussed in terms of price and emissions. Additionally, the following three different scenarios are considered:

- Scenario 1, Only the TTW CO_{2eq} emissions are taxed
- Scenario 2, the WTW CO_{2eq} emissions are taxed and grey ammonia is used
- Scenario 3, The WTW CO_{2eq} emissions are taxed and green ammonia is used

7.1. Price assumptions

This section explains which assumptions are made for the costs of: equipment, fuel and carbon tax. The costs that are discussed during this section are the business-as-usual cost. The prices of equipment were given in us dollars per kW, this is converted to euro/kW, with the exchange rate of 0.89 €/\$ from 17 July 2023.

7.1.1. Price of equipment

The prices for the engines and SOFC are shown in Table 7.1. The price for the dual-fuel ammonia/hydrogen engine was not given, but this price is assumed to be the same for an ammonia/MGO dual-fuel engine. The price of a SOFC is based on the price of a hydrogen fuel cell. For both fuel cells, hydrogen is required to generate electricity, and therefore, this assumption can be made.

Table 7.1: The price for engines for the different configurations [9].

ICE	Cost [€/kW]
MGO	356
DF MGO NH3	713
DF NH3 H2	713
SOFC NH3	1,336

Table 7.2 shows the cost for the tank and add-on. These costs include the extra cost for tank systems and add-ons such as a diesel particle filter. The cost of a SCR is not included into these add-on costs, but it is factored into the sustainability factor as explained in Section 6.1. Furthermore, the tank and add-on costs for the dual-fuel ammonia/hydrogen setup were not provided. For the ammonia/hydrogen configuration, there is no MGO present, and mainly ammonia is stored and a very small fraction of hydrogen stored. Therefore, the price of the dual-fuel ammonia/hydrogen tank and add-on cost was assumed to be 300 \$/kw higher than for the ammonia/MGO tank add-on cost. The tank and add-on cost for an ammonia SOFC are also not given, there is no hydrogen present, and therefore the costs are assumed to be 200 \$/kw higher than for the ammonia/MGO tank add-on cost.

The cost for the battery is shown in Table 7.3. During this research, three different batteries with three different C-ratings are used. However, for all these batteries, the same price is used. In reality,

Table 7.2: The price for tank and add-on cost for the different configurations[9].

Tank and add-on	Cost [€/kW]
MGO	0
DF MGO NH3	535
DF NH3 H2	802
SOFC NH3	713

the higher the C-rating, the higher the price of the battery. During this research, for every configuration with a certain installed power, optimization was done to minimize the battery capacity. Once the minimal capacity is determined, optimization is carried out to find the lowest C-rating possible. Therefore, without incorporating different prices for the batteries with a different C-rating, the battery with the lowest C-rating possible was chosen as the preferred option to keep the analysis consistent.

Table 7.3: The cost for a marine battery [128].

Energy storage cost	[€/kWh]
Battery	445

7.1.2. Price of fuel

The fuel prices are based on the latest available bunker prices. On 18 July 2023 the average MGO price from the 20 biggest ports in the world was 789 €/ton [129]. Furthermore, in may 2023 the average ammonia price according to the S&P global commodity insights was 356 €/ton [130]. Finally, the price of green ammonia was assumed at 1197 €/ton, Lindstad et al, discussed a high and a low price for green ammonia, which is dependant on the price of electricity [9]. For this research the average between the high and the low price of green ammonia was used.

Table 7.4: Latest fuel prices according to bunker rapports [9], [129], [130].

Fuel type	Cost [€/ton]
MGO	769
Ammonia (grey)	356
Ammonia (green)	1,197

7.1.3. Carbon cost

In 2022 the average price of carbon was approximately 82 \in /ton. This will likely rise in the future and therefore, a carbon price of 100 \in /ton is assumed as is shown in table 7.5. Every ton of CO_{2eq} that is emitted is 100% taxed with the carbon price.

Table 7.5: The assumed carbon tax for the business-as-usual scenario.

Carbon cost	[€/ton CO _{2eq}]
Carbon tax	100

44 7. Results

7.2. Final setup of each configuration

A brief summary of each cheapest configuration according to the business-as-usual prices is presented in Table 7.6. For all configurations except for configuration 5 (Ammoniadrive + battery), the same setup is the cheapest in all three scenarios. The total costs of these setups are discussed in Section 7.4

The power for the ICE and SOFC is rounded to 1,000 kW, due to the step size of a 1,000 kW that was chosen during the simulations. For the conventional configuration and for configuration 2 (DF MGO NH3), the power is 100%, which is the currently total installed power of the Vox Amalia. The installed cracker power is not rounded, because the cracker power is calculated based on the hydrogen rate exiting the SOFC, as is mentioned in Section 4.6.

Furthermore, the battery for configuration 4 (SOFC NH3 + battery) and 5 (Ammoniadrive + battery) is 2 to 7 times larger than for configuration 1 (MGO + battery) and 3 (DF MGO NH3 + battery). A reason for the large battery, for configuration 4 (SOFC NH3 + battery) and 5 (Ammoniadrive + battery), is that a SOFC and a dual-fuel NH3/H2 ICE is (almost) unable to handle transient and the stack load is kept constant. Unlike the other configuration, where the engine load can be lowered. Therefore excess of energy that cannot be stored, because the battery is full, needs to be wasted or destroyed. Therefore in order to minimize the amount of fuel that needs to be destroyed, a large battery is required.

System efficiency is the total amount energy present in the fuel that was used divided by the total amount of energy required during the 30 days of the simulation. The total power demand during the 30 days simulation was 29.1 TJ. Due to the addition of a battery, the engine for configuration 1 (MGO inc battery) and 3 (DF MGO NH3 + battery), operates at a more efficient engine load and therefore the fuel consumption is lower. This results in a higher system efficiency. Furthermore, the system efficiency of configuration 4 (SOFC NH3 + battery) is 4%, higher than the conventional configuration. However, a SOFC operates at a more than 10% higher efficiency than a MGO engine, so a higher system efficiency was expected for the configuration operating a SOFC instead of a MGO engine. Configuration 4 (SOFC NH3 + battery) has to waste energy, due to the inability of the SOFC to lower its power output. Therefore, difference of the system efficiencies for configuration 1 (MGO + battery) and 4 (SOFC NH3 + battery) is closer than the difference in power train efficiency between the configuration. The energy destroyed is the amount of energy that could not be used as the SOFC or ICE output could not be lowered, when the power demand was lower than the power output. Only for configuration 4 (SOFC NH3 + battery) and 5, energy is destroyed.

Table 7.6: The summary of the cheapest setup for each configuration and normalized for every column.

Configuration [-]	ICE [%]	SOFC [%]	Cracker [%]	Battery [%]	System efficiency [%]	Energy destroyed [TJ]
Conventional	100	0	0	0	92	0
1 MGO + battery	73	0	0	23	93	0
2 DF MGO NH3	100	0	0	0	85	0
3 DF MGO NH3 + battery	82	0	0	13	91	0
4 SOFC NH3 + battery	0	100	0	100	100	74
5 Ammoniadrive + battery	47	31	100	48	85	100

A brief summary of the cheapest setup for configuration 5 (Ammoniadrive + battery) for all three scenarios is shown in table 7.7. For scenario 1, an approximately twice as large ICE is installed than for scenario 2 and 3. The main reason is that for scenario 1, ammonia is only taxed with the TTW CO_{2eq} emissions and grey (cheaper than green) ammonia is used. Therefore, an ICE is feasible although the lower efficiency, because the SOFC have to be replaced and are more expensive.

Table 7.7: The summary of the cheapest setup for configuration 5 for each scenario and normalized for every column.

Configuration [-]	Scenario	ICE [%]	SOFC [%]	Cracker [%]	Battery [%]	system efficiency [%]	Difference dredged material [%]
5 Ammoniadrive + battery	1	47	31	100	48	85	-3
5 Ammoniadrive + battery	2	22	69	40	60	91	-3
5 Ammoniadrive + battery	3	17	75	33	62	91	-3

The setup of each configuration results in a different total weight of the vessel and this is summarized in Table 7.8. An increase in weight results in a decrease of dredged material as is discussed in Section 3.8.2. The weight of the ICE, SOFC, cracker, battery and fuel is take into account to determine the difference in dredged material. The higher the installed power or battery power, the higher the weight for these components is. More tons of fuel is necessary for the configurations that use ammonia as

a fuel, because the lower heating value of ammonia is lower than that of MGO (18.6 vs 42.7 MJ/kg). Furthermore, configuration 4 (SOFC NH3 + battery) and 5 (Ammoniadrive + battery) are the heaviest and these configurations dredge 3% less material than the conventional configuration.

Table 7.8: The weight of t	ne fuel and equipment of	each configuration and	normalized for every column.

Configuration [-]	ICE [%]	SOFC [%]	Cracker [%]	Battery [%]	MGO [%]	Ammonia [%]	Delta dredged material [%]
Conventional	100	0	0	0	100	0	-
1 MGO + battery	74	0	0	35	96	0	0
2 DF MGO NH3	100	0	0	0	80	25	-1
3 DF MGO NH3 + battery	82	0	0	14	69	28	-1
4 SOFC NH3 + battery	0	100	0	100	0	85	-3
5 Ammoniadrive + battery	48	31	100	49	0	100	-3

The batteries for configuration 4 (SOFC NH3 + battery) encountered the most cycles. Every the battery was loaded and unloaded 92 times. This means that over the lifetime of the vessel (25 years), the battery go through approximately 20,000 cycles. This is lower than the 50,000 cycles that were mention in Section 5.1. Therefore, the batteries do not have to be replaced during the lifetime of the vessel.

7.3. Carbon dioxide equivalent emissions for each configuration

Table 7.9 provides a summary of the CO_{2eq} emissions for each configuration (cheapest setup parameters) and for all three scenarios. In scenarios 1 and 3, configurations that solely utilize ammonia as a fuel have the lowest CO_{2eq} emissions. Configuration 2 and 3 also have lower $CO_{[2eq]}$ emissions than the configurations on MGO in scenario 1 and 3. Configuration 4 (SOFC NH3 + battery) even achieves carbon neutrality in scenarios 1 and 3. In scenario 2, when grey ammonia is used instead of green ammonia, configuration 2 (MGO inc battery) becomes the most environmentally friendly option in terms of CO_{2eq} emissions, due to the high CO_{2eq} emissions of grey ammonia.

Table 7.9: The dredged material expressed in carbon dioxide equivalent.

Configuration	Scenario 1 [% CO _{2eq} /m3]	Scenario 2 [% CO _{2eq} /m3]	Scenario 3 [% CO _{2eq} /m3]
Conventional	100	100	100
1 MGO + battery	96	95	95
2 DF MGO NH3	84	119	83
3 DF MGO NH3 + battery	73	111	71
4 NH3 SOFC + battery	0	124	0
5 Ammoniadrive + battery	6	137	2

7.4. Weekly costs

Table 7.10 summarizes the weekly costs for each component in each configuration for scenario 1. For the conventional configuration and configuration 1 (MGO inc battery) the D+I and the M&R are the lowest. This is due to the lower equipment cost for MGO engines than for equipment with ammonia. Additionally, the D+I for configuration 4 and 5 is more than 50% higher than the other configurations, due to the high replacement cost of the SOFC.

Furthermore, the fuel cost for MGO are only slightly cheaper than for configurations on ammonia. The price per ton of ammonia is approximately 2 times lower than the price of a ton MGO. However, when the same efficiencies are considered, a ton of MGO generates more than 2 times the amount of energy, that 1 ton of ammonia can generate. The carbon cost are the highest for the conventional configuration, because this configurations uses the most amount of MGO and MGO has higher TTW CO_{2eq} emissions than ammonia.

Additionally, configuration 1 (MGO inc battery), burns less MGO than the conventional configuration and therefore less CO_{2eq} emissions are produced and this results in a lower carbon cost. The same applies for configuration 2 (DF MGO NH3) and 3 (DF MGO NH3 + battery) where less MGO is used for configuration 3 (DF MGO NH3 + battery). This means that the addition of a battery results in a lower fuel consumption and carbon output. Configuration 4 (SOFC NH3 + battery) has no carbon cost

46 7. Results

due to the absence of WTT \mathcal{CO}_2 emissions for a SOFC that is powered by ammonia. For configuration 5 (Ammoniadrive + battery) only a small amount of \mathcal{CO}_{2eq} is emitted by the ICE that results in a low carbon cost.

The crew cost are equal for each configuration, because the same crew is assumed for each configuration.

The cost for insurance are dependent on the vessel of the value as mentioned in Section 6.7. The higher the value of the vessel is, the higher the insurance cost are. Therefore, the conventional configuration has the lowest carbon cost and configuration 5 has the highest insurance cost. The wear and tear cost are dependent on the amount of dredged material and configuration 4 and 5 dredge less material in a week than the other configuration.

When all of these 8 weekly costs are summed up, the weekly cost are calculated. The configuration with the lowest weekly cost is configuration 1, followed by, conventional, 3, 2, 5 and finally 4.

Table 7.10: The weekly costs for each configuration in scenario 1, where grey ammonia is used and only the TTW emissions are taxed and normalized in every column.

Configuration [-]	D+I[%]	M&R[%]	Fuel[%]	Carbon[%]	Lubricant[%]	Insurance[%]	Crew[%]	W&T[%]	Total[%]
Conventional	100	148	100	100	100	100	100	100	100
1 MGO + battery	101	101	96	96	75	100	100	100	99
2 DF MGO NH3	110	108	110	82	100	108	100	100	105
3 DF MGO NH3 + battery	108	107	102	87	81	108	100	100	100
4 SOFC NH3 + battery	179	116	99	71	0	119	100	96	113
5 Ammoniadrive + battery	150	113	116	6	44	116	100	96	109

For scenario 2, grey ammonia is used and the WTW emissions are taxed. Therefore, in scenario 2, only the carbon and thus the total cost changes with regards to scenario 1. The WTW CO_{2eq} emissions for MGO are 1.69 times higher than for grey ammonia. However, in order to generate the same amount of energy with an ICE, 2.30 times more ammonia has to be burned. Therefore, when the engines have the same efficiency, 1.36 more CO2 equivalent emissions are emitted in the WTW cycle when using grey ammonia instead of MGO. Therefore, the carbon cost for scenario 2 for configurations that use ammonia as a fuel are higher than for configurations that only use MGO. The result is that configuration 4 and 5 have the highest weekly cost for scenario 2. The weekly cost for each configuration for scenario 2 are summarized in table 7.11.

Table 7.11: The weekly costs for each configuration in scenario 2, where grey ammonia is used and WTW emissions are taxed and normalized in every column.

Configuration []	D : I[0/1	M 0 D (0/ 1	Fuelf0/1	Carbon[0/1	Lubricant[0/1	Incurance[0/1	Crow[0/1	1A/0 T[0/1	Total[0/1
Configuration [-]	D+I[%]	M&R[%]	Fuel[%]	Carbon[%]	Lubricant[%]	Insurance[%]	Crew[%]	W&T[%]	Total[%]
Conventional	100	100	100	100	100	100	100	100	100
1 MGO + battery	101	101	97	96	75	100	100	100	99
2 DF MGO NH3	110	108	110	118	100	108	100	50	101
3 DF MGO NH3 + battery	108	107	102	110	81	108	100	50	105
4 SOFC NH3 + battery	179	116	99	120	0	119	96	48	127
5 Ammoniadrive + battery	164	114	107	132	19	116	96	48	126

For the last scenario (3), green ammonia is used and the WTW CO_{2eq} emissions are taxed. Only the fuel cost and the carbon cost will change in comparison with scenario 1. The carbon cost for green ammonia are the same as for scenario 1, due to the absence of WTT CO_{2eq} emissions for green ammonia. Due to the high cost for green ammonia, all configurations that use green ammonia, become much more expensive than configurations that use MGO as a fuel. The price of green ammonia is approximately 3.4 times higher than the price for grey ammonia as was mentioned in Section 7.1.2. This results in an 3.4 times increase of fuel price for configuration 4 and 5. Furthermore, the fuel price increases 1.6 and 1.8 times for configuration 2 and 3 respectively.

7.5. Cost of dredged material

Table 7.13 presents the cost of dredged material (\in /m3), for each configuration. The cost of dredged materials is the total weekly cost divided by the total dredged material in a week. Across all three scenarios it is not economically feasible to use ammonia as a fuel for a TSHD. However, for scenario 1, configuration 3 is only 2 cents/m3 more expensive than sailing on MGO. For scenario 2 and 3 the cost for sailing on ammonia become increasingly higher due to the high WTW CO_{2eq} emissions for grey

Table 7.12: The weekly costs for each configuration in scenario 3, where green ammonia is used and only the WTW emissions are taxed.

Configuration [-]	D+I[%]	M&R[%]	Fuel[%]	Carbon[%]	Lubricant[%]	Insurance[%]	Crew[%]	W&T[%]	Total[%]
Conventional	100	100	100	100	100	100	88	100	1089
1 MGO + battery	101	101	97	96	75	100	88	100	101
2 DF MGO NH3	110	108	180	82	100	108	88	100	124
3 DF MGO NH3 + battery	108	107	179	71	81	108	88	100	122
4 SOFC NH3 + battery	179	116	331	0	0	119	88	96	174
5 Ammoniadrive + battery	163	114	364	3	25	116	88	96	176

ammonia and the high cost of green ammonia. When comparing the cost per dredged material instead of the weekly cost, it becomes clear that configuration 4 and 5 are even more expensive, due to its lower production.

Table 7.13: The cost of dredged material for each configuration.

Configuration [-]	sc1 [% €/m3]	sc2 [% €/m3]	sc3 [% €/m3]
Conventional	100	100	100
1 MGO + battery	98	98	92
2 DF MGO NH3	106	110	124
3 DF MGO NH3 + battery	101	105	120
4 NH3 SOFC + battery	112	126	173
5 Ammoniadrive + battery	110	126	173

48 7. Results

7.6. Sensitivity analysis

The total cost of dredged material is a function of different parameters. The price assumption from Section 7.1 will be used, but only one parameter will change every time. In this section the following five parameters will be investigated:

- · Carbon tax
- Ammonia cost
- MGO cost
- · SOFC cost
- · SOFC degradation

The prices of fuel is uncertain and can rapidly change in the future. Furthermore, the price of carbon can also change, when the climate targets are accelerated. Additionally, the price of new technology often becomes lower as the technology develops and also lifetime of the technology can improve. It is expected that these parameters will have a significant influence on the cost of dredged material.

7.6.1. Carbon tax

Figure 7.1 illustrates the costs of dredged material for each configuration for scenario 1 across a range of carbon taxes. Notably, a carbon tax leads to higher costs per unit of dredged material for all configurations except configuration 5 and configuration 4 for a lesser extent for scenario 1. For scenario 1 the carbon price has to double

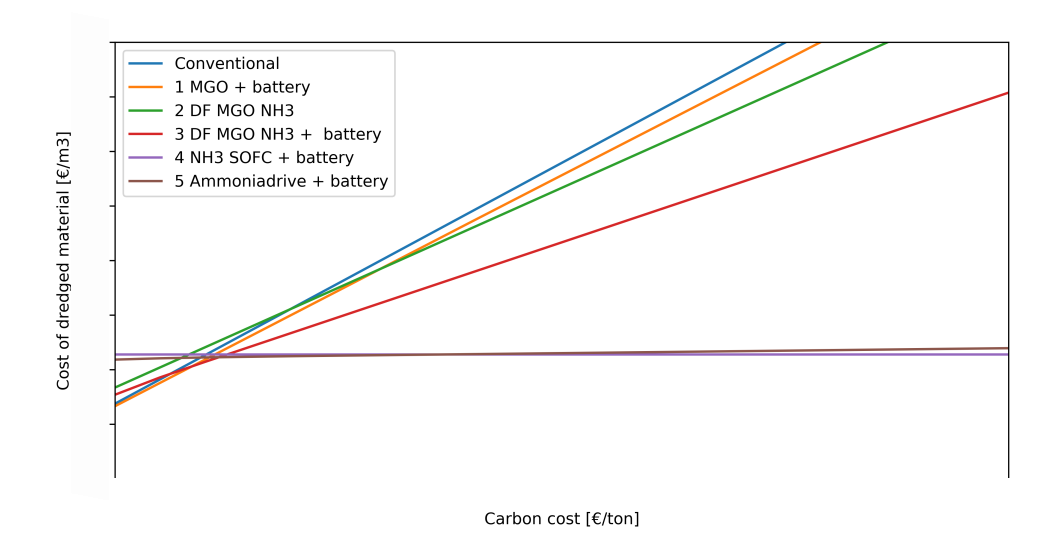


Figure 7.1: The cost of dredged material for different carbon tax for every configuration for and for scenario 1.

For scenario 2, configurations on MGO have a lower price per dredged material than the other configurations regardless of the carbon cost, as is illustrated in Figure 7.2. From Table 2.2, it is evident that the WTW emissions per ton of grey ammonia are approximately sixty percent lower compared to a ton of MGO. However, ammonia has a 2.30 times lower, lower heating value. Therefore, to generate the same amount of energy as one ton of MGO can produce, 2.30 times more tons of ammonia need to be used. Consequently, the WTW CO_{2eq} emissions for grey ammonia will always be higher than those for MGO.

The figure for scenario 3 can be found in Appendix B.1.1. For scenario 3 the carbon price has to increase with 600% for ammonia to become economically feasible. Currently it is unclear if in the future the carbon tax will apply to WTW or TTW emissions [131].

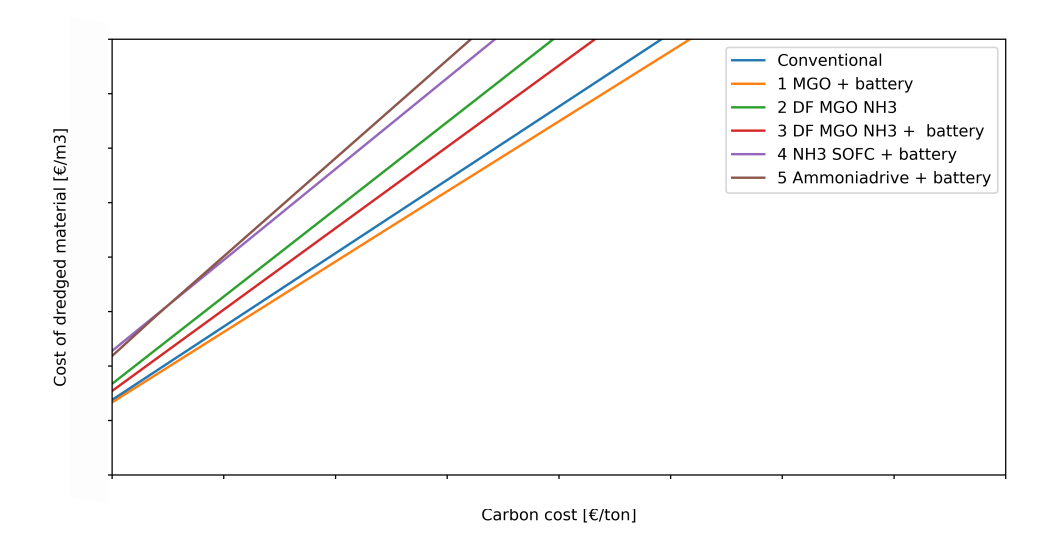


Figure 7.2: The cost of dredged material for different carbon tax for every configuration for and for scenario 2.

7.6.2. MGO cost

The cost of fuel can vary significantly over time, particularly during periods of war or geopolitical instability. Therefore, the future cost for MGO is uncertain. To explore the impact of varying MGO costs on the cost of dredged material, Figure 7.3 illustrates the relationship for scenario 1. It is important to note that the cost of MGO will only affect the prices of configurations that utilize MGO as a fuel. Therefore, the cost of dredged material for configuration 4 and 5 is constant for a varying cost of MGO. The price of MGO has to increase with 50%, 100, 300% for the respective scenarios for ammonia to become economically feasible.

The Figures for scenario 2 and 3 can be found in Appendix B.1.2. On 17 June 2022 the average MGO price was 1257 €/ton, and therefore it is not unlikely that the price of MGO can rise again in the future [129]. A

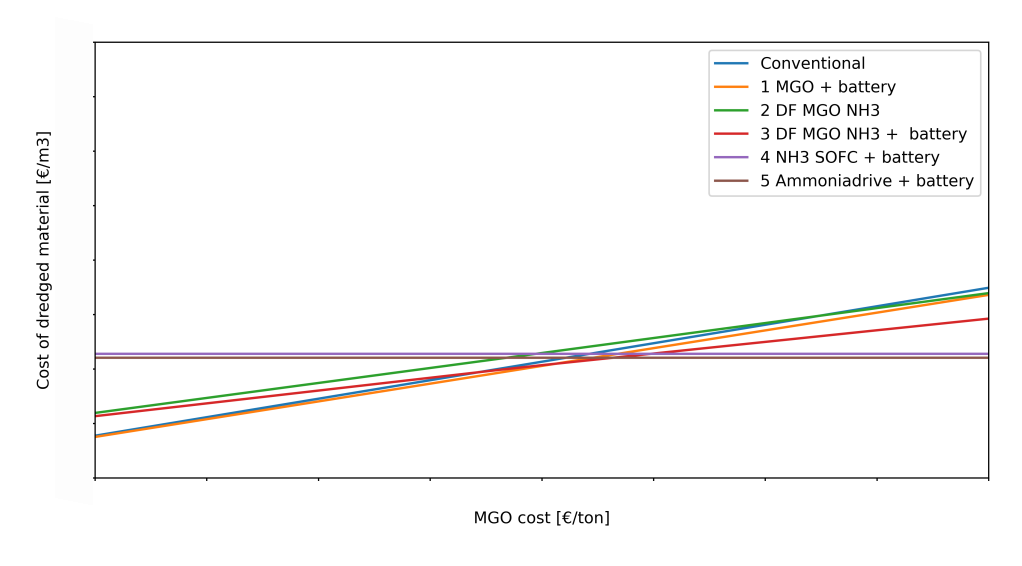


Figure 7.3: The cost of dredged material for different MGO cost for every configuration for scenario 1.

50 7. Results

7.6.3. Ammonia cost

Currently, ammonia is not produced in large scale meant for fuel supply. The current ammonia production is used for chemical use or fertilizer production. Therefore, the cost of ammonia can heavily vary in the future. The price for grey and green ammonia is different. The cost of ammonia directly influences the cost of dredged material for the configurations that use ammonia as a fuel as can be seen in Figure 7.4. The price of ammonia has to decrease by 50%, 100%, 75% for the respective scenarios for the configurations on ammonia to become the best option in terms of cost. The figures for scenario 2 and 3 can be found in the Appendix B.1.3

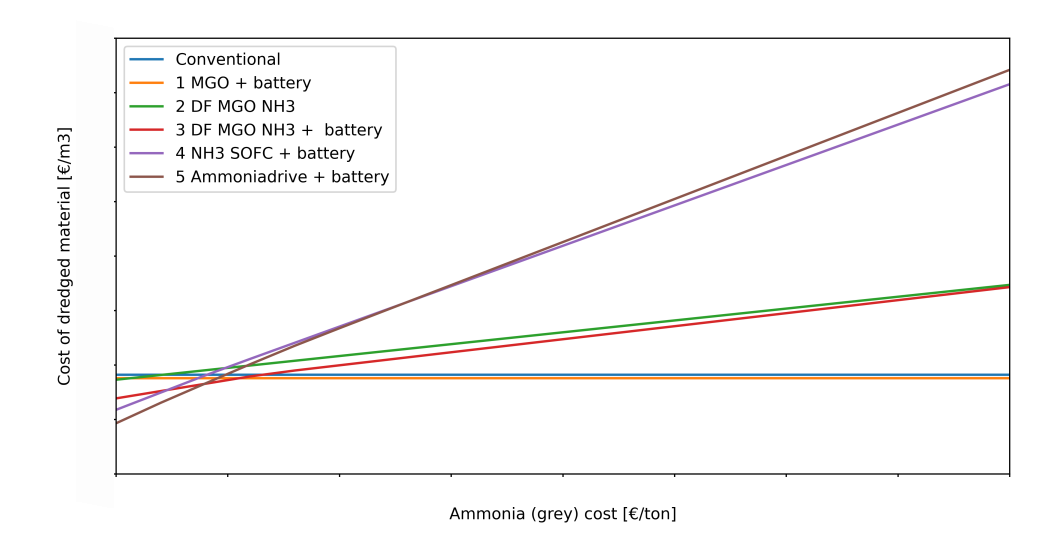


Figure 7.4: The cost of dredged material for different ammonia (grey) cost for every configuration for scenario 1.

The price of grey ammonia is strongly related to the price of natural gas and the natural gas price was in 2022 triple the price of the current gas price. This means that the price of grey ammonia could decrease in the future, however it is certain that the price of ammonia will increase if the gas prices rise again. An grey ammonia price of 0 €/ton is unrealistic. In order for the green ammonia price to decrease, the supply for green ammonia has to be increased. The supply of green ammonia will only be increased if the demand for green ammonia increases.

7.6.4. SOFC cost

The price of SOFC that uses ammonia is not certain, because it has a low technology readiness level. The cost of this equipment can still change as the technology develops. Figure 7.5 illustrates that the price of an SOFC only affects the configurations equipped with an SOFC. For scenario 1 the SOFC cost have to decrease by 75% for ammonia to become an economically feasible option. Regardless of the price of the SOFC, for scenario 2 & 3 MGO is always the cheaper option.

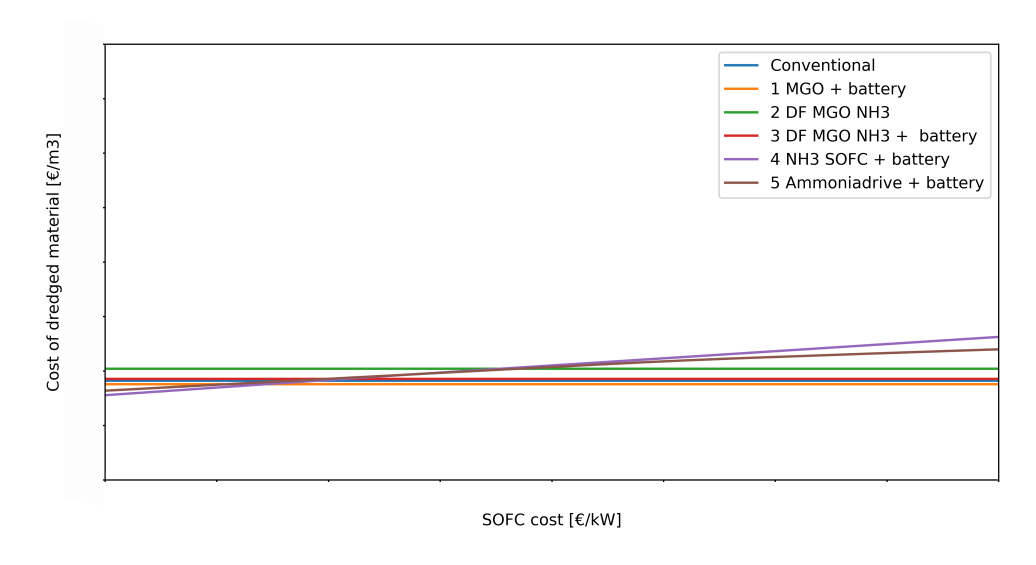


Figure 7.5: The cost of dredged material for different SOFC cost for every configuration for scenario 1.

In the future the manufacturing cost for an SOFC system can be as low as 166 €/kW if 50,000 systems are produced annually [132]. To reach a lower price, the production of SOFC systems needs to be drastically increased.

52 7. Results

7.6.5. SOFC degradation

Currently, with the business-as-usual parameters, the SOFC has a degradation of 0.5% for every 1000 hours of operation. This means that in the 25 year lifetime of the vessel, the SOFC has the be replaced 3 times. In Figure 7.6 it is shown that at when the degradation of a SOFC is lower or equal to 0.1%, configuration 4 is the cheapest option for scenario 1. When the SOFC degradation is 0.1% per 1000 hours, then no replacement is necessary in the 25 year lifespan of the vessel. The figure for scenario

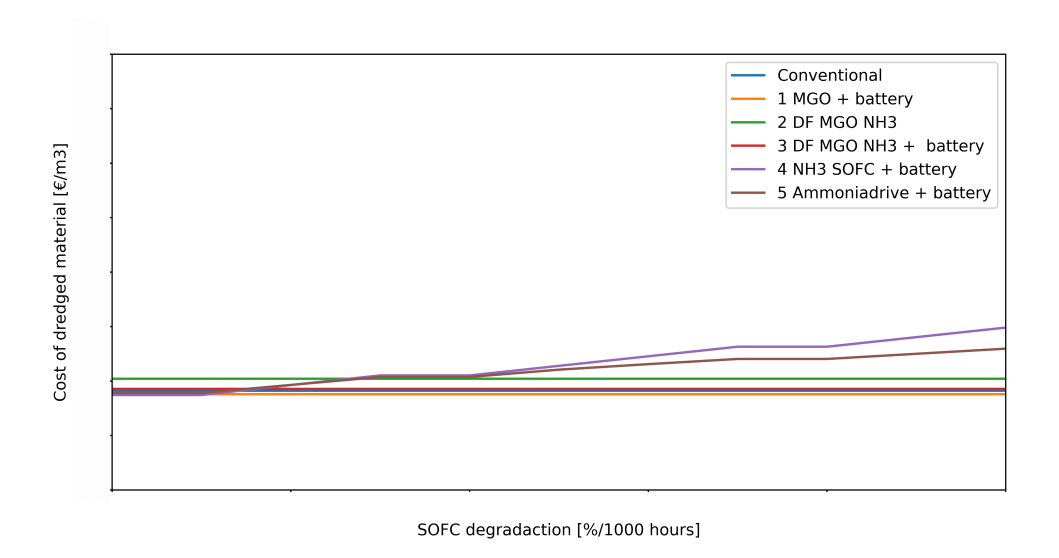


Figure 7.6: The cost of dredged material for different SOFC degradation for every configuration for scenario 1.

3 is shown in Appendix B.1.5.

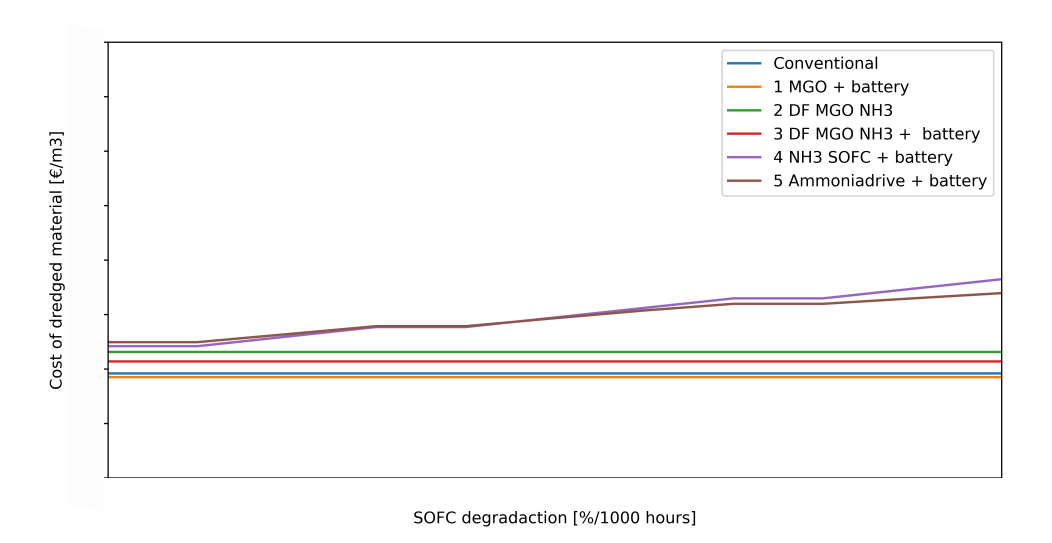


Figure 7.7: The cost of dredged material for different SOFC degradation for every configuration for scenario 2.

Currently the SOFC degradation is 1%, every 1000 hours and the target for the future is 0.2% for every 1000 hours.

7.7. Conclusion

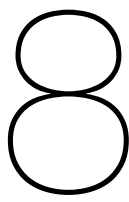
First of all , ammonia can definitely decarbonize a TSHD. As for every configuration that uses green ammonia as a fuel the WTW \mathcal{CO}_{2eq} emissions are reduced. Furthermore, for the configurations that

7.7. Conclusion 53

are using a SOFC, the WTW ${\it CO}_{\it 2eq}$ emissions are zero or near zero.

Currently, with the business-as-usual parameters it is not economically feasible to use ammonia as a fuel for a trailing suction hopper dredger across all three scenarios. The price of drive train systems and green ammonia is still to expensive. However, the future prices of fuel, carbon, and SOFC and it degradation are not 100% certain and likely to vary significantly.

Thus, ammonia can be an economically viable option to decarbonize a TSHD when the price of ammonia (Scenario: 50%, 100%, 75%) and SOFC (Scenario: 75%, -, -) decreases, or the price of MGO (Scenario: 50%, 100%, 300%) and carbon (Scenario: 100%, -, 600%) increases for all scenarios respectively



Discussion

This research shows that it can be economically feasible to decarbonize a TSHD with an installed power of 23 MW, By using ammonia if and only if the carbon or MGO price rises or the ammonia or SOFC price decreases. A TSHD configuration was deemed economically feasible if it was cheaper to use ammonia than a configuration using MGO. It was clear that grey ammonia, due to its high WTT ${\cal CO}_{2eq}$ emissions could hardly decarbonize a TSHD because its higher WTW ${\cal CO}_{2eq}$ emissions than MGO, when assuming equal power train efficiencies.

During a previous study of Valeria-Medina et all concluded that an ultra-large container vessel that would use an ammonia engine with an integrated cracker would cost (CAPEX and OPEX over lifetime) almost twice as much over the total lifetime of the vessel [84]. However, this study did not include a carbon tax in the total lifetime cost of the vessel. In that study, the carbon tax was not included in the total lifetime cost of a vessel. Green ammonia was assumed as fuel, and therefore the CO_{2eq} WTW emissions were assumed low. If the carbon tax was included in the total cost over the lifetime, then the cost difference between a vessel on conventional fuels and an ammonia vessel would be lower.

Another study of Wu et all found that an ammonia SOFC has a comparable cost to an HFO ICE over the lifespan of a container ship [133]. A container vessel has a more constant operational profile, and transient loads are less present than on a TSHD. A container vessel will be sailing for a long time, while a TSHD will only sail for a couple of hours and then switch to another operational mode, such as dredging. Due to the constant sailing operation of a container vessel, a configuration with a SOFC is more attractive for a container vessel than for a TSHD, because less energy has to be wasted during longer operational modes. Therefore, it is reasonable to conclude that for a TSHD with the business-as-usual parameters, an ammonia SOFC is more expensive than an MGO configuration.

Additionally, a study of Cornelius investigated the cost of an SOFC-powered TSHD and concluded that an SOFC with ammonia can reduce carbon emissions [134]. This is in line with my research, where a SOFC fueled with green ammonia was assumed to have no WTW carbon emissions.

During this research, approximately 200 simulations have been conducted. To more accurately determine the lowest price for each configuration, a wider range of setups should be simulated. Also, the step size for the installed power was set at 1,000 kW, for time constraint reasons. For each output of fuel consumption, for every simulation that passed all the tests, the costs were calculated. A better optimized result can be achieved when the simulation optimizes to the lowest cost per dredged material $[\epsilon/m^3]$ directly.

Furthermore, a more sophisticated power management strategy can be applied to the setups, allowing engines to be shut off or turned on as required. This can reduce the amount of wasted energy in setups where an SOFC or ammonia/hydrogen ICE is present. Currently, the Ammoniadrive + battery and the ammonia SOFC + battery configuration waste a significant amount of energy. By implementing a more sophisticated power management strategy, these two configurations will be more energy efficient over the 30 days. Therefore, these configurations will become economically more attractive.

During this research, only the power supply was changed, and the power demand was kept unchanged as measured for the TSHD in operation over a 30 day period. The high transient loads in the power demand (which were incorporated in the model, the model stopped if the transient load was to high) posed issues for the configurations that use ammonia. If the transient loads can be reduced, it

would be beneficial for an ICE and a SOFC running on ammonia. For a configuration consisting of a SOFC, with the absence of transient loads, the battery capacity and/or the C-rating of the battery can be reduced. Furthermore, a dual-fuel ammonia/hydrogen ICE could also be possible without a battery then.

Additionally, the used transient load capabilities (the chosen maximum change of engine load per second which result in a maximum dP/dt) have a direct influence on ICE or SOFC load and thus the fuel consumption during the simulation of the configurations. All configurations except configuration 4 and 5 were assumed to have a unlimited transient load behaviour.

For configuration 4 (Ammonia SOFC + battery) the transient load capabilities were assumed at to completely absent. The SOFC had a constant power output over time, meaning the load would not increase or decrease. The result is that energy is destroyed, when the battery is full and the power demand is lower than the power output. This will results in a higher fuel consumption than. A system with SOFC stacks that can be turned on or off could be a solution.

For configuration 5 (Ammoniadrive + battery) the transient load capabilities for the ICE were set at a maximum change of engine load per second of 2%. Meaning that the ICE could increase its engine load with 2% each second. Also, the minimum engine load for configuration 5 was set at the optimum (85% of the installed ICE capacity) engine load. Meaning that the engine load for this configuration could not go below the optimum engine load. The reason for this choice is that if the engine load would be decreased to a low power output when the power demand was low, due to the low maximum transient load capabilities, the engine output could not have increased fast enough to cope with the high power demand. Due to this choice in the simulation, this configuration will waste/destroy energy, when the battery is full and the power output is higher than the power demand. Therefore, the full consumption is higher than preferred in this configuration.

The fuel consumption for all configurations is based on the fuel consumption of the Vox Amalia during operation. When estimating the fuel consumption, the trend of the fuel consumption could be accurately estimated (after using a correction factor) within 0% difference. However, for individual weeks the fuel consumption is not accurately estimated. For the simulation the fuel consumption was estimated for only 30 days (more than 4 weeks). However, the total costs (and thus cost of fuel) is extrapolated to a 25 year lifetime. The fuel consumption will be different for different projects in reality, due the different power demand. The kustlijnzorg project was a project with a very high power demand. Thus in the 25 year lifespan of the vessel, the Vox Amalia will also dredge on projects with a lower power demand. Therefore fuel consumption on other projects will be lower than is estimated in this simulation. Furthermore, the fuel is estimated with one engine instead of the three main engines and a correction factor is used to still get an accurate fuel estimation.

The fuel consumption of a dual-fuel ammonia/MGO engine and a dual-fuel ammonia/hydrogen engine was estimated with a correction factor. This factor was based on the TRL and the poor combustion characteristics of ammonia.

Furthermore, the extra weight due to the different tanks is not taken into account. An ammonia tanks needs to be pressurized to 8 bar, while an MGO can be stored at ambient conditions. Therefore, an ammonia tank is more heavy than a MGO tank. This would further increase the weight of configurations that use ammonia and this is not incorporated in this research. Additionally, the physical implementation of the SOFC, engines, ammonia and storage is not taken into account. As mentioned ammonia will be stored pressurized, and therefore a cylindrical tank will be used. Thus, ammonia tanks cannot be placed where the MGO tanks are located now.

It was assumed that the battery of the TSHD was full at the start of the 30 day simulation. The costs for a full battery were not incorporated. The cost for a charging the battery once would result in a weekly cost, that is less than 0.2% of the total weekly costs. Therefore, these cost could be neglected for the cost calculations. Additionally, it is assumed that the battery is charged with green electricity in the port. Therefore, the emissions that are emitted for charging the battery at the port are assumed to be zero.

Also, the loading process of a hopper is assumed to be constant over time, which is not the case in reality. Therefore, the influence of a lower hopper capacity on the production capacity could be more accurately estimated in the future. Moreover, the additional safety measures required for handling ammonia are not included.

This work has given high level insight into different power train configurations based on ammonia as a marine fuel. A model was used for simulations with assumptions for the transient load and fuel

56 8. Discussion

consumption as a output. The aspects discussed above should be taken into account in future work to get more in-depth insight into which configuration is applicable for powering a future-proof TSHD. It is expected that the configurations on ammonia become economically more attractive from a more in-depth analysis for the transient loads and a power management system. When the practical side of the ammonia configuration (safety and storage) is investigated more in depth, issues of the physical implication may arise.



Conclusion

The research objective was to determine if it is economically viable to use ammonia as a fuel to decarbonize a trailing suction hopper dredger (TSHD). This question is answered with the following findings;

Ammonia has the advantage over other alternative fuels, there is already an industry in the production of ammonia. However, the production for both grey and green ammonia is currently not on a scale that is ready to support the maritime industry. Furthermore, the price of technology is 50% cheaper for ammonia in comparison with hydrogen, and ammonia can be carbon-free when produced green and used in combination with a fuel cell.

Ammonia can both be used as fuel in an internal combustion engine (ICE) and a fuel cell. Ammonia has poor combustion properties, and therefore, a promoter such as hydrogen or MGO is required to promote combustion. Moreover, the transient load capability of ammonia in combination with an ICE is low, and a solid oxide fuel cell (SOFC) has almost no transient load capabilities. The set transient load capability for ammonia in an ICE is 600 kW/s with an installed power of 30,000 kW.

The cycle of a TSHD consists of sailing empty, dredging, sailing full, and discharging. In each of these operations, different consumers are used. During dredging and discharging, the power demand is the highest due to the use of both the propellers, dredge pumps, and jet pumps.

The transient loads during dredging are mainly due to the change in propulsion power during dredging. This propulsion power is a function of drag force and vessel speed. During dredging the vessel speed changes significantly. furthermore, is the friction force of the draghead dependant on the soil characteristics and the failure mechanism of the soil. A sudden change in mixture density can result in a sudden change in power demand.

Due to the high transient load experienced during dredging, the power supply needs to be able to handle these transient loads. In that way the transient loads can be handled by a battery. Additionally, the transient loads can be handled with MGO. Furthermore, the ammonia drive concept is an integration between an ICE, SOFC, and a battery. While the SOFC on ammonia is unable to handle transient loads, the ICE with ammonia has an maximum change of engine load per second of 2%, and a battery can handle the transient depending on the C-rating.

A model was created to determine the minimal installed power and battery capacity. This model also checked if the configuration could handle the dP/dt. During this research, the following three scenarios have been investigated:

- Scenario 1, Only the TTW CO_{2eq} emissions are taxed
- Scenario 2, the WTW CO_{2eq} emissions are taxed and grey ammonia is used
- Scenario 3, The WTW CO_{2eq} emissions are taxed and green ammonia is used

Currently, with the business-as-usual parameters, it is not economically viable to use ammonia as a fuel because it is cheaper to use MGO in combination with a battery for all three scenarios. It is clear that ammonia can decarbonize a TSHD for scenarios 1 and 3. Furthermore, for scenario 2, grey ammonia cannot decarbonize a TSHD by definition.

58 9. Conclusion

A sensitivity analysis has been done on fuel costs, carbon taxes, the component price of the SOFC, and the degradation of the SOFC.

First of all, if the carbon tax doubles (€200/ton), then ammonia is an economically feasible option for scenario 1. For scenario 2, ammonia is not a feasible option, regardless of the price of carbon. For scenario 3, the carbon tax has to be €700/kW, which seems unlikely in the near future.

If the current MGO price (€769/ton) increases by 50%, 100%, and 300% for scenarios 1, 2, and 3, then ammonia is an economically feasible fuel for a TSHD. An increase of 50% is certainly possible in the near future.

The price of grey ammonia needs to halve to €200/ton to make it the best option in terms of cost for scenario 1. For scenario 2, when grey ammonia is provided at no cost, then sailing on ammonia becomes cheaper. When the price of green ammonia also drops to €300/ton, then ammonia is economically feasible to use as a fuel.

When the cost of an SOFC system decreases by 4 times with respect to the current price (€1336/kW), then ammonia becomes an economically feasible option. For scenarios 2 and 3, even when the SOFC system is supplied for free, configurations using ammonia are the more expensive option.

If the SOFC does not need replacement in the 25-year lifetime of a TSHD, then ammonia is an economically feasible option for scenario 1. However, for scenarios 2 and 3, regardless of the SOFC degradation, configurations on MGO are a better option in terms of cost than configurations that use ammonia as a fuel.

Thus, ammonia can be an economically viable option to decarbonize a TSHD when the price of ammonia (Scenario: 50%, 100%, 75%) and SOFC (Scenario: 75%, -, -) decreases, or the price of MGO (Scenario: 50%, 100%, 300%) and carbon (Scenario: 100%, -, 600%) increases for all scenarios respectively. Currently, the production of commercially available drivetrain configurations on ammonia is not available. Improvements in transient load capabilities and efficiency of ammonia drivetrain systems can reduce fuel consumption and improve the economic feasibility of certain configurations. Furthermore, green ammonia production needs to be developed and increased before it can be globally used as a maritime fuel.

9.1. Recommendations

In the future all configurations could be better optimized. For example, during the simulations, the installed power and battery capacity was adjusted with increments of 1,000 kW. If this step size is changed to 100 kW. Then, each configuration would be more optimized for the power demand. Additionally, the simulation itself could simulate to the lowest cost per dredged material directly with a precision of 1 kW instead of the steps of 1,000 kW. The result would be a lower total cost for each configuration.

Also, a more detailed power management strategy can be developed in future research. A power management system were engines are turned on and off are an interesting addition. When the power demand is lower, then less engines could possibly be used. The influence of a changing stack load should also be investigated in the future. During this research the stack load was kept constant at 80%.

The simulation for the fuel consumption can be done for multiple projects in the future. For this research only the project with the highest power demand was chosen. A high power demand results in a high fuel consumption. During the 25 year lifespan of the Vox Amalia, the Vox Amalia will dredge on different projects where each a project has a different power demand and thus a different weekly fuel consumption. When a variety of projects is used for the fuel consumption, the fuel consumption will be more accurate for the lifespan of a vessel.

The loading process of a hopper dredger could be investigated in more detail in future research. During this research the loading process of a hopper was assumed to be linear over time. However, in reality at the start of the dredging process, the production is the highest and when the hopper is almost full, the production is the lowest. If this effect is incorporated, a more accurate estimation for the weekly dredge production can then be made when the weight of the vessel changes due to the addition of extra fuel or batteries.

The weight of the ammonia tanks is not incorporated in the weight calculations. If this additional weight would be incorporated, then the total weight of a vessel would change. This would then result in a different weekly dredge production. However, this difference is expected to be small.

The volumetric constraints are not taken into account during this research. The available space on a

9.1. Recommendations 59

TSHD and the space required for the new equipment (SOFC, battery and fuel) should be investigated. It is possible that there is not enough space on board and that the hopper or the range of the vessel need to be decreased in order for a configuration to be physically feasible.

Finally, the power demand can be investigated more in-depth in the future. Opportunities to reduce the transient loads during dredging or discharging should be investigated. If these transient load can be reduced, then configurations on ammonia can become economically more attractive.

- [1] European Commission, Reducing emissions from the shipping sector, 2022. [Online]. Available: https://climate.ec.europa.eu/eu-action/transport-emissions/reducing-emissions-shipping-sector en.
- [2] U. states environmental protection agency, *Overview of Greenhouse gases*, May 2022. [Online]. Available: https://www.epa.gov/ghgemissions/overview-greenhouse-gases.
- [3] J. van 't Hoff, J. Alkema, L. van der Graaf, et al., Baggerwerken 5b Sleephopperzuiger, 2010th ed. Gouda, nl: Vereniging van Waterbouwers, 2010.
- [4] A. T. Wijayanta, T. Oda, C. W. Purnomo, T. Kashiwagi, and M. Aziz, "Liquid hydrogen, methyl-cyclohexane, and ammonia as potential hydrogen storage: Comparison review," *International Journal of Hydrogen Energy*, vol. 44, no. 29, pp. 15 026–15 044, 2019, ISSN: 0360-3199. DOI: https://doi.org/10.1016/j.ijhydene.2019.04.112. [Online]. Available: https://www.sciencedirect.com/science/article/pii/S0360319919315411.
- [5] N. Salmon and R. Bañares-Alcántara, "Green ammonia as a spatial energy vector: A review," Sustainable Energy Fuels, vol. 5, pp. 2814–2839, 11 2021. DOI: 10.1039/D1SE00345C. [Online]. Available: http://dx.doi.org/10.1039/D1SE00345C.
- [6] A. Valera-Medina, H. Xiao, M. Owen-Jones, W. I. David, and P. Bowen, "Ammonia for power," *Progress in Energy and combustion science*, vol. 69, pp. 63–102, 2018.
- [7] J. Humphreys, R. Lan, and S. Tao, "Development and recent progress on ammonia synthesis catalysts for haber–bosch process," *Advanced Energy and Sustainability Research*, vol. 2, no. 1, p. 2000043,
- [8] I. Dincer and C. Zamfirescu, "A review of novel energy options for clean rail applications," *Journal of Natural Gas Science and Engineering*, vol. 28, pp. 461–478, 2016.
- [9] E. Lindstad, B. Lagemann, A. Rialland, G. M. Gamlem, and A. Valland, "Reduction of maritime ghg emissions and the potential role of e-fuels," *Transportation Research Part D: Transport and Environment*, vol. 101, p. 103 075, 2021.
- [10] D. Erdemir and I. Dincer, A perspective on the use of ammonia as a clean fuel: Challenges and solutions, 2021.
- [11] J. R. Bartels, A feasibility study of implementing an Ammonia Economy. Iowa State University, 2008.
- [12] A. Afif, N. Radenahmad, Q. Cheok, S. Shams, J. H. Kim, and A. K. Azad, "Ammonia-fed fuel cells: A comprehensive review," *Renewable and Sustainable Energy Reviews*, vol. 60, pp. 822–835, 2016.
- [13] S. Giddey, S. Badwal, and A. Kulkarni, "Review of electrochemical ammonia production technologies and materials," *International Journal of Hydrogen Energy*, vol. 38, no. 34, pp. 14 576–14 594, 2013.
- [14] A. Araújo and S. Skogestad, "Control structure design for the ammonia synthesis process," *Computers & Chemical Engineering*, vol. 32, no. 12, pp. 2920–2932, 2008.
- [15] A. Yapicioglu and I. Dincer, "A review on clean ammonia as a potential fuel for power generators," *Renewable and sustainable energy reviews*, vol. 103, pp. 96–108, 2019.
- [16] G. Mallouppas, C. Ioannou, and E. A. Yfantis, "A review of the latest trends in the use of green ammonia as an energy carrier in maritime industry," *Energies*, vol. 15, no. 4, 2022, ISSN: 1996-1073. DOI: 10.3390/en15041453. [Online]. Available: https://www.mdpi.com/1996-1073/15/4/1453.

[17] A. T. Wijayanta and M. Aziz, "Ammonia production from algae via integrated hydrothermal gasification, chemical looping, n2 production, and nh3 synthesis," *Energy*, vol. 174, pp. 331–338, 2019.

- [18] M. Aziz, A. T. Wijayanta, and A. B. D. Nandiyanto, "Ammonia as effective hydrogen storage: A review on production, storage and utilization," *Energies*, vol. 13, no. 12, p. 3062, 2020.
- [19] Engineering Toolbox, Fuels Higher and Lower Calorific Values, 2003. [Online]. Available: https://www.engineeringtoolbox.com/fuels-higher-calorific-values-d 169.html.
- [20] inchem, ICSC 0001 HYDROGEN. [Online]. Available: https://inchem.org/documents/icsc/icsc/eics0001.htm.
- [21] inchem, ICSC 0414 AMMONIA (ANHYDROUS). [Online]. Available: https://www.inchem.org/documents/icsc/icsc/eics0414.htm.
- [22] inchem, ICSC 0291 METHANE. [Online]. Available: https://inchem.org/documents/icsc/icsc/eics0291.htm.
- [23] Neste, SAFETY DATA SHEET Marine Diesel Oil DMB grade (MDODMB), Dec. 2017.
- [24] Fuels and chemicals Autoignition temperatures. [Online]. Available: https://www.engineeringtoolbox.com/fuels-ignition-temperatures-d 171.html.
- [25] A. Klerke, C. H. Christensen, J. K. Nørskov, and T. Vegge, "Ammonia for hydrogen storage: Challenges and opportunities," *Journal of Materials Chemistry*, vol. 18, no. 20, pp. 2304–2310, 2008.
- [26] Y. Wang, S. Zheng, J. Chen, Z. Wang, and S. He, "Ammonia (nh3) storage for massive pv electricity," *Energy Procedia*, vol. 150, pp. 99–105, 2018.
- [27] A. Züttel, "Hydrogen storage methods," *Naturwissenschaften*, vol. 91, no. 4, pp. 157–172, 2004.
- [28] Y. Kojima, "A green ammonia economy," in 10th annual NH 10th annual NH3 fuel conference, 2013.
- [29] B. Veldhuizen, L. van Biert, K. Visser, and H. Hopman, "Comparative analysis of alternative fuels for marine sofc systems," Oct. 2022.
- [30] A. Buis and NASA, *The Atmosphere: Getting a Handle on Carbon Dioxide*, Nov. 2022. [Online]. Available: https://climate.nasa.gov/news/2915/the-atmosphere-getting-a-handle-on-carbon-dioxide/.
- [31] R. H. Thurston, A History of the Growth of the Steam-Engine. D. Appleton, 1878, vol. 24.
- [32] Z. Mario, Device for operating internal combustion engines with mixtures of ammonia, hydrogen, and nitrogen prepared from ammonia, US Patent 2,140,254, Dec. 1938.
- [33] W. Corporation, "World's first full scale ammonia engine test an important step towards carbon free shipping," Jun. 2020. [Online]. Available: https://www.wartsila.com/media/news/30-06-2020-world-s-first-full-scale-ammonia-engine-test---an-important-step-towards-carbon-free-shipping-2737809.
- [34] H. Kobayashi, A. Hayakawa, K. K. A. Somarathne, and E. C. Okafor, "Science and technology of ammonia combustion," *Proceedings of the Combustion Institute*, vol. 37, no. 1, pp. 109–133, 2019.
- [35] C. Lhuillier, P. Brequigny, F. Contino, and C. Mounaim-Rousselle, "Experimental study on ammonia/hydrogen/air combustion in spark ignition engine conditions," *Fuel*, vol. 269, p. 117 448, 2020.
- [36] A. J. Reiter and S.-C. Kong, "Combustion and emissions characteristics of compression-ignition engine using dual ammonia-diesel fuel," *Fuel*, vol. 90, no. 1, pp. 87–97, 2011.
- [37] C. Lhuillier, P. Brequigny, F. Contino, and C. Mounaim-Rousselle, "Combustion characteristics of ammonia in a modern spark-ignition engine," in *Conference on Sustainable Mobility*, 2019.
- [38] B. Zincir, "A short review of ammonia as an alternative marine fuel for decarbonised maritime transportation," *Proceedings of the ICEESEN2020, Kayseri, Turkey*, pp. 19–21, 2020.

[39] K. Kamasamudram, C. Henry, N. Currier, and A. Yezerets, "N□o formation and mitigation in diesel aftertreatment systems," *SAE International Journal of Engines*, vol. 5, no. 2, pp. 688–698, 2012.

- [40] B. Chandrasekhar, *Concept of Marine Compression Ignition Engines*, May 2021. [Online]. Available: https://www.marinesite.info/2021/05/concept-of-marine-compression-ignition.html.
- [41] P. J. Feibelman and R. Stumpf, "Comments on potential roles of ammonia in a hydrogen economy— a study of issues related to the use of ammonia for on-board vehicular hydrogen storage," *Sandia Natl. Lab*, 2006.
- [42] C. S. Mørch, A. Bjerre, M. P. Gøttrup, S. C. Sorenson, and J. Schramm, "Ammonia/hydrogen mixtures in an si-engine: Engine performance and analysis of a proposed fuel system," *fuel*, vol. 90, no. 2, pp. 854–864, 2011.
- [43] P. Dimitriou and R. Javaid, "A review of ammonia as a compression ignition engine fuel," *International Journal of Hydrogen Energy*, vol. 45, no. 11, pp. 7098–7118, 2020.
- [44] A. J. Reiter and S.-C. Kong, "Demonstration of compression-ignition engine combustion using ammonia in reducing greenhouse gas emissions," *Energy & Fuels*, vol. 22, no. 5, pp. 2963–2971, 2008.
- [45] E. S. Starkman, H. Newhall, R. Sutton, T. Maguire, and L. Farbar, "Ammonia as a spark ignition engine fuel: Theory and application," *Sae Transactions*, pp. 765–784, 1967.
- [46] P. Mishra, How Spark Ignition Engine Works? Dec. 2017. [Online]. Available: https://www.mechanicalbooster.com/2017/10/spark-ignition-engine.html.
- [47] K. Ryu, G. E. Zacharakis-Jutz, and S.-C. Kong, "Effects of gaseous ammonia direct injection on performance characteristics of a spark-ignition engine," *Applied energy*, vol. 116, pp. 206–215, 2014.
- [48] S. Frigo and R. Gentili, "Analysis of the behaviour of a 4-stroke si engine fuelled with ammonia and hydrogen," *International Journal of Hydrogen Energy*, vol. 38, no. 3, pp. 1607–1615, 2013.
- [49] I. maritime organization, Nitrogen Oxides (NOx) Regulation 13. [Online]. Available: https://www.imo.org/en/OurWork/Environment/Pages/Nitrogen-oxides-(NOx)-%5C%E2%5C%80%5C%93-Regulation-13.aspx.
- [50] L. Liu, Y. Wu, and Y. Wang, "Numerical investigation on the combustion and emission characteristics of ammonia in a low-speed two-stroke marine engine," *Fuel*, vol. 314, p. 122727, 2022.
- [51] M. energy solutions, "MAN B&W two-stroke engine operating on ammonia," Tech. Rep., Nov. 2020. [Online]. Available: https://www.man-es.com/docs/default-source/document-sync/man-b-w-two-stroke-engine-operating-on-ammonia-eng.pdf?sfvrsn=c4bb6fea 0.
- [52] M. P. Ruggeri, J. Luo, I. Nova, E. Tronconi, K. Kamasamudram, and A. Yezerets, "Novel method of ammonium nitrate quantification in scr catalysts," *Catalysis Today*, vol. 307, pp. 48–54, 2018.
- [53] G. Feick and R. Hainer, "On the thermal decomposition of ammonium nitrate. steady-state reaction temperatures and reaction rate," *Journal of the American Chemical Society*, vol. 76, no. 22, pp. 5860–5863, 1954.
- [54] G. J. Bartley and C. A. Sharp, "Brief investigation of scr high temperature n□o production," *SAE International Journal of Engines*, vol. 5, no. 2, pp. 683–687, 2012.
- [55] C. Song, "Fuel processing for low-temperature and high-temperature fuel cells: Challenges, and opportunities for sustainable development in the 21st century," *Catalysis today*, vol. 77, no. 1-2, pp. 17–49, 2002.
- [56] O. of energy efficiency & renewable energy, *Fuel Cells*. [Online]. Available: https://www.energy.gov/eere/fuelcells/fuel-cells.
- [57] G. Jeerh, M. Zhang, and S. Tao, "Recent progress in ammonia fuel cells and their potential applications," *Journal of Materials Chemistry A*, vol. 9, no. 2, pp. 727–752, 2021.

[58] T. Tronstad, H. H. Åstrand, G.-P. Haugom, and L. Langfeldt, "Study on the use of fuel cells in shipping," 2017.

- [59] L. Carrette, K. A. Friedrich, and U. Stimming, "Fuel cells: Principles, types, fuels, and applications," *ChemPhysChem*, vol. 1, no. 4, pp. 162–193, 2000.
- [60] G. B. Gharehpetian and M. Mousavi, *Distributed generation systems: design, operation and grid integration*. Butterworth-Heinemann, 2017.
- [61] L. van Biert, M. Godjevac, K. Visser, and P. Aravind, "A review of fuel cell systems for maritime applications," *Journal of Power Sources*, vol. 327, pp. 345–364, 2016.
- [62] F. Garzon, T. Lopes, T. Rockward, J.-M. Sansiñena, B. Kienitz, and R. Mukundan, "The impact of impurities on long-term pemfc performance," *Ecs Transactions*, vol. 25, no. 1, p. 1575, 2009.
- [63] M. Ni, D. Y. Leung, and M. K. Leung, "An improved electrochemical model for the nh3 fed proton conducting solid oxide fuel cells at intermediate temperatures," *Journal of Power Sources*, vol. 185, no. 1, pp. 233–240, 2008.
- [64] H. R. Ellamla, I. Staffell, P. Bujlo, B. G. Pollet, and S. Pasupathi, "Current status of fuel cell based combined heat and power systems for residential sector," *Journal of Power Sources*, vol. 293, pp. 312–328, 2015.
- [65] S. Giddey, S. Badwal, C. Munnings, and M. Dolan, "Ammonia as a renewable energy transportation media," *ACS Sustainable Chemistry & Engineering*, vol. 5, no. 11, pp. 10 231–10 239, 2017.
- [66] J. Staniforth and R. M. Ormerod, "Clean destruction of waste ammonia with consummate production of electrical power within a solid oxide fuel cell system," *Green Chemistry*, vol. 5, no. 5, pp. 606–609, 2003.
- [67] ShipFC, World's first ammonia fuel cell taking shape Zpirit, Jan. 2021. [Online]. Available: https://shipfc.eu/worlds-first-ammonia-fuel-cell-taking-shape/.
- [68] M. Kishimoto, H. Muroyama, S. Suzuki, *et al.*, "Development of 1 kw-class ammonia-fueled solid oxide fuel cell stack," *Fuel Cells*, vol. 20, no. 1, pp. 80–88, 2020.
- [69] S. Vora, Overview of SOFC Program at DOE NETL. [Online]. Available: https://netl.doe.gov/sites/default/files/netl-file/21SOFC Vora16.pdf.
- [70] A. Chellappa, C. Fischer, and W. Thomson, "Ammonia decomposition kinetics over ni-pt/al2o3 for pem fuel cell applications," *Applied Catalysis A: General*, vol. 227, no. 1-2, pp. 231–240, 2002.
- [71] S. Chiuta, R. C. Everson, H. W. Neomagus, P. Van der Gryp, and D. G. Bessarabov, "Reactor technology options for distributed hydrogen generation via ammonia decomposition: A review," *International journal of hydrogen energy*, vol. 38, no. 35, pp. 14 968–14 991, 2013.
- [72] Large-scale ammonia cracker to enable 1 million tonnes of hydrogen imports via port of Rotterdam, Dec. 2022. [Online]. Available: https://www.portofrotterdam.com/en/news-and-press-releases/large-scale-ammonia-cracker-to-enable-1-million-tonnes-of-hydrogen-imports.
- [73] I. DE VOS, I. TINGA, E. FOEKEMA, and B. VAN DER ZWAAN, "The ammoniadrive research project," *SWZ Maritime*, vol. 143, no. 7/8, pp. 24–27, 2022.
- [74] A. public schools, NFPA 704 Hazard Identification System Albuquerque Public Schools. [Online]. Available: https://www.aps.edu/risk-management/chemical-management/nfpa-704-hazard-identification-system.
- [75] N. L. of Medicine, NPFA Hazard Classification. [Online]. Available: https://webwiser.nlm.nih.gov/substance?substanceId=315.
- [76] H. Berrien Zettler, Highly Hazardous Chemical's anhydrous ammonia (NH(3)). | Occupational Safety and Health Administration, Jun. 1994. [Online]. Available: https://www.osha.gov/laws-regs/standardinterpretations/1994-06-02.
- [77] P. H. England, Ammonia: health effects, incident management and toxicology, Aug. 2019. [Online]. Available: https://www.gov.uk/government/publications/ammonia-properties-incident-management-and-toxicology.

[78] C. on Acute Exposure Guideline Levels *et al.*, "Acute exposure guideline levels for selected airborne chemicals: Volume 6.," *Acute exposure guideline levels for selected airborne chemicals: volume 6.*, 2008.

- [79] R. P. Padappayil and J. Borger, "Ammonia toxicity," in *StatPearls [Internet]*, StatPearls Publishing, 2022.
- [80] R. A. Michaels, "Emergency planning and the acute toxic potency of inhaled ammonia.," *Environmental health perspectives*, vol. 107, no. 8, pp. 617–627, 1999.
- [81] N. J. D. of Health, "Hazardous Substance Fact Sheet," Tech. Rep., Feb. 2016. [Online]. Available: https://nj.gov/health/eoh/rtkweb/documents/fs/0084.pdf.
- [82] NOS, "Ammoniakwold boven Servische stad, tientallen mensen vergiftigd," Dec. 2022. [Online]. Available: https://nos.nl/artikel/2457716-ammoniakwolk-boven-servischestad-tientallen-mensen-vergiftigd.
- [83] E. E. F. M. Association, "Guidance for transportation ammonia by rail," Tech. Rep., 2017. [Online]. Available: https://cefic.org/app/uploads/2018/12/Transporting-Ammonia_ByRail-by-EFMA-2007-GUIDELINES-ROAD-SUBSTANCE.
- [84] A. Valera-Medina and R. Banares-Alcantara, *Techno-economic challenges of green ammonia* as an energy vector. Academic Press, 2020.
- [85] K. Mori, A. Takamura, and T. Shimose, "Stress corrosion cracking off ti and zr in hcl-methanol solutions," *Corrosion*, vol. 22, no. 2, pp. 29–31, 1966.
- [86] Z. Salamonowicz, M. Majder-Lopatka, A. Dmochowska, W. Rogula-Kozlowska, A. Piechota-Polanczyk, and A. Polanczyk, "Ammonia dispersion in the closed space of an ammonia engine room with forced ventilation in an industrial plant," *Atmosphere*, vol. 13, no. 7, 2022, ISSN: 2073-4433. DOI: 10.3390/atmos13071062. [Online]. Available: https://www.mdpi.com/2073-4433/13/7/1062.
- [87] B. V. marine & offshore, "Ammonia-fuelled ships tentative rules NR671," Paris, fr, Tech. Rep. NR671, Jul. 2022. [Online]. Available: https://erules.veristar.com/dy/data/bv/pdf/671-NR_2022-07.pdf.
- [88] ClassNK, "Part C 'guidelines for the safety of ships using ammonia as a fuel'," Tech. Rep. [Online]. Available: https://www.classnk.or.jp/hp/pdf/research/rd/2022/05_e07.pdf.
- [89] W. R. Center, Surface Water: The Role and Hazard of Ammonia in the Surface Water Groundwater. [Online]. Available: https://www.knowyourh2o.com/outdoor-4/ammonia-in-groundwater-runoff-and-streams.
- [90] S. M. Levit, "A literature review of effects of ammonia on fish," *Montana*, 2010.
- [91] Allianz, Safety and Shipping Review 2022 | AGCS, May 2022. [Online]. Available: https://www.agcs.allianz.com/news-and-insights/reports/shipping-safety.html.
- [92] G. ter Meulen, "Draghead analysis: An analysis of the draghead's physical processes to determine the trailing forces and the production," 2018.
- [93] W. Shi, "Dynamics of energy system behaviour and emissions of trailing suction hopper dredgers," 2013
- [94] E. Ovrum and T. Bergh, "Modelling lithium-ion battery hybrid ship crane operation," *Applied Energy*, vol. 152, pp. 162–172, 2015.
- [95] M. van Leeuwen, "Hybrid solutions for cutter suction dredgers: A feasibility study on the application of electrical energy storage," 2017.
- [96] M. Gallucci, "The ammonia solution: Ammonia engines and fuel cells in cargo ships could slash their carbon emissions," *IEEE Spectrum*, vol. 58, no. 3, pp. 44–50, 2021. DOI: 10.1109/ MSPEC.2021.9370109.
- [97] T. Nguyen and R. F. Savinell, "Flow batteries," *The Electrochemical Society Interface*, vol. 19, no. 3, p. 54, 2010.

[98] J. R. Miller and A. Burke, "Electrochemical capacitors: Challenges and opportunities for real-world applications," *The electrochemical society interface*, vol. 17, no. 1, p. 53, 2008.

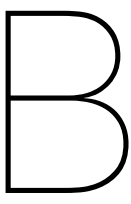
- [99] O. Alnes, S. Eriksen, and B.-J. Vartdal, "Battery-powered ships: A class society perspective," *IEEE Electrification Magazine*, vol. 5, no. 3, pp. 10–21, 2017.
- [100] P. Manimekalai, R. Harikumar, and S. Raghavan, "An overview of batteries for photovoltaic (pv) systems," *International Journal of Computer Applications*, vol. 82, no. 12, 2013.
- [101] E. .-. P. B. A. Software, *C-Rate of Batteries and Fast charging*. [Online]. Available: https://energsoft.com/blog/f/c-rate-of-batteries-and-fast-charging.
- [102] S.-J. Park, Y.-W. Song, B.-S. Kang, *et al.*, "Depth of discharge characteristics and control strategy to optimize electric vehicle battery life," *Journal of Energy Storage*, vol. 59, p. 106477, 2023.
- [103] J. F. Peters, M. Baumann, B. Zimmermann, J. Braun, and M. Weil, "The environmental impact of li-ion batteries and the role of key parameters—a review," *Renewable and Sustainable Energy Reviews*, vol. 67, pp. 491–506, 2017.
- [104] Yara, Yara Birkeland | Yara International, Sep. 2022. [Online]. Available: https://www.yara.com/news-and-media/media-library/press-kits/yara-birkeland-press-kit/.
- [105] J. Xie, P. Yang, Y. Wang, T. Qi, Y. Lei, and C. M. Li, "Puzzles and confusions in supercapacitor and battery: Theory and solutions," *Journal of Power Sources*, vol. 401, pp. 213–223, 2018.
- [106] J. R. Miller, "Perspective on electrochemical capacitor energy storage," *Applied Surface Science*, vol. 460, pp. 3–7, 2018.
- [107] J. L. Garcia, "9 electric power systems," in *Cubesat Handbook*, C. Cappelletti, S. Battistini, and B. K. Malphrus, Eds., Academic Press, 2021, pp. 185–197, ISBN: 978-0-12-817884-3. DOI: https://doi.org/10.1016/B978-0-12-817884-3.00009-6. [Online]. Available: https://www.sciencedirect.com/science/article/pii/B9780128178843000096.
- [108] R. Vellacheri, A. Al-Haddad, H. Zhao, W. Wang, C. Wang, and Y. Lei, "High performance supercapacitor for efficient energy storage under extreme environmental temperatures," *Nano Energy*, vol. 8, pp. 231–237, 2014.
- [109] L. Nègre, B. Daffos, V. Turq, P.-L. Taberna, and P. Simon, "lonogel-based solid-state supercapacitor operating over a wide range of temperature," *Electrochimica Acta*, vol. 206, pp. 490– 495, 2016.
- [110] İ. I. GÜRTEN, "Scalable activated carbon/graphene based supercapacitors with improved capacitanceretention at high current densities," *Turkish Journal of Chemistry*, vol. 45, no. 3, pp. 927–941, 2021.
- [111] Y. Wang, J. Wang, X. Zhang, D. Bhattacharyya, and E. M. Sabolsky, "Quantifying environmental and economic impacts of highly porous activated carbon from lignocellulosic biomass for highperformance supercapacitors," *Energies*, vol. 15, no. 1, p. 351, 2022.
- [112] V. engineering, Spartacus Cutter Suction Dredger. [Online]. Available: https://vuykrotterdam.com/projects/spartacus-cutter-suction-dredger.
- [113] C. van Rhee, "Lecture Notes OE44045," Tech. Rep., Apr. 2018.
- [114] R. Ferguson and M. Church, "A simple universal equation for grain settling velocity," *Journal of sedimentary Research*, vol. 74, no. 6, pp. 933–937, 2004.
- [115] C. Energy, Corvus Blue Whale Corvus Energy, Feb. 2023. [Online]. Available: https://corvusenergy.com/products/energy-storage-solutions/corvus-blue-whale/.
- [116] C. Energy, Corvus Dolphin Energy Corvus Energy, Feb. 2023. [Online]. Available: https://corvusenergy.com/products/energy-storage-solutions/corvus-dolphin-energy/.
- [117] Echandia, Technical Data Sheet ECHANDIA ENERGY & ECHANDIA POWER, Jan. 2022.

[118] A. Rajewski, "Evaluating internal combustion engine's performance," Dec. 2018. [Online]. Available: https://www.wartsila.com/insights/article/evaluating-internal-combustion-engine-s-performance.

- [119] S. Farhad and A. Nazari, "Introducing the energy efficiency map of lithium-ion batteries," *International Journal of Energy Research*, vol. 43, no. 2, pp. 931–944, 2019.
- [120] M. A. Dijkman, "Solving the lng load response challenge," 2016.
- [121] R. Bray, C. I. Research, and I. Association, *A Guide to Cost Standards for Dredging Equipment* 2009. CIRIA, 2009.
- [122] ciria, "Guide to cost standards for dredging equipment indexation 2023," Tech. Rep., 2023. [Online]. Available: https://www.ciria.org/CIRIA/Resources/Free_publications/C684.aspx.
- [123] J. van 't Hoff, *Baggerwerken 11 planning en kostenbegroting*, 2019th ed. Den Haag, nl: Vereniging van waterbouwers, 2010.
- [124] "Rough costprice calculation of TSHD's and CSD's," Tech. Rep.
- [125] E. council of the european union, "General approach EU ETS," Tech. Rep., Jun. 2022. [Online]. Available: https://data.consilium.europa.eu/doc/document/ST-10796-2022-INIT/x/pdf.
- [126] T. ECONOMICS, EU Carbon Permits 2023 Data 2005-2022 Historical 2024 Forecast Price Quote. [Online]. Available: https://tradingeconomics.com/commodity/carbon.
- [127] R. N. Bray, A. Bates, and J. Land, *Dredging: a handbook for engineers*. 1997.
- [128] M. E. Solutions, "Batteries on board ocean-going vessels," Tech. Rep., Sep. 2019. [Online]. Available: https://staticl.squarespace.com/static/5f0d42f16639a745affd633e/t/5ffac248fb26793593c04d70/1610269269784/batteries-on-board-ocean-going-vessels.pdf.
- [129] Rotterdam Bunker Prices, Jul. 2023. [Online]. Available: https://shipandbunker.com/prices/emea/nwe/nl-rtm-rotterdam#MGO.
- [130] H. E.-E. M. Perez, "S&P Global Commodity Insights," Jun. 2023. [Online]. Available: https://www.spglobal.com/commodityinsights/en/market-insights/latest-news/energy-transition/051023-interactive-ammonia-price-chart-natural-gas-feedstock-europe-usgc-black-sea.
- [131] E. Parliament, "Raising ambition levels at the IMO for 2050," Tech. Rep., Jun. 2023. [Online]. Available: https://www.europarl.europa.eu/RegData/etudes/BRIE/2023/740089/IPOL BRI(2023)740089 EN.pdf.
- [132] R. Scataglini, M. Wei, A. Mayyas, S. H. Chan, T. Lipman, and M. Santarelli, "A direct manufacturing cost model for solid-oxide fuel cell stacks," *Fuel Cells*, vol. 17, no. 6, pp. 825–842, 2017.
- [133] S. Wu, B. Miao, and S. H. Chan, "Feasibility assessment of a container ship applying ammonia cracker-integrated solid oxide fuel cell technology," *International Journal of Hydrogen Energy*, vol. 47, no. 63, pp. 27166–27176, 2022.
- [134] T. Cornelius, Evaluation study for an ammonia-fed and solid-oxide fuel cell powered trailing suction hopper dredger for Van oord Offshore Contractors.



Power of the past projects -



Appendix B

B.1. Results B.1.1. Carbon tax

— Conventional — 1 MGO + battery — 2 DF MGO NH3 — 3 DF MGO NH3 + battery — 4 NH3 SOFC + battery — 5 Ammoniadrive + battery

Figure B.1: The cost of dredged material for different carbon tax for every configuration for scenario 3.

B.1. Results 69

B.1.2. MGO cost

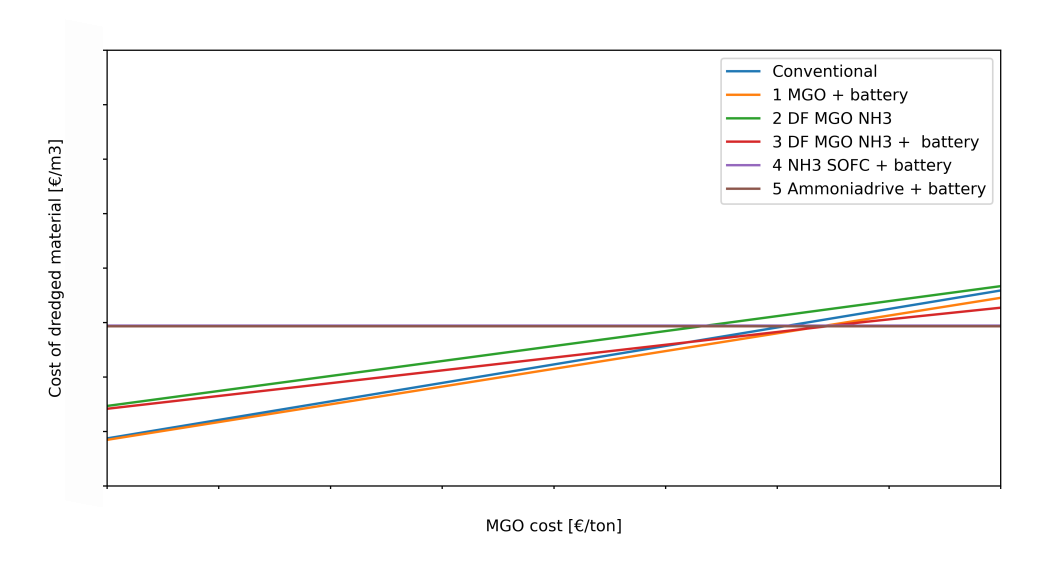


Figure B.2: The cost of dredged material for different MGO cost for every configuration for scenario 2.

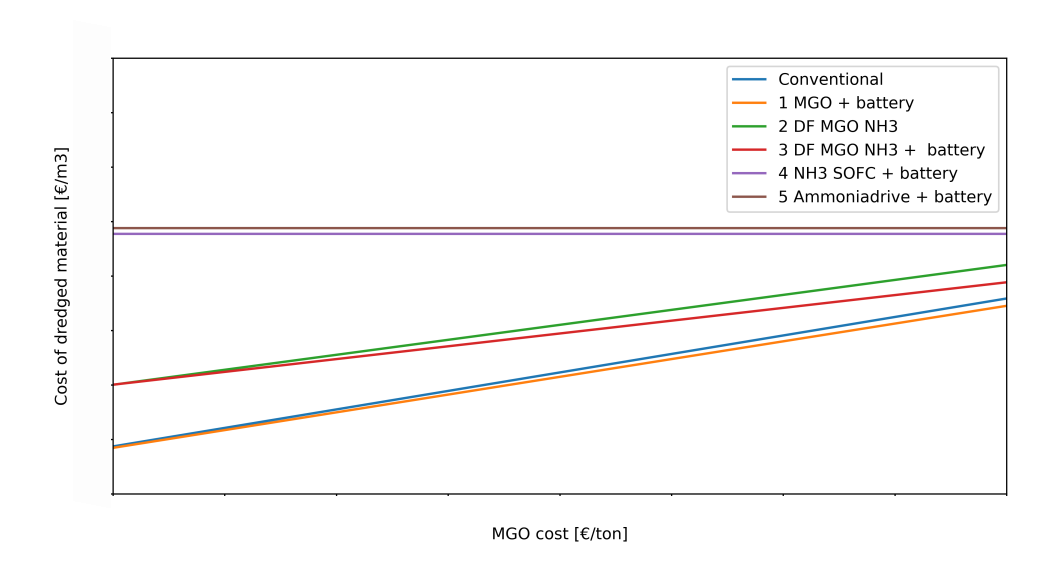


Figure B.3: The cost of dredged material for different MGO cost for every configuration for scenario 3.

70 B. Appendix B

B.1.3. Ammonia cost

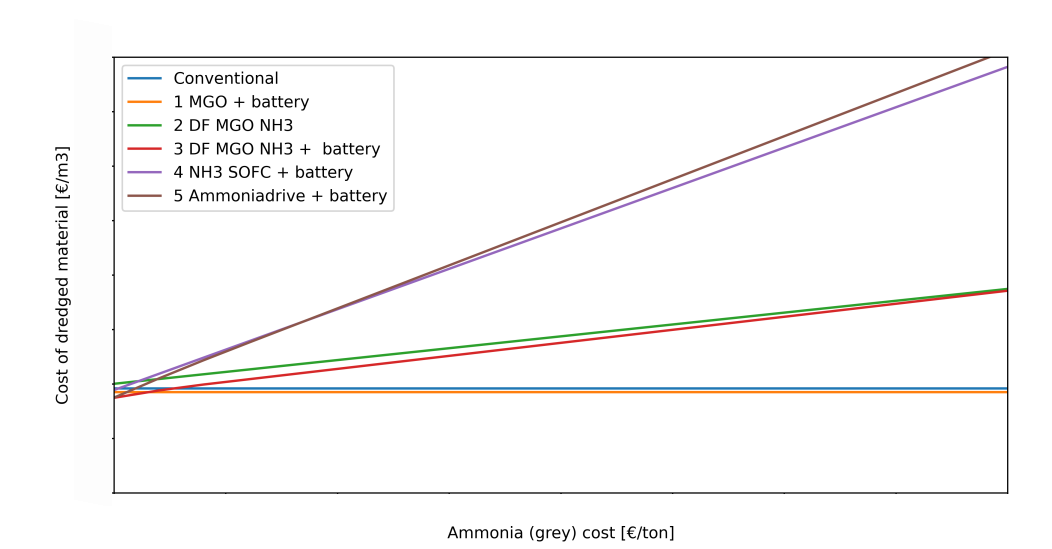


Figure B.4: The cost of dredged material for different ammonia (grey) cost for every configuration for scenario 2.

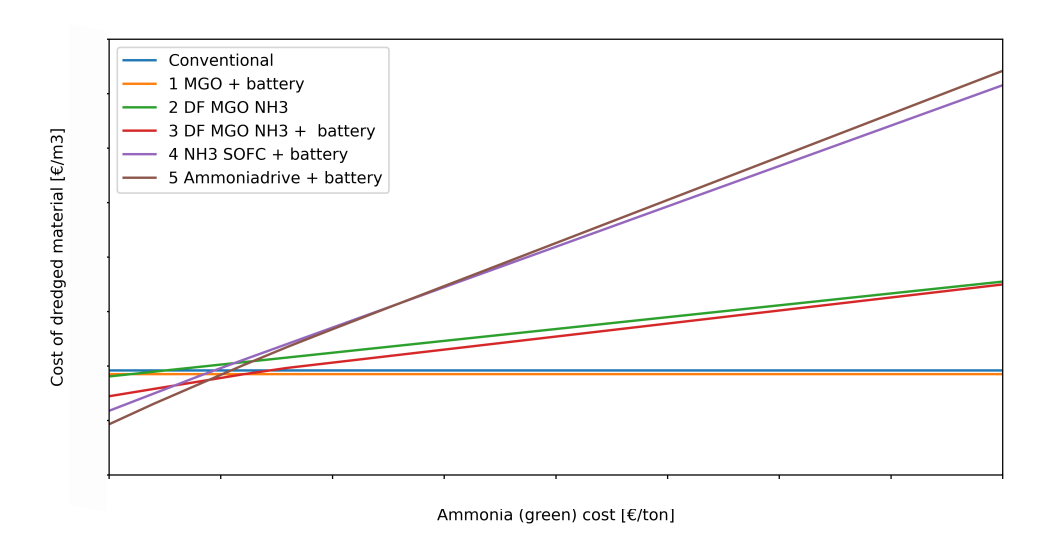


Figure B.5: The cost of dredged material for different ammonia (green) cost for every configuration for scenario 3.

B.1. Results 71

B.1.4. SOFC cost

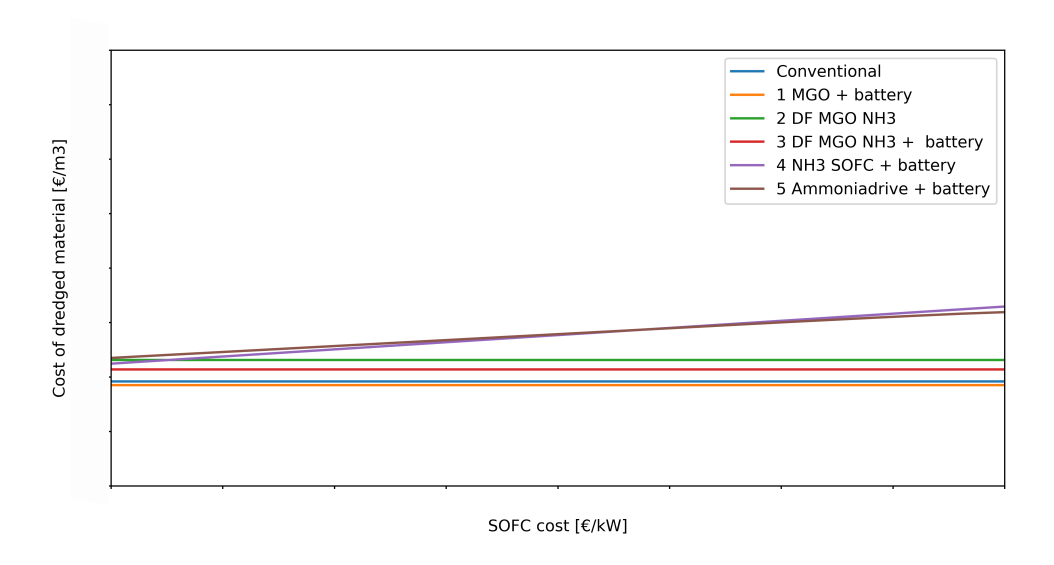


Figure B.6: The cost of dredged material for different SOFC cost for every configuration for scenario 2.

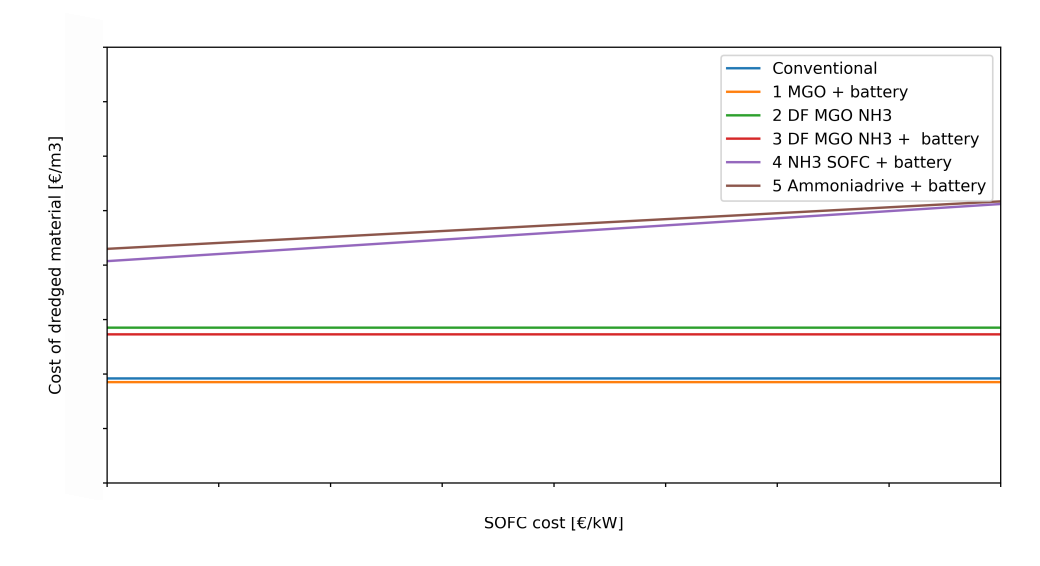


Figure B.7: The cost of dredged material for different SOFC cost for every configuration for scenario 3.

72 B. Appendix B

B.1.5. SOFC degradation

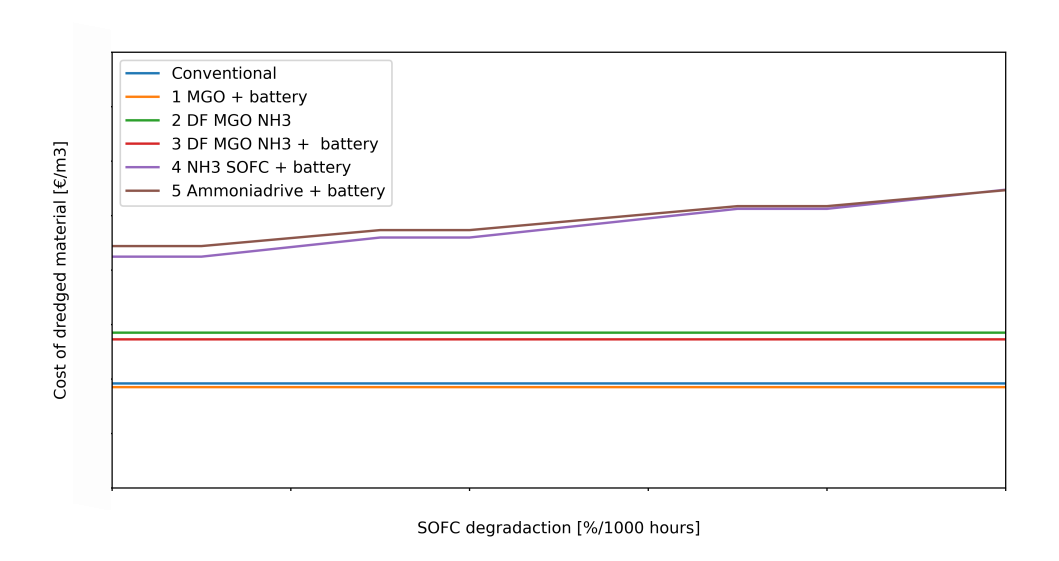
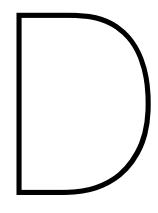


Figure B.8: The cost of dredged material for different SOFC degradation for every configuration for scenario 3.



Python code

C.1. simulation



Simulations